NASA CONTRACTOR REPORT

NASA CR-239

NASA CR-239

DEVELOPMENT OF SATISFACTORY LATERAL-DIRECTIONAL HANDLING QUALITIES IN THE LANDING APPROACH

by Robert L. Stapleford, Donald E. Johnston, Gary L. Teper, and David H. Weir

Prepared under Contract No. NAS 2-864 *by*
SYSTEMS TECHNOLOGY, INC.
Hawthorne, Calif.
for

NATIONAL AERONAUTICS AND SPACE ADMINISTRATION • WASHINGTON, D. C. • JULY 1965

NASA CR-239

DEVELOPMENT OF SATISFACTORY LATERAL-DIRECTIONAL HANDLING QUALITIES IN THE LANDING APPROACH

By Robert L. Stapleford, Donald E. Johnston,
Gary L. Teper, and David H. Weir

Prepared under Contract No. NAS 2-864 by
SYSTEMS TECHNOLOGY, INC.
Hawthorne, Calif.

for

NATIONAL AERONAUTICS AND SPACE ADMINISTRATION

For sale by the Clearinghouse for Federal Scientific and Technical Information
Springfield, Virginia 22151 – Price $4.00

FOREWORD

This report was prepared under Contract NAS2-864 between Systems Technology, Inc., Hawthorne, California, and the National Aeronautics and Space Administration. The NASA project monitor was Maurice D. White. The STI technical directors were Irving L. Ashkenas and Duane T. McRuer. The STI project engineer was Robert L. Stapleford.

The authors gratefully acknowledge the fine work of the STI production department in the preparation of this report.

ABSTRACT

27946

An analytical method is presented for developing satisfactory lateral-directional handling qualities in the landing approach. The method includes the following three steps:

1. Analysis of the handling qualities of the basic airframe to determine what deficiencies, if any, exist.
2. Determination of stability augmentation requirements for satisfactory handling qualities.
3. Assessment of the operational tradeoffs among the various mechanizational possibilities.

Twelve factors for the handling-quality evaluations of steps 1 and 2 are developed. Preliminary estimates of the values necessary for a good pilot rating are derived from previous studies and from tests of several supersonic transport configurations evaluated on the Transport Landing Simulator of the Ames Research Center of the NASA.

The operational tradeoffs considered in step 3 include reliability, maintainability, and cost.

CONTENTS

		Page
I.	INTRODUCTION.	1
	A. General	1
	B. Outline of the Report	3
II.	BASIC MANEUVERS.	5
	A. Tracking the Localizer Beam	5
	B. Large Turns.	6
	C. Engine-Out Recovery	7
	D. Decrab	8
III.	HANDLING-QUALITY FACTORS.	10
	A. Closed-Loop Control	10
	B. Roll/Sideslip Ratio	17
	C. Turn Coordination.	17
	D. Roll Response	20
	E. Decrab	21
IV.	CONFIGURATION REVIEW	23
	A. Subsonic Jet	23
	B. SCAT 16, Bare Airplane	25
	C. SCAT 16, Tested Augmentation	26
	D. SCAT 16, Alternate Augmentation	29
	E. SCAT 17A, Bare Airplane.	31
	F. SCAT 17A, Tested Augmentation.	32
	G. SCAT 17A, Alternate Augmentation.	34
	H. SCAT 17B, Bare Airplane.	35
	I. SCAT 17B, Tested Augmentation.	36
	J. Desirable Values	64
V.	STABILITY AUGMENTER MECHANIZATION.	66
	A. Ground Rules	67
	B. Selection of Mechanizations	69

Page

VI. SUMMARY 80

REFERENCES. 82

APPENDIX A – TRANSFER FUNCTIONS. 84

APPENDIX B – NUMERICAL DATA 87

APPENDIX C – PILOT MODEL 91

APPENDIX D – UNIFIED SERVO ANALYSIS METHOD 96

APPENDIX E – MULTILOOP ANALYSIS TECHNIQUE 100

APPENDIX F – REDUNDANCY IN STABILITY AUGMENTERS 102

FIGURES

		Page
1.	Tracking the Localizer Beam.	6
2.	Typical Root Loci for Bank-Angle-to-Aileron Feedback .	12
3.	Typical Root Loci for Heading-to-Aileron Feedback . .	13
4.	Typical Root Loci for Yaw-Rate-to-Rudder Feedback . .	16
5.	Subsonic Jet, Bank-Angle Closure	38
6.	Subsonic Jet, Heading Closure	39
7.	Subsonic Jet, Yaw-Rate Closure.	40
8.	SCAT 16, Bare Airplane, Bank-Angle Closure.	41
9.	SCAT 16, Bare Airplane, Heading Closure.	42
10.	SCAT 16, Bare Airplane, Yaw Rate Closure	43
11.	SCAT 16, Tested Augmentation, Bank-Angle Closure. . .	44
12.	SCAT 16, Tested Augmentation, Heading Closure. . . .	45
13.	SCAT 16, Tested Augmentation, Yaw-Rate Closure . . .	46
14.	Sideslip-to-Rudder Feedback.	28
15.	SCAT 16, Alternate Augmentation, Bank-Angle Closure. .	47
16.	SCAT 16, Alternate Augmentation, Heading Closure. . .	48
17.	SCAT 16, Alternate Augmentation, Yaw-Rate Closure . .	49
18.	SCAT 17A, Bare Airplane, Bank-Angle Closure	50
19.	SCAT 17A, Bare Airplane, Heading Closure	51
20.	SCAT 17A, Bare Airplane, Yaw-Rate Closure	52
21.	SCAT 17A, Tested Augmentation, Bank-Angle Closure . .	53
22.	SCAT 17A, Tested Augmentation, Heading Closure . . .	54
23.	SCAT 17A, Tested Augmentation, Yaw-Rate Closure . . .	55

Page

24. SCAT 17A, Alternate Augmentation, Bank-Angle Closure . 56

25. SCAT 17A, Alternate Augmentation, Heading Closure . . 57

26. SCAT 17A, Alternate Augmentation, Yaw-Rate Closure . . 58

27. SCAT 17B, Bare Airplane, Bank-Angle Closure 59

28. SCAT 17B, Bare Airplane, Yaw-Rate Closure 60

29. SCAT 17B, Tested Augmentation, Bank-Angle Closure . . 61

30. SCAT 17B, Tested Augmentation, Heading Closure . . . 62

31. SCAT 17B, Tested Augmentation, Yaw-Rate Closure . . . 63

32. Probable Number of Landings Without Augmentation. . . 76

33. Probable Number of Maintenance Actions and Augmenter "Cost" 77

D-1. Example of the Combined Use of Root Locus and Bode Diagrams 97

TABLES

		Page
I	Summary of Handling-Quality Factors	65
II	SCAT 16 Mechanization (Per Channel)	71
III	SCAT 17A Mechanization (Per Channel)	72
IV	SCAT 17B Mechanization (Per Channel)	73
V	Augmenter Comparison Summary.	75
B-I	Reference Dimensions	87
B-II	Dimensionless Stability Derivatives	88
B-III	Dimensional Stability Derivatives	89
B-IV	Transfer Function Factors.	90
F-I	Multiplicity Matrix.	109

SYMBOLS

A	Polynomial coefficient
a_y	Lateral acceleration sensed by accelerometer at the center of gravity
a_y'	Lateral acceleration sensed by accelerometer a distance l_x forward (parallel to the X axis) of the center of gravity and a distance l_z below (parallel to the Z axis) the center of gravity
b	Wing span
C	Cost, weight, and bulk index
C_l	Rolling moment coefficient, Roll moment/$(1/2)\rho V_{T_o}^2 Sb$
C_{l_β}	Roll coefficient due to sideslip, $\partial C_l/\partial\beta$
$C_{l_{\delta_a}}$	Aileron rolling coefficient, $\partial C_l/\partial\delta_a$
$C_{l_{\delta_r}}$	Rudder rolling coefficient, $\partial C_l/\partial\delta_r$
C_{l_p}	Roll damping coefficient, $\partial C_l/\partial(pb/2V_{T_o})$
C_{l_r}	Roll coefficient due to yaw rate, $\partial C_l/\partial(rb/2V_{T_o})$
C_n	Yawing moment coefficient, Yawing moment/$(1/2)\rho V_{T_o}^2 Sb$
C_{n_β}	Static directional stability, $\partial C_n/\partial\beta$
$C_{n_{\delta_a}}$	Aileron yawing coefficient, $\partial C_l/\partial\delta_a$
$C_{n_{\delta_r}}$	Rudder yawing coefficient, $\partial C_l/\partial\delta_r$
C_{n_p}	Yawing coefficient due to roll rate, $\partial C_n/\partial(pb/2V_{T_o})$
C_{n_r}	Yaw damping coefficient, $\partial C_n/\partial(rb/2V_{T_o})$
C_y	Lateral force coefficient, Lateral force/$(1/2)\rho V_{T_o}^2 S$
C_{y_β}	Lateral force coefficient due to sideslip, $\partial C_y/\partial\beta$
$C_{y_{\delta_a}}$	Aileron lateral force coefficient, $\partial C_y/\partial\delta_a$
$C_{y_{\delta_r}}$	Rudder lateral force coefficient, $\partial C_y/\partial\delta_r$

g	Acceleration due to gravity
$G(s)$	Transfer function
I_x	Moment of inertia about X axis
I_z	Moment of inertia about Z axis
I_{xz}	Product of inertia
j	$\sqrt{-1}$
K	Gain
l_x	Distance accelerometer is forward of the center of gravity, measured parallel to the X axis
l_z	Distance accelerometer is below the center of gravity, measured parallel to the Z axis
L	Rolling acceleration due to aerodynamic moments
L_β	$\rho S V_{T_o}^2 b C_{l_\beta}/2I_x$
L_δ	$\rho S V_{T_o}^2 b C_{l_\delta}/2I_x$
L_p	$\rho S V_{T_o} b^2 C_{l_p}/4I_x$
L_r	$\rho S V_{T_o} b^2 C_{l_r}/4I_x$
L_i'	$\dfrac{L_i + (I_{xz}/I_x)N_i}{1 - (I_{xz}^2/I_x I_z)}$, where i refers to any motion or input quantity
m	Mass
M	Probable maintenance hours per flight
N	Yawing acceleration due to aerodynamic moments
N_β	$\rho S V_{T_o}^2 b C_{n_\beta}/2I_z$
N_δ	$\rho S V_{T_o}^2 b C_{n_\delta}/2I_z$
$N_{\lambda_\delta}(s)$	Airframe motion quantity/control deflection transfer function numerator
N_p	$\rho S V_{T_o} b^2 C_{n_p}/4I_z$

N_r	$\rho S V_{T_o} b^2 C_{n_r}/4I_Z$
N_i'	$\frac{N_i + (I_{xz}/I_z)L_i}{1 - (I_{xz}^2/I_x I_z)}$, where i refers to any motion or input quantity
p	Roll rate, angular velocity about the X axis, positive right wing down
P_F	Probability of system failure per flight
P_M	Probability of maintenance required per flight
r	Yaw rate, angular velocity about the Z axis, positive nose right
s	Laplace operator, $s = \sigma + j\omega$
S	Wing area
T_i	Time constant particularized by the subscript
U_o	Steady-state (trim) linear velocity along the X axis
v	Linear velocity along the Y axis
V_{T_o}	Total steady-state (trim) linear velocity, $\sqrt{U_o^2 + W_o^2}$
W_o	Steady-state (trim) linear velocity along the Z axis
y	Lateral deviation from the localizer beam
Y	Side acceleration due to aerodynamic forces
Y(s)	Transfer function
Y_δ	$\rho S V_{T_o}^2 C_{y_\delta}/2m$
Y_δ^*	$\rho S V_{T_o} C_{y_\delta}/2m$
Y_v	$\rho S V_{T_o} C_{y_\beta}/2m$
α_o	Steady-state (trim) angle of attack, $\tan^{-1} \frac{W_o}{U_o}$
β	Sideslip angle, $\tan^{-1} \frac{v}{V_T}$
δ_a	Aileron deflection, positive for left-wing-down rolling moment

δ_r	Rudder deflection, positive for nose-left yawing moment
$\Delta(s)$	Denominator of airframe transfer functions
ζ_i	Damping ratio of second-order mode, particularized by the subscript
θ_o	Steady-state (trim) pitch angle of the X axis with respect to the local horizontal, positive for nose up
ρ	Mass density of air
σ	The real portion of the complex variable $s = \sigma + j\omega$
φ	Roll angle
ψ	Heading
ω	The imaginary portion of the complex variable $s = \sigma + j\omega$
ω_{co}	Heading-control crossover frequency, see page 14
ω_i	Undamped natural frequency of second-order mode, particularized by the subscript

SECTION I

INTRODUCTION

A. GENERAL

An important function of the control system designer is to determine the best augmentation system for a given airplane. This determination may be divided into three sequential steps:

1. Analysis of the handling qualities of the basic airframe to determine what deficiencies, if any, exist.
2. Determination of stability augmentation requirements for satisfactory handling qualities.
3. Assessment of the operational tradeoffs among the various mechanizational possibilities.

This report presents a method for performing these three steps. Although the analyses presented here were done for the lateral-directional augmentation of large transport-type aircraft in the landing approach, portions of the method are applicable to other aircraft types in other flight regimes.

In recent years there has been a considerable advance in the ability to analytically predict handling-quality characteristics (Refs. 1 – 4); the proposed method uses such analytical prediction methods. By examining the various maneuvers the pilot will have to perform, a number of parameters or factors which should have important effects on handling qualities are determined. In some instances a particular phenomenon may be described by any of several factors, and in the present study a selection based on computational simplicity has been made.

A key problem in this analytical technique is the definition of what are good and what are bad values of the selected parameters. For the particular flight task considered here it has been possible to make preliminary estimates by comparing the analytical results with the simulator study reported in Ref. 5. Additional analytical and simulator

studies should be made to provide better quantitative criteria. Such studies would undoubtedly also aid in better defining the important handling-quality factors.

The second step, determining the stability augmentation requirements, is intimately connected to the first step. If we can define what constitutes satisfactory handling qualities, the determination of possible types of augmentation is relatively simple. Otherwise, we are reduced to an educated trial-and-error simulation of various augmentation schemes and combinations until one or more satisfactory types are found.

In the third step the various ways of mechanizing the satisfactory augmentation are assessed. The best system will probably not reflect simultaneously all of the desired virtues of being the most reliable, the lightest, the cheapest, and the easiest to maintain but will be a compromise among these, and other, operational factors. The most difficult part of the third step is to obtain realistic numerical values for various parameters, such as the mean-time-between-failures for a particular component in the actual operating environment. Once the numerical values are available it is a straightforward task to evaluate the operational factors for each competing system. The final selection can then be made in a logical fashion with full knowledge of the trade-offs involved.

The method proposed here evolved during a study of the lateral-directional handling-quality problems of a supersonic transport during landing approach. The configurations being considered were: one SCAT 16* variable-sweep design, two SCAT 17 (noted here as SCAT 17A and SCAT 17B) canard-delta-wing designs, and a currently operational subsonic jet which was used as a standard for comparison. The SCAT configurations considered were only interim designs and do not represent actual proposed configurations. These configurations were tested on

*The SCAT designations used here refer to the family of Supersonic Commercial Air Transports studied and reported on by the NASA in recent years.

the NASA's fixed-base Transport Landing Simulator at the Ames Research Center, as described in Ref. 5. That report also describes augmentation schemes derived during the simulator tests. The pilot ratings and comments from those tests have been compared with the analytical factors developed here to provide the initial estimates of the parameter values which are the boundaries between good and bad ratings.

It should be noted that the vehicle characteristics which are used throughout this report are those used on the simulator; certain relatively unimportant terms, such as $C_{y_{\delta_r}}$, were omitted from the simulation.

B. OUTLINE OF THE REPORT

Section II briefly discusses each maneuver the pilot may have to perform in a landing approach. The physical characteristics which should have the most effect on the pilot's ability to perform the maneuvers are pointed out.

Section III translates the physical characteristics into twelve specific handling-quality factors. The significance of each factor to one or more of the maneuvers is indicated.

Section IV is a review of the handling-quality factors for the subsonic jet and the three supersonic transport designs with and without various types of augmentation. All but two of the configurations were tested on the NASA's simulator (Ref. 5). The two untested configurations involve alternate augmentation schemes.

Examples of assessments of several means for mechanizing stability augmenters are contained in Section V. The minimum complexity augmentation scheme for each of the three supersonic transport designs is considered. A mechanization compatible with the reliability requirements of each is selected. Finally, a comparison is made of the operational factors for the augmentation system for each of the three designs.

Section VI is a summary.

Literal expressions for the vehicle transfer functions used in this report are given in Appendix A.

Appendix B is a summary of the numerical data on the various configurations.

Appendices C, D, and E are brief outlines of special analytical techniques utilized in this report. If the reader is unfamiliar with any of these, it is recommended that he read the appropriate appendices before making a detailed study of the body of the report. The subjects of the appendices are:

C. Pilot Model (Transfer Function Representation of the Pilot)

D. Unified Servo Analysis Method

E. Multiloop Analysis Technique

F. Redundancy in Stability Augmenters

SECTION II

BASIC MANEUVERS

Any study of the factors which affect the handling qualities of an airplane should start with a consideration of the basic maneuvers that the pilot must perform. This section discusses the important maneuvers and the related pilot tasks which are required during an approach and landing. The pilot's difficulty in performing these tasks should be the primary factor in his evaluation of the airplane's handling qualities. For those configurations which were tested on the NASA simulator, all of the maneuvers discussed in this section were actually performed.

A. TRACKING THE LOCALIZER BEAM

When making an instrument approach the pilot's primary lateral task is to keep the airplane on the localizer beam, i.e., to "track" the beam through deviations displayed on his ILS instrument. The pilot closes the loop by maneuvering the airplane to zero the deviation, preferably by using ailerons alone to make corrections.

Because of the long time required to correct a lateral offset it is generally impossible for the pilot to track the beam by closing only the lateral-deviation loop. To provide anticipation or lead he also closes two other aileron loops, roll angle and heading. (Roll angle control is additionally desirable because of the necessity for limiting maximum bank angles during approach.) The complete multiloop situation is shown in Fig. 1, where Y_ϕ, Y_ψ, and Y_y are the pilot's controller transfer functions for roll angle, heading, and lateral deviation. Pilot closure of the roll and heading loops is discussed in subsection III-A. The lateral-deviation loop is not considered as a separate factor here because this closure is normally of very low bandwidth which is set primarily by the bandwidth of the heading closure. If the airplane has good heading control, the lateral-deviation control will be good.

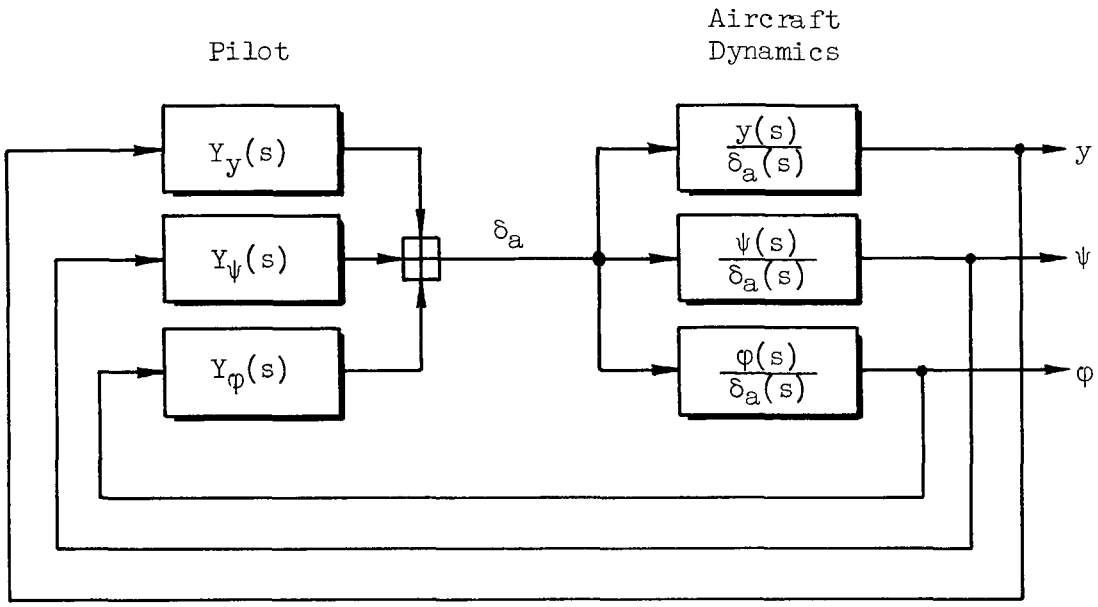

Note: Instrument and control system dynamics are neglected

Figure 1. Tracking the Localizer Beam

While the pilot is tracking the localizer, and during other maneuvers, the airplane may be disturbed by side gusts. For the configurations being considered here an important effect of the gusts will be to disturb the aircraft's roll attitude. The single most significant parameter in determining the severity of the roll disturbances is the magnitude of the roll-to-sideslip ratio in the Dutch-roll mode, $|\varphi/\beta|_{DR}$. This parameter is discussed in subsection III-B.

B. LARGE TURNS

While tracking the localizer the pilot will be making small turns to stay on the beam, but at other times, such as in turning onto the beam or in a sidestep maneuver, larger turns will be necessary. Large turns are distinguished from small ones by a longer turning time and by a greater emphasis on coordination for maneuver judgment and passenger comfort. The pilot makes large turns by bringing the airplane up to and holding a steady bank angle. In an airplane with good roll dynamics the desired bank angle is reached by commanding a roll rate with a step

aileron, holding the aileron and hence a steady roll rate until the airplane nearly reaches the desired bank angle, and then neutralizing the aileron, which quickly brings the airplane to a zero roll rate, constant bank angle condition.

The roll subsidence time constant and the maximum roll rate available are two parameters which affect the pilot's evaluation of the airplane's handling qualities (Ref. 1 and 4). The pilot would like the airplane to respond rapidly, which implies a small roll time constant. The most desirable maximum roll rate, p_{max}, is a compromise between values considered too sluggish and too sensitive. The two parameters are discussed in subsection III-D.

The difficulty of coordinating large turns is related to the rudder motions required or the sideslip time histories if the rudder is not used.* Much simpler, albeit less informative, measures of the difficulty are the initial rudder position and rate for perfect coordination with a step aileron input. These two parameters, plus the amount of rudder required to maintain a coordinated steady-state turn, are described in subsection III-C.

C. ENGINE-OUT RECOVERY

The primary effect of an engine failure on a conventional multiengine aircraft is a large yawing moment input. The problem is particularly severe in an aborted approach if the failure occurs shortly after go-around power has been applied. As the airplane yaws it will develop an appreciable sideslip, and because of the L'_r and L'_β terms may also roll significantly.

The analytical determination of how much difficulty the pilot will have in regaining control before the sideslip and roll have become too large is an extremely complicated task. This problem has not been

*British experimental and analytical studies of large turns (sidestep maneuver) are described in Ref. 6-9.

completely resolved, but certain factors which should have important effects have been noted. The initial yawing–sideslipping motion will primarily excite the Dutch-roll mode; consequently two factors which should be important are the pilot's ability to damp the Dutch-roll mode with rudder proportional to yaw rate, and the magnitude of φ/β in the Dutch-roll mode. The second factor gives an indication of the amount of rolling motion which will result from the engine failure. Pilot damping of the Dutch roll by $r \rightarrow \delta_r$ feedback is discussed in subsection III-A and $|\varphi/\beta|_{DR}$ is discussed in subsection III-B.

Additional factors which are probably significant, but which are not specifically included in the analyses because the variations among the SST configurations are relatively small, are:

1. L'_r — initially the primary source of roll acceleration. The L'_β contribution is normally of the same sign and within a few seconds is of larger magnitude.

2. $L'_{\delta_r}/N'_{\delta_r}$ — determines the amount of roll acceleration introduced when the pilot puts in rudder to offset the engine yawing moment. The roll due to rudder will normally be of the same sign as that due to yaw rate and sideslip.

3. N'_β — one of the prime factors in determining the magnitude of the sideslip response to engine failure.

D. DECRAB

When approaching in a crosswind the pilot may hold a crab angle so that the airplane is headed into the relative wind and the ground track is along the runway centerline. Shortly before touchdown the pilot must decrab fairly rapidly so that the airplane lands headed down the runway centerline with little lateral drift velocity. This is primarily done by kicking the rudder, but aileron control is also required to keep the wings level.

For good handling qualities the pilot must have enough rudder power so that he can yaw the airplane through the decrab angle before the lateral drift velocity builds up to an excessive level. He must also have sufficient aileron power to keep the wings level, with some reserve for counteracting gust disturbances. Two simple measures of rudder and aileron power are discussed in subsection III-E.

Another factor, which also includes the effects of other parameters such as directional stiffness, is the amount of time required to yaw the airplane through a specified angle. An equivalent factor which is easier to compute is the yaw angle which can be achieved in a specified time; this latter factor is used in the comparisons of Section IV and is described in detail in subsection III-E.

Some of the factors which are important for engine-out recovery are also significant for decrab as there are many similarities between the two maneuvers. Particularly important is the pilot control of yaw rate with rudder as this provides nearly all the damping of the Dutch-roll mode while the pilot is trying to keep the nose aligned with the runway centerline; this loop closure is discussed in subsection III-A.

SECTION III

HANDLING-QUALITY FACTORS

From the previous discussions it should be clear that numerous handling-quality factors must be considered to assess each configuration. In this section twelve of the factors which appear to be the most significant will be described. Some of the factors may be expressed as explicit parameters which can be assigned a numerical value while others require interpretation of pilot loop closures. Additional discussion has been provided as appropriate to aid in the understanding of the latter type of factor.

Because many of these factors are important for several of the basic maneuvers and there are a great many interrelationships among the factors, it is impossible to divide them into independent groups. In the following presentation the twelve factors are divided into five categories, with each category being a grouping of the factors with the most interdependence.

It should be noted that by approaching the problem from the viewpoint of pilot difficulties in performing various maneuvers, certain handling-quality parameters, such as Dutch-roll frequency and damping, are not considered explicitly. The effects of the conventional parameters are included indirectly in that they affect the numerical values of some factors and affect pilot loop closures by changing the transfer function poles and zeros.

For some of the factors past research provides an indication of desirable values, and these are noted in the discussion. For the other factors desirable values will be stated on the basis of analysis of the NASA simulator experiments (Section IV).

A. CLOSED-LOOP CONTROL

Three loop closures will be considered as handling-quality factors: simultaneous bank angle and heading to aileron, and yaw rate to rudder.

The control of bank angle with aileron forms the basic inner loop for all lateral control. Typical root loci for a pure-gain bank-angle-to-aileron feedback are shown in Fig. 2. Note that the usual second-order form of the φ/δ_a numerator has a frequency, ω_φ, which can be greater than or less than the Dutch-roll frequency, ω_d. It can be seen in Fig. 2 that when $\omega_\varphi/\omega_d < 1$ the Dutch-roll mode may be stabilized (damping increased somewhat) by controlling the bank angle, whereas if $\omega_\varphi/\omega_d > 1$ the feedback destabilizes the Dutch roll.

The most common stability problem in bank-angle feedback is that due to $\omega_\varphi/\omega_d > 1$. In fact, ω_φ/ω_d is frequently used as a handling-quality parameter (Ref. 1, 2, and 3). Although ω_φ/ω_d will not be used explicitly as a handling-quality factor in this report, its effects are included by considering bank-angle control as a factor; however, bank-angle control depends on more than the ω_φ/ω_d ratio. Other parameters which are important are ω_d, ζ_φ, ζ_d, and the roll-subsidence time constant, T_R (Ref. 1, 2, and 3). The key point to be made here is that for a good pilot rating the pilot must be able to control bank angle with ailerons alone without destabilizing the Dutch-roll mode. This closure is treated as a handling-quality factor in this report.

When flying the localizer beam, heading control with the aileron is an outer loop and bank angle to aileron is an inner loop. The need for the $\varphi \rightarrow \delta_a$ inner loop can be seen in Fig. 3 (these root loci are for the subsonic jet in landing approach). The effects of inner loop closures appear in modifications to the effective values of $1/T_s$, $1/T_R$, ω_d, ζ_d as determined from plots similar to Fig. 2. Without the inner loop the closed-loop system is unstable for all gains if the spiral mode is unstable; if the spiral is stable it couples with the free s to form a second-order mode which goes unstable at a very low frequency and for a very small gain. Consequently, even if the spiral mode is stable the heading response will be poor because the dominant mode* is restricted to low frequencies.

*The dominant mode is that mode which contains the largest portion of the response to a command input.

$$\frac{\phi}{\delta_a} = \frac{A_\phi\left(s^2 + 2\zeta_\phi\omega_\phi s + \omega_\phi^2\right)}{\left(s + \frac{1}{T_s}\right)\left(s + \frac{1}{T_R}\right)\left(s^2 + 2\zeta_d\omega_d s + \omega_d^2\right)}$$

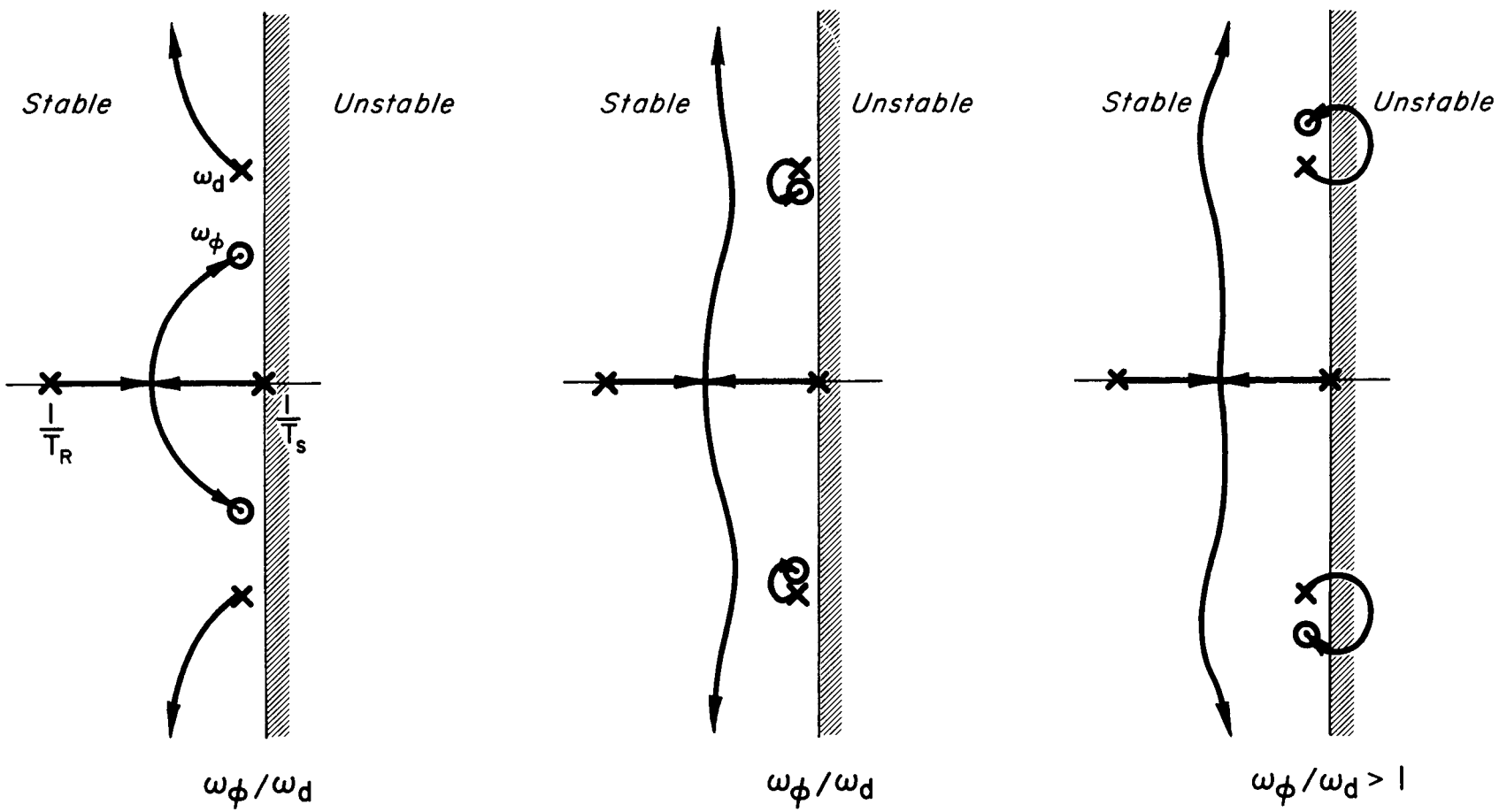

Figure 2. Typical Root Loci for Bank-Angle-to-Aileron Feedback

$$\frac{\psi}{\delta_a} = \frac{N'_{\delta_a}}{\cos\theta_0} \frac{\left(s + \frac{1}{T_{\psi_1}}\right)\left(s + \frac{1}{T_{\psi_2}}\right)\left(s + \frac{1}{T_{\psi_3}}\right)}{s\left(s + \frac{1}{T_s}\right)\left(s + \frac{1}{T_R}\right)\left(s^2 + 2\zeta_d\omega_d\, s + \omega_d^2\right)}$$

- or -

$$\frac{\psi}{\delta_a} = \frac{N'_{\delta_a}}{\cos\theta_0} \frac{\left(s + \frac{1}{T_{\psi_1}}\right)\left(s^2 + 2\zeta_\psi\omega_\psi\, s + \omega_\psi^2\right)}{s\left(s + \frac{1}{T_s}\right)\left(s + \frac{1}{T_R}\right)\left(s^2 + 2\zeta_d\omega_d\, s + \omega_d^2\right)}$$

Note: $\frac{1}{T_{\psi_3}}$ *is too large to be seen in these sketches*

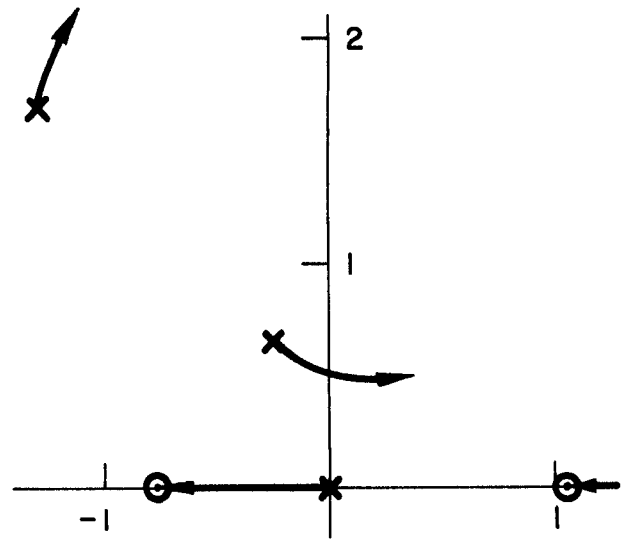

High-Gain Roll Inner Loop

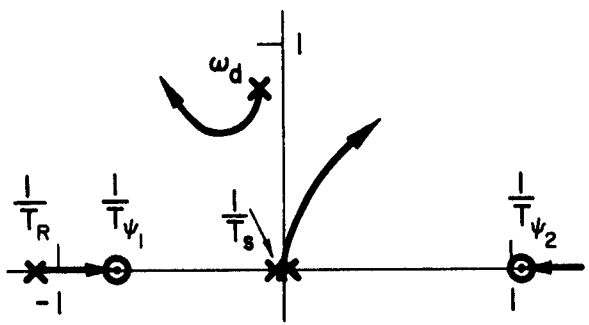

No Inner Loop

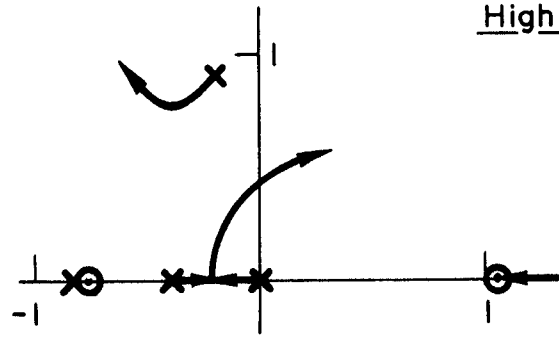

Low-Gain Roll Inner Loop

Figure 3. Typical Root Loci for Heading-to-Aileron Feedback

A low gain $\varphi \rightarrow \delta_a$ inner loop increases $1/T_s$, decreases $1/T_R$, and slightly modifies the Dutch-roll mode. As the gain in the heading closure is increased, the new spiral mode and the free-s are driven together, couple, and finally, for high enough gain, go unstable. The heading response can be greatly improved over the no-inner-loop case because the dominant mode can be of much higher frequency. Because of the frequency separation, the heading closure has a negligible effect on the $\varphi \rightarrow \delta_a$ inner loop.

For a high-gain inner loop, the spiral and roll-subsidence modes have coupled so that the airplane now has two second-order modes, one of which is located near the zeros of the φ/δ_a transfer function and the second pair at higher frequency. In this case it is the pair of roots near the φ/δ_a zeros that are driven unstable by the heading loop and the dominant mode in the heading response is the first-order pole which originated at the free s. The heading-loop gain is limited by the requirement of keeping the second-order mode from going unstable; this in turn limits the location of the dominant first-order mode. Whether the high-gain inner loop provides better heading response than the low-gain inner loop depends primarily on the damping of the second-order mode in the high-gain case and on the locations of the ψ/δ_a zeros.

For the comparison of various configurations it is desirable to have a simple quantitative parameter which is a valid indicator of relative speeds of heading response. The parameter ω_{co}, crossover frequency, appears to be useful as that indicator because ω_{co} is an approximation to the dominant response frequency and the bandwidth of the heading control. The crossover frequency is easily determined from the Bode plot of the $\psi \rightarrow \delta_a$ loop by the following steps which also provide the definition of ω_{co}:

1. Determine the zero-db line for the highest loop gain which provides a gain margin of at least 6 db and a phase margin of at least 45 deg.
2. Locate the intersection of that zero-db line and the low frequency asymptote, K/s.

3. The frequency at which that intersection occurs is ω_{co}.

It should be reiterated that good heading control also depends on favorable locations for the zeros of the φ/δ_a and ψ/δ_a numerators. The zeros of the latter change drastically with relatively small changes in the aerodynamic derivatives $C_{n_{\delta_a}}$ and C_{n_p}. In practice both of these are difficult to predict and may vary substantially with minor configuration changes. Consequently the values of $C_{n_{\delta_a}}$ and C_{n_p} and the heading control may change significantly during the design evolution.

The third loop closure to be considered as a handling-quality factor is the control of yaw rate with rudder to damp the Dutch-roll mode. The yaw-rate-to-rudder numerator is third order with one root usually near the roll-subsidence mode and a second-order pair of very low frequency, ω_r, and damping. Examples of good and bad closures are shown in Fig. 4. Normally ω_r/ω_d is very small so that the yaw-rate-to-rudder feedback can add a great deal of damping to the Dutch roll. For ω_r/ω_d near 1 this feedback can do little to damp the Dutch roll and in an extreme case may reduce the damping.

The conditions which can produce a poor yaw rate closure can be seen from the approximate factors of Ref. 10.

$$\frac{\omega_r}{\omega_d} \doteq \sqrt{\frac{g\left[-L'_\beta + (L'_{\delta_r}/N'_{\delta_r})N'_\beta\right]}{U_o L'_p (N'_\beta - L'_\beta \tan \alpha_o)}} \qquad (1)$$

This equation clearly indicates that the elements which can contribute to a poor yaw rate closure are:

1. Low speed
2. Low directional stability
3. Low roll damping
4. High dihedral effect

$$\frac{r}{\delta_r} = \frac{N'_{\delta_r}\left(s + \frac{1}{T_r}\right)\left(s^2 + 2\zeta_r\omega_r s + \omega_r^2\right)}{\left(s + \frac{1}{T_s}\right)\left(s + \frac{1}{T_R}\right)\left(s^2 + 2\zeta_d\omega_d s + \omega_d^2\right)}$$

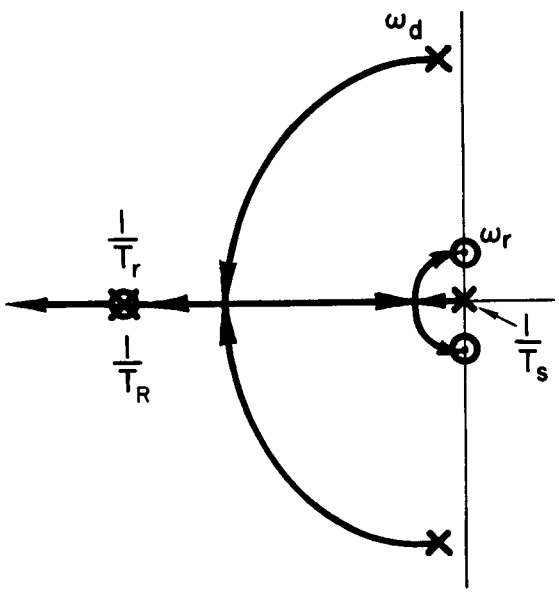

Low ω_r/ω_d
(good ability to damp Dutch Roll)

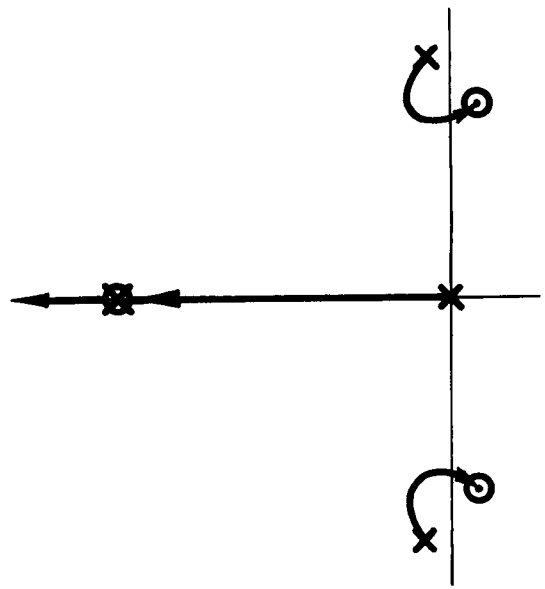

$\omega_r/\omega_d \approx 1$
(poor ability to damp Dutch Roll)

Figure 4. Typical Root Loci for Yaw-Rate-to-Rudder Feedback

The approximation of Eq 1 is given only to indicate the effects of various parameters. In the comparisons of Section IV the exact r/δ_r transfer functions are used.

B. ROLL/SIDESLIP RATIO

The magnitude of φ/β in the Dutch-roll mode is a measure of the roll response to yaw inputs—inadvertent rudder motions, engine out, rudder to decrab, and side gusts. Consequently it is desirable to have the magnitude of φ/β small. Normally (Ref. 1),

$$\left|\frac{\varphi}{\beta}\right|_{DR} \doteq \frac{|L'_\beta|}{\omega_d \sqrt{\omega_d^2 + (1/T_R)^2}} \qquad (2)$$

From Eq. 2 it can be seen that $|\varphi/\beta|_{DR}$ can be reduced by decreasing the effective dihedral (reducing L'_β), increasing the directional stiffness (increasing the Dutch-roll frequency), or increasing the roll damping (decreasing the roll-subsidence time constant).

The approximation of Eq. 2 is given only to indicate the effects of various parameters. In the comparisons of Section IV the exact values of $|\varphi/\beta|_{DR}$ (as determined from the ratio of numerators) are used.

C. TURN COORDINATION

The problem of turn coordination can be examined from two aspects, the rudder deflection necessary to keep the sideslip zero or the amount of sideslip which develops in an aileron-alone turn. The first approach will be used here since in commercial transports there is considerable emphasis on maintaining zero sideslip for piloting precision and passenger comfort.

Sample calculations for a step aileron input have shown that the rudder motion to maintain zero sideslip is quite complicated. Generally the difficulty in coordinating turns can be at least qualitatively

determined by examining the three factors considered in this subsection:

1. The initial step rudder deflection required for perfect coordination with a step aileron input.

2. The initial (immediately after the step) rate of change of rudder deflection required for perfect coordination with a step aileron input.

3. The rudder required to coordinate a steady-state turn.

For a step aileron input a step in rudder position is also necessary so that the resultant angular acceleration is about the airplane velocity vector. Thus, the ratio of the initial rudder step to the aileron input is (for $C_{y_{\delta_a}} = C_{y_{\delta_r}} = 0$)

$$\left(\frac{\delta_r}{\delta_a}\right)_o = -\left(\frac{N'_{\delta_a}}{N'_{\delta_r}}\right)_{SA} \tag{3}$$

where the subscript SA indicates that the derivatives are evaluated in stability axes. For body axes inclined nose-up an angle α_o with respect to the velocity vector, Eq. 3 becomes

$$\left(\frac{\delta_r}{\delta_a}\right)_o = -\left(\frac{N'_{\delta_a} - L'_{\delta_a} \tan \alpha_o}{N'_{\delta_r} - L'_{\delta_r} \tan \alpha_o}\right) \tag{4}$$

The initial rudder rate is necessary to counteract the effects of the cross-coupling term N'_p and the gravity term in the side force equation. In a perfectly coordinated turn

$$\beta(s) = \frac{N_{\beta\delta_a}(s)}{\Delta(s)}\delta_a(s) + \frac{N_{\beta\delta_r}(s)}{\Delta(s)}\delta_r(s) = 0 \tag{5}$$

Therefore the rudder required for coordination is

$$\delta_r(s) = -\frac{N_{\beta\delta_a}(s)}{N_{\beta\delta_r}(s)}\,\delta_a(s) \tag{6}$$

The above can be used to calculate the initial rudder position and rate (from that position) for a step aileron by means of the initial value theorem of Laplace transforms. The required rudder rate is given by

$$\left(\frac{\dot{\delta}_r}{\delta_a}\right)_o = \left[\frac{\left(L'_{\delta_a}N'_{\delta_r} - L'_{\delta_r}N'_{\delta_a}\right)\left(\frac{g}{V_{T_o}}\cos\theta_o - N'_p\right)}{\left(N'_{\delta_r}\right)^2}\right]_{SA} \tag{7}$$

or in body axes

$$\left(\frac{\dot{\delta}_r}{\delta_a}\right)_o = \frac{L'_{\delta_a}N'_{\delta_r} - L'_{\delta_r}N'_{\delta_a}}{\left(N'_{\delta_r}\cos\alpha_o - L'_{\delta_r}\sin\alpha_o\right)^2}$$

$$\times\left[\frac{g}{V_{T_o}}\cos(\theta_o - \alpha_o) - N'_p\cos^2\alpha_o\right.$$

$$\left. + (L'_p - N'_r)\sin\alpha_o\cos\alpha_o + L'_r\sin^2\alpha_o\right] \tag{8}$$

If $(\delta_r/\delta_a)_o$ and $(\dot{\delta}_r/\delta_a)_o$ are of opposite sign, extra precautions in the interpretation of the results should be taken. When these two parameters are of opposite sign their effects tend to cancel and it may be that, even though the magnitudes of both are large, little sideslip would develop if the pilot did not apply rudder.

The necessity for holding large amounts of rudder in a steady-state turn is an undesirable characteristic. For constant-altitude steady-state

turns within the bank angles normally used for commercial transports, the rudder required for zero sideslip implies $r \doteq (g/V_{T_o})\varphi$ is well approximated by

$$\left(\frac{\delta_r}{\varphi}\right)_{ss} \doteq \frac{-g}{V_{T_o}}\left(\frac{L'_{\delta_a}N'_r - L'_rN'_{\delta_a}}{L'_{\delta_a}N'_{\delta_r} - L'_{\delta_r}N'_{\delta_a}}\right)_{SA} \tag{9}$$

or in body axes

$$\left(\frac{\delta_r}{\varphi}\right)_{ss} \doteq \frac{-g}{V_{T_o}}\left[\frac{\left(L'_{\delta_a}N'_r - L'_rN'_{\delta_a}\right)\cos\alpha_o + \left(L'_pN'_{\delta_a} - L'_{\delta_a}N'_p\right)\sin\alpha_o}{L'_{\delta_a}N'_{\delta_r} - L'_{\delta_r}N'_{\delta_a}}\right] \tag{10}$$

D. ROLL RESPONSE

The roll response characteristics are principally defined by the roll-subsidence time constant and the maximum roll rate. The roll-rate response to aileron inputs is predominantly a first-order lag, T_R. Superimposed on the first-order response are oscillations which are due to the Dutch-roll mode. For most maneuvers the spiral mode will have a small effect because of the very low frequency of this mode.

The time to achieve a steady roll rate (following a step aileron input) and the time to stop rolling after the aileron has been neutralized are both proportional to the roll-subsidence time constant, T_R. Therefore it is desirable to have a small value of T_R. The only experimental data on the effects of T_R on pilot rating (Ref. 4) indicate that T_R must be less than 1.3 sec for a satisfactory rating; however, these experiments were for fighter aircraft operating at combat speeds. While it might appear that values of T_R somewhat greater than 1.3 sec should be acceptable for commercial transports in the approach condition, the NASA simulator studies of the SST configuration show a definite pilot desire for values less than 1 sec.

The maximum roll rate is a direct measure of the airplane's roll power. For this parameter the Ref. 4 experiments showed that excessively large or small values are unacceptable; if p_{max} is too small the pilot complains that the airplane is sluggish and if p_{max} is too large he complains that the airplane is too sensitive. As would be expected, the numerical values of p_{max} for satisfactory ratings in Ref. 4 are not applicable here. The minimum p_{max} for a satisfactory rating was 60 deg/sec, while in the NASA simulator studies of SST approaches values of 10–15 deg/sec were satisfactory.

Neglecting the small effects of the spiral mode, a very good approximation of the maximum roll rate can be found from the φ/δ_a transfer function, i.e.,

$$p_{max} \doteq \left(\frac{\omega_\varphi}{\omega_d}\right)^2 T_R L'_{\delta_a} (\delta_a)_{max} \tag{11}$$

E. DECRAB

A key factor in the decrab maneuver is rudder power, and a good indication of rudder power is the yaw angular acceleration produced by the rudder. Consequently, the dimensional derivative N'_{δ_r} will be used as a handling-quality factor.

To determine the aileron power required to maintain the wings level, the details of the decrab maneuver must be considered. If the pilot kicks the rudder to yaw the airplane's nose to the right, the rudder will also produce a left-wing-down roll acceleration. The airplane is prevented from rolling very much in this direction by the L'_r term which lags the rudder term ($\dot{r} \doteq N'_{\delta_r}\delta_r$) and gives a right-wing-down acceleration. The L'_β term, which lags the L'_r term ($\dot{\beta} \doteq -r$), also produces a right-wing-down acceleration and after the first few seconds is the dominant source of roll motion. The primary requirement on aileron power appears to be the ability to cancel the L'_β or dihedral term; therefore, L'_β/L'_{δ_a} will be used as a handling-quality factor.

The third decrab parameter to be considered is the yaw angle which can be obtained in a specified time. It will be assumed that the pilot puts in a step rudder deflection and holds it while using the ailerons to keep the wings level. With the wings held level the yaw response is the same as it would be with an infinite-gain bank angle feedback. Using the multiloop analysis technique described in Appendix E gives

$$\frac{r}{\delta_r} = \lim_{Y_\varphi \to \infty} \frac{N_{r\delta_r} + Y_\varphi N^{\varphi\ r}_{\delta_a \delta_r}}{\Delta + Y_\varphi N_{\varphi_{\delta_a}}} = \frac{N^{\varphi\ r}_{\delta_a \delta_r}}{N_{\varphi_{\delta_a}}} \tag{12}$$

For $C_{y_{\delta_a}} = C_{y_{\delta_r}} = 0$ the $\varphi \rightarrow \delta_a$, $r \rightarrow \delta_r$ coupling numerator is given by

$$N^{\varphi\ r}_{\delta_a \delta_r} = \left(L'_{\delta_a} N'_{\delta_r} - L'_{\delta_r} N'_{\delta_a}\right)(s - Y_v) \tag{13}$$

Consequently, the yaw angle for a step rudder input is

$$\Delta\psi(t) = \mathcal{L}^{-1} \frac{\left(L'_{\delta_a} N'_{\delta_r} - L'_{\delta_r} N'_{\delta_a}\right)(s - Y_v)(\delta_r)_s}{A_\varphi s^2 (s^2 + 2\zeta_\varphi \omega_\varphi s + \omega_\varphi^2)} \tag{14}$$

For the comparisons of the next section it is assumed that the full rudder authority of 25 deg is used and the angle is evaluated at a time of 2 sec, which is considered near the desirable maximum for the decrab maneuver. It should be noted that for the approach speeds being considered a crosswind of 25 knots gives a crab angle of approximately 10 deg.

As discussed in the previous section, there are other parameters besides the three considered above which are important in the decrab. Nevertheless, these three, combined with some of the factors discussed earlier in this section, should give a fair indication of piloting problems in decrab.

SECTION IV

CONFIGURATION REVIEW

This section reviews the handling qualities of the subsonic jet, which is used as a standard for comparison, and the three SST configurations with and without various methods of augmentation. The major emphasis is on the handling-quality factors described in Section III. A tabular summary of these factors for all configurations is given in Table I,* page 65. The review of each configuration considers the factors in the left-to-right order listed in the table; the configurations are reviewed in the vertical order shown. For those configurations which were tested on the NASA's approach simulator (all but two), the correlation between major comments of the pilots and the handling-quality factors will be discussed. The factors which appear to be deficient for each configuration are indicated by shading.

A. SUBSONIC JET

Pilot closure of the $\varphi \rightarrow \delta_a$ loop requires that the pilot generate a moderate amount of lead to provide damping for the higher frequency mode which originates at the Dutch roll (see Fig. 5).** The plots of Fig. 5 are for a pilot lead of 0.67 sec, which is certainly adequate and may be slightly more than actually used. Although the closure does require pilot lead, the amount is not great enough to significantly degrade pilot opinion (Ref. 11).

---

*This table has been prepared as a fold-out so the reader can readily refer to it while reading this section.

**To fully understand the manner in which the closed-loop results described below (and summarized in the first three columns of Table I) are obtained requires a working knowledge of the material given in Appendices C and D. However, the casual reader will still be able to obtain an (imperfect) appreciation for the effects of importance by reading only the text. The root locus and Bode plots for all the pilot closures are together at the back of this section, page 38-63.

To evaluate the $\psi \rightarrow \delta_a$ control it is necessary to make some assumption as to how the pilot has closed the $\varphi \rightarrow \delta_a$ inner loop. Throughout the comparisons of this section it will be assumed that the pilot closes the $\varphi \rightarrow \delta_a$ loop with a phase margin of 45 deg. Fortunately, the heading-loop bandwidth is relatively insensitive to the gain in the $\varphi \rightarrow \delta_a$ loop; therefore, a comparison based on this assumption should be valid even if the pilot is actually using a somewhat higher or lower gain.

Closure of the $\psi \rightarrow \delta_a$ loop with the inner $\varphi \rightarrow \delta_a$ loop closed as above is shown in Fig. 6. For a 6-db gain margin the crossover frequency, ω_{co}, is only 0.12 rad/sec and the dominant first order is slightly higher, 0.16 sec^{-1}. Table I shows this value to be lower than that for all other configurations except SCAT 16, bare airplane (ω_{co} = 0.10 rad/sec). Since the pilot complained of the poor heading control on the SCAT 16, bare airplane, it would seem that the same problem might exist on the subsonic jet as the two values of ω_{co} are quite close; however, there is nearly a two to one difference in the frequency of the dominant first-order modes, 0.16 sec^{-1} for the subsonic jet versus 0.085 sec^{-1} for the SCAT 16. Although detailed pilot comments on the subsonic jet are not available, it is known that many of these aircraft have been equipped with yaw dampers and that the airline pilots prefer to have the damper on during approach. This is a significant point as a yaw damper can greatly improve the heading control (increase ω_{co}) as well as eliminate the need for pilot lead in the $\varphi \rightarrow \delta_a$ closure.

The pilot's ability to damp the Dutch roll with $r \rightarrow \delta_r$ feedback is very good, as shown in Fig. 7.

The magnitude of φ/β, 1.4, is comparatively small and there is no significant problem due to the roll sensitivity to lateral inputs.

The turn coordination is very good. The angular acceleration due to the ailerons is about the velocity vector so no initial rudder

displacement is necessary for a step aileron input. The initial rudder rate and the steady-state value are also low.

The roll response is satisfactory but could be improved; an increase in maximum roll rate would appear desirable.

The rudder is quite powerful; N'_{δ_r} and the yaw angle achievable in 2 sec are greater than for any other configuration. Aileron power appears marginal; for a 10-deg sideslip, nearly full aileron authority is necessary to offset the dihedral effect.

B. SCAT 16, BARE AIRPLANE

As shown in Fig. 8, pilot closure of the $\varphi \rightarrow \delta_a$ loop can significantly increase the Dutch-roll frequency and damping even if the pilot doesn't use lead. Thus, the $\varphi \rightarrow \delta_a$ closure is considered very good.

The $\psi \rightarrow \delta_a$ closure is shown in Fig. 9. For a 6-db gain margin the crossover frequency is slightly less than 0.1 rad/sec and the dominant first-order mode is only 0.085 sec^{-1}. Table I shows this value to be considerably smaller than that for the other SCAT configurations. The primary cause for the poor heading control is the low value of $\zeta_\varphi \omega_\varphi$,* which is in turn due to a low value of N'_r (see Appendix B). A secondary cause is the existence of low-frequency zeros in the ψ numerator. The correlation with the pilot commant, "Low directional stability, difficult to hold a heading," is obvious.

The pilot's ability to damp the Dutch roll by feeding $r \rightarrow \delta_r$ is very good, as shown in Fig. 10.

The magnitude of φ/β for SCAT 16 is considerably less than for SCAT 17A or 17B because of the reduced dihedral effect obtained with the wings extended for the approach. As a result this configuration will be less roll-sensitive to lateral inputs.

---

*With the $\varphi \rightarrow \delta_a$ loop closed there is a pair of poles near the ω_φ zeros of the φ/δ_a transfer function. The damping ($\zeta\omega$) of these poles determines the magnitude of the peak on the $\psi \rightarrow \delta_a$ Bode and consequently is the main factor in setting the maximum gain and the crossover frequency.

The turn coordination characteristics show that initially a large amount of rudder into the turn is necessary to limit sideslip, but the steady-state value is quite low. The pilots did object to the large amount of adverse sideslip which developed in turn entries.

The roll-response time constant is very good, but the maximum roll rate may be a little low; however, there was no record of a pilot complaint.

For the decrab maneuver, the yaw acceleration due to rudder and the yaw angle achievable are low. This coupled with the difficulty in maintaining a heading could explain the pilot's difficulties in making crosswind landings.

In summary, the major deficiencies of this configuration are the difficulty in maintaining heading, the large adverse sideslip in turn entries, and low rudder power. In spite of these problems the overall pilot rating is marginally satisfactory for normal operation.

C. SCAT 16, TESTED AUGMENTATION

The augmentation determined by experiments on the NASA approach simulator is

$$C_{n_\beta} = 2 \times \text{basic}$$
$$C_{n_r} = 3 \times \text{basic}$$
$$C_{n_p} = -1 \times \text{basic}$$

that is, a β-to-rudder feedback so that the effective C_{n_β} is twice the bare-airplane value (this also changes the effective C_{l_β}), an r-to-rudder feedback so that the effective C_{n_r} is three times the bare-airplane value (this also changes the effective C_{l_r}), and a p-to-rudder feedback so that the effective C_{n_p} is the negative of the bare-airplane value (this also changes the effective C_{l_p}).

The pilot closure of the $\varphi \rightarrow \delta_a$ loop is shown in Fig. 11. By comparison with Fig. 8 it can be seen that the augmentation has increased the Dutch-roll damping and increased ω_φ so that the ω_φ and

ω_d roots nearly cancel. As for the bare airplane, the $\varphi \rightarrow \delta_a$ control is very good and the pilot does not have to generate any lead.

The $\psi \rightarrow \delta_a$ loop is shown in Fig. 12. The heading control is much better than for the bare airplane because the augmentation has increased $\zeta_\varphi \omega_\varphi$ and has modified the ψ/δ_a numerator so that a pair of zeros nearly cancel the low frequency second-order mode which previously limited the heading-loop gain and bandwidth. The heading control is now very good, with the crossover frequency of 0.59 rad/sec set by a 45-deg phase margin. The dominant first-order mode is at 0.65 sec^{-1}.

The pilot's ability to damp the Dutch roll by an $r \rightarrow \delta_r$ feedback is still very good, as seen in Fig. 13.

The magnitude of φ/β is essentially unchanged as the slight increase in Dutch-roll frequency has been offset by an increase in the magnitude of I'_β.

The coordination problem on turn entries has been eased by creating a proverse yaw due to roll rate ($C_{n_p} > 0$) to offset the adverse aileron yaw. This is evidenced by the change in the initial rudder rate for coordination from a large positive value to a large negative one. As mentioned in Section III, the canceling effects of different signs of the initial position and rate may result in negligible sideslip if the pilot does not use the rudder. In fact, the pilot commented that reversing the sign of C_{n_p} made turn entries much easier.

The augmentation of C_{n_r} has resulted in a large increase in the amount of rudder required to hold a steady turn, a feature the pilots complained about. This problem could be overcome by using a washout in the $r \rightarrow \delta_r$ feedback rather than a pure gain; the washout would eliminate the steady-state feedback of opposing rudder during a turn.

The augmentation gives a slight improvement in the roll-subsidence time constant and a considerable increase in the maximum roll rate (due to the increase in ω_φ). The roll response should be very good.

The rudder power is still low; in fact, the achievable yaw angle has been reduced. The pilots indicated that they would prefer a more powerful rudder.

The augmentation included a $\beta \rightarrow \delta_r$ feedback to increase the directional stiffness. During the decrab maneuver this feedback will deflect the rudder in opposition to the pilot's input and slow down the yaw motion. One solution is to have small limits on the augmenter authority so that the pilot can easily overpower it; but, in doing so, he effectively cuts out all rudder feedbacks.

Another solution is to use large augmenter authority with the pilot's rudder input effectively acting as a sideslip command. From Fig. 14 it can be seen that the sideslip response to the pilot's rudder input is

$$\frac{\beta}{\delta_{r_p}} = \left(\frac{K_2 K_3 N_{\beta\delta_r}}{\Delta + K_2 K_3 N_{\beta\delta_r}} \right) \frac{K_1}{K_3}$$

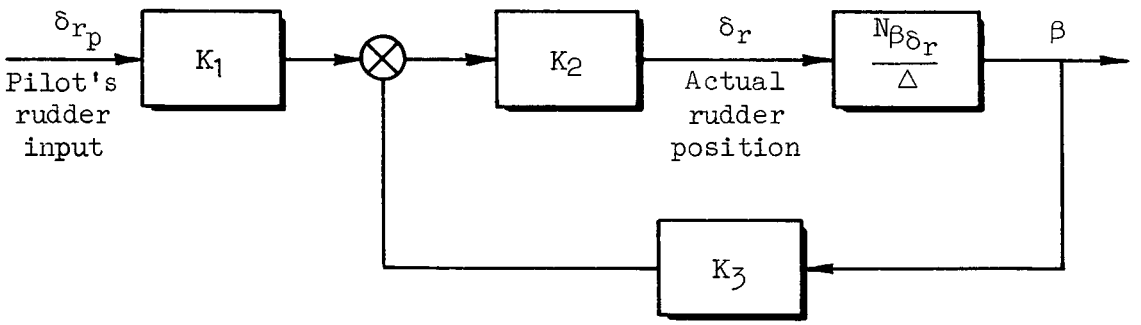

Figure 14. Sideslip-to-Rudder Feedback

Thus the response to the pilot's input can be increased without changing the loop gain by

1. Increasing K_1
2. Increasing K_2 and reducing K_3 so that $K_2 K_3$ is constant
3. Combination of the above

All these methods allow a high loop gain without making it difficult for the pilot to kick out a crab angle; however, there is the potential problem of a severe disturbance in case of a hard-over failure in the augmenter. Various mechanizational techniques for eliminating hard-over failures, such as hard-over detectors, are described in Section V.

D. SCAT 16, ALTERNATE AUGMENTATION

This article describes an alternate method of augmentation which was not tested on the simulator. The basic objective is to provide the simplest possible augmentation, i.e., a minimum number of feedbacks using only easily sensed quantities.

Two major deficiencies of the bare airplane (heading control and turn coordination) can be alleviated by increasing the Dutch-roll frequency and damping. To increase frequency it was decided to use a lateral acceleration feedback to rudder rather than a sideslip feedback. An accelerometer should be easier to install, more reliable, and simpler to maintain than a sideslip sensor.

Normally an accelerometer is located forward of the c.g. so that the $\dot{r}$ term compensates for the acceleration due to rudder side force, Y_{δ_r}. The rudder center-of-rotation (located a distance $-Y_{\delta_r}/N'_{\delta_r}$ forward of the c.g.) is often a good location. Since the simulator dynamics used $Y_{\delta_r} = 0$, the c.g. was chosen as the accelerometer location. The feedback proposed is

$$\delta_r = K_y a_y$$

where

$$K_y = 3.24 \frac{\text{rad}}{\text{ft/sec}^2}$$

For damping, a washed-out yaw-rate-to-rudder feedback was selected with the gain set to give a damping ratio of 0.5, i.e.,

$$\delta_r = K_r \frac{s}{s + a} r$$

where

$$a = 0.5 \text{ rad/sec}$$

$$K_r = 22.2 \text{ sec}$$

Pilot closure of $\varphi \rightarrow \delta_a$ is shown in Fig. 15. Note the additional nearly canceling pole and zero which result from the washout in the $r \rightarrow \delta_r$ augmentation. The closure is again very good with no pilot lead required.

The $\psi \rightarrow \delta_a$ closure is shown in Fig. 16. Because of the augmentation, the second-order poles which go unstable have been moved to higher frequency and damping. In addition, the numerator zeros have been improved somewhat by being shifted to higher frequencies. The net result is a significant improvement in the heading control over that of the bare airplane, although not as good as the tested augmentation.

The $r \rightarrow \delta_r$ control is very good (see Fig. 17) and the need for the pilot to use the rudder to damp the Dutch roll is greatly reduced because of the high damping supplied by the augmentation.

Although the magnitude of φ/β has increased slightly, the greatly increased directional stiffness (ω_d = 1.79 rad/sec compared to 0.64 rad/sec for the bare airplane and 0.68 rad/sec for the tested augmentation) will significantly reduce the roll response of the airplane to side gusts or an engine failure.

Although the initial rudder position and rate for turn coordination are the same unsatisfactory values as for the bare airplane, the increased directional stiffness with the proposed augmentation should actually greatly reduce the amount of sideslip in aileron-alone turns.

The roll-subsidence time constant is essentially unchanged and the maximum roll rate has been increased by the increase in ω_φ/ω_d. The roll-response factors are nearly equal to those for the tested augmentation.

The lateral-acceleration-to-rudder feedback has produced a large increase in the magnitude of the effective L'_β (because of L'_{δ_r}) and has thereby greatly increased L'_β/L'_{δ_a}. The increased directional stiffness and yaw damping have also reduced the achievable yaw angle. Both the aileron required to keep the wings level and the achievable yaw angle could be improved to nearly the bare-airplane values by using the pilot's rudder input as an acceleration command (in the same manner described in subsection C for a sideslip command).

E. SCAT 17A, BARE AIRPLANE

The $\varphi \rightarrow \delta_a$ closure for a pilot lead of 0.67 sec is shown in Fig. 18. This moderate amount of lead is necessary to provide a reasonable amount of Dutch-roll damping when the pilot is closing the $\varphi \rightarrow \delta_a$ loop. Without the lead the allowable pilot gain would be rather limited and heading control would be poor.

An interesting point on this configuration is that the value of ω_φ/ω_d, 0.62, is less than the 0.75 required to avoid roll rate reversals (Ref. 1 and 3). One pilot reported that he noticed the reversal but did not consider it highly objectionable. The reason for the acceptance of this characteristic is not clearly understood.

Even with the pilot lead in the $\varphi \rightarrow \delta_a$ loop the heading control is only fair (see Fig. 19). The crossover frequency is 0.20 rad/sec and the dominant first-order mode is at 0.18 sec^{-1}.

The $r \rightarrow \delta_r$ control (Fig. 20) is not as good as for the previous configuration, ζ_{max} being only 0.35, because of the relatively large value of ω_r/ω_d due to the high dihedral and low roll damping (Eq 1).

The magnitude of φ/β is quite high and, as would be expected, the pilot complained about the large roll motions caused by side gusts, engine failure, and the decrab maneuver.

A moderate amount of rudder is needed for turn entries and, although considerably less than for the SCAT 16, was still considered objectionable. The rudder required for steady-state turns does not appear excessive.

The airplane is quite sluggish in roll because of the relatively high roll time constant and slightly low maximum roll rate, a deficiency noted by the pilots.

The rudder power is much better than for the SCAT 16, but the aileron required to offset the effective dehedral is quite high. The aileron authority (15 deg) is not large enough to cancel the L'_β term for a 10-deg sideslip.

In summary, the configuration does not have any one serious problem, but instead is somewhat deficient in a number of areas. The most serious defect appears to be the tendency for the airplane to roll sharply whenever disturbed laterally by side gusts, engine failure, or the decrab maneuver. The over-all rating of the configuration was unsatisfactory to unacceptable for normal operation.

F. SCAT 17A, TESTED AUGMENTATION

This subsection describes the handling qualities of the SCAT 17A with the augmentation which was derived during the experiments on the NASA approach simulator. The augmentation consisted of β, p, and r feedbacks to aileron so that the effective derivatives were

$$C_{l_\beta} = 0.6 \times \text{basic}$$

$$C_{l_p} = 1.5 \times \text{basic}$$

$$C_{l_r} = 0 \times \text{basic}$$

and to rudder so that

$$C_{n_\beta} = 2 \times \text{basic}$$

$$C_{n_p} = -1 \times \text{basic}$$

$$C_{n_r} = 2 \times \text{basic}$$

Note that the actual values of the augmented derivatives are somewhat different than those listed above because the control cross-coupling terms, $C_{n_{\delta_a}}$ and $C_{l_{\delta_r}}$, were neglected in determining the feedback gains to be used.

Pilot closure of the $\varphi \rightarrow \delta_a$ loop is shown in Fig. 21. With the increased Dutch-roll damping, pilot lead is no longer necessary. The value of ω_φ/ω_d has also been increased to the point where the roll reversal no longer occurs.

The increased damping combined with a favorable shift in the ψ/δ_a zeros gives a significant improvement in the heading control; the crossover frequency is nearly doubled (see Fig. 22).

The reduced dihedral and increased roll damping have improved the $r \rightarrow \delta_r$ control through a reduction in ω_r/ω_d (see Fig. 23). There is also less need for the pilot to damp the Dutch roll as it is quite well damped by the augmentation.

The magnitude of φ/β has been reduced to two-thirds of its original value. This coupled with the increased roll and yaw damping significantly decreases the roll response to lateral inputs; however, the pilots indicated that they would prefer an even smaller $|\varphi/\beta|_{DR}$.

The initial rudder position for turn coordination is unchanged, but the initial rate is reduced to a small negative value by the change in C_{n_p}. The rudder for coordinating turn entries is reduced, but that required for steady turns has more than doubled because of the yaw damper. The steady-state requirement was considered excessive by the pilots, but could be reduced by a washout in the $r \rightarrow \delta_r$ feedback, as previously discussed in the SCAT 16 case. It is worth mentioning that a larger C_{n_r} augmentation would have been used had it not increased the steady-state-turn requirement.

The roll response is improved considerably by a 50-percent increase in maximum roll rate (through increasing ω_φ/ω_d) and a 25-percent decrease in the roll time constant.

For the decrab maneuver, the aileron required to offset the dihedral has been slightly reduced, but is still quite large. There has been a significant reduction in achievable yaw angle, but this could be increased by using the pilot's rudder input as a sideslip command.

G. SCAT 17A, ALTERNATE AUGMENTATION

This article describes an alternate method of augmentation which was not tested on the simulator. As for the SCAT 16 (subsection D), the basic objective is to provide the simplest possible augmentation.

One peculiarity of this configuration is worth special notice, that is, the aerodynamic derivative C_{y_β} is positive. Because of this reversal in sign a conventional accelerometer feedback would decrease the directional stiffness. One might consider changing the sign of the feedback, but two potential problems strongly discourage this:

1. Probable reversal of C_y at large β could cause an instability.

2. Because C_{y_β} would be negative over the rest of the flight envelope, either the feedback could be turned on only after the airplane is in the final approach condition or large gain changes would have to be made prior to final approach.

With an accelerometer feedback eliminated from consideration, the most logical augmentation for this airplane is a roll damper ($p \rightarrow \delta_a$) to decrease the rolling response to lateral inputs. A roll damper, however, will do little to improve the heading control. It was found that an aileron-to-rudder interconnect could improve the heading control by favorable shifts in the φ and ψ numerators. An interconnect ratio of 1:1 appears to be satisfactory. With the roll damper set to give a roll time constant of 0.5 sec, the augmentation is

$$\delta_r = \delta_a = K_p p$$

where $K_p = 1.23$ sec

Pilot closure of the $\varphi \rightarrow \delta_a$ loop with the interconnect and roll damper is shown in Fig. 24. The roll damper has added a considerable amount of Dutch-roll damping, the rudder interconnect has increased ω_φ, and the $\varphi \rightarrow \delta_a$ closure is very good without pilot lead.

The heading closure is shown in Fig. 25. The combined effects of an increased $1/T_R$ and a more favorable location of the ψ/δ_a zeros gives heading control which is much better than the bare airplane and is essentially the same as the tested augmentation.

The increased roll damping has also significantly reduced ω_r/ω_d and improved the pilot's ability to damp the Dutch roll by the $r \rightarrow \delta_r$ closure (see Fig. 26).

The magnitude of φ/β has been cut nearly in half from the bare airplane. This means an important reduction in the roll response to lateral inputs.

The interconnect eliminates the initial rudder position for turn entries, but the rate is unchanged. The resultant rudder requirements for coordination during turn entries should be modest. The interconnect has increased the rudder requirement for steady-state turns to about the same level (considered excessive) as the tested augmentation.

The roll damper has reduced the roll time constant, but has also lowered the maximum roll rate to 7 deg/sec. The maximum roll rate could be increased by using a very limited authority augmenter or by using the pilot's aileron input as a roll-rate command.

Although the rudder acceleration and achievable yaw angle are good, the amount of aileron to offset the dihedral appears to be objectionably large.

Because of the problems of the rudder required for steady turns and the aileron required for decrab, the handling qualities of this configuration may not be acceptable for normal operation without additional augmentation.

H. SCAT 17B, BARE AIRPLANE

The dynamics of this configuration are rather unusual. Because of the large positive value of C_{n_p}, the roll-subsidence and spiral modes have been coupled into a lateral phugoid. Thus the lateral characteristics

consist of two second-order modes of low frequency but relatively high damping ratio.

Pilot closure of the $\varphi \rightarrow \delta_a$ loop with a lead of 0.67 sec is shown in Fig. 27. The figure clearly shows that this is a very bad closure; the pilot is destabilizing the lateral phugoid and actual stability is critically dependent on the pilot lead. The pilot is capable of generating much higher leads, but extreme leads always lead to poor ratings. One pilot commented that the only way he could fly the airplane was by pulsing the ailerons. By applying a large acceleration for a short time the pilot can get a reasonable roll rate, and after he neutralizes the ailerons the roll rate decays slowly because of the low frequencies of the lateral modes.

Because of the very poor quality of the $\varphi \rightarrow \delta_a$ closure, heading control was not even considered.

The $r \rightarrow \delta_r$ closure is also very bad (Fig. 28). As with the $\varphi \rightarrow \delta_a$ loop, the closure destabilizes the lateral phugoid. The pilot experienced extreme difficulty controlling the airplane whenever he used the rudders.

The remaining handling-quality factors are unimportant as the closed-loop control is so bad that the configuration was rated unacceptable even for emergency conditions.

I. SCAT 17B, TESTED AUGMENTATION

This subsection describes the augmentation which was tested on the NASA simulator. Because this simple augmentation was successful, no attempt was made to derive an alternate augmentation system.

The sole augmentation was a roll damper with gain such that

$$C_{l_p} = 2.5 \times \text{basic}$$

or

$$\delta_a = K_p p$$

where

$$K_p = 1.7 \text{ sec}$$

As will be shown shortly, the roll damper makes a remarkable improvement in both $\varphi \rightarrow \delta_a$ and $r \rightarrow \delta_r$ control. It decouples the lateral phugoid back into a roll-subsidence and a spiral mode. It improves the $r \rightarrow \delta_r$ closure by greatly reducing ω_r.

The $\varphi \rightarrow \delta_a$ closure is shown in Fig. 29. Although the feedback reduces the Dutch-roll damping slightly, the damping was originally high enough so the effect is unimportant. This closure is very good; no pilot lead is required.

The heading control, Fig. 30, is considerably better than any other configuration because of the good Dutch-roll damping and the favorable location of the ψ/δ_a zeros.

Figure 31 shows the $r \rightarrow \delta_r$ closure which is now very good because of the effects of the roll damper on ω_r and the lateral phugoid.

While the magnitude of φ/β has been greatly reduced, one might suspect that it is still somewhat too large; simulator tests with reduced C_{l_β} did show a slight improvement in pilot rating.

The turn coordination appears good and there were no pilot complaints. The rudder requirements for turn entry are quite small and rather than put in top rudder, or rudder out-of-the-turn (the initial rudder rate required is negative), the pilot probably accepts the small amount of sideslip for aileron-alone entries. The steady-turn requirement is moderate.

The roll response is very good, with a low time constant and relatively large maximum roll rate.

The rudder power is good, N'_{δ_r} and the achievable yaw angle are quite large. The aileron required to overcome the dihedral is high and, although a pilot complaint on this specific point was not noted, simulator tests showed that a reduced L'_β improved pilot rating.

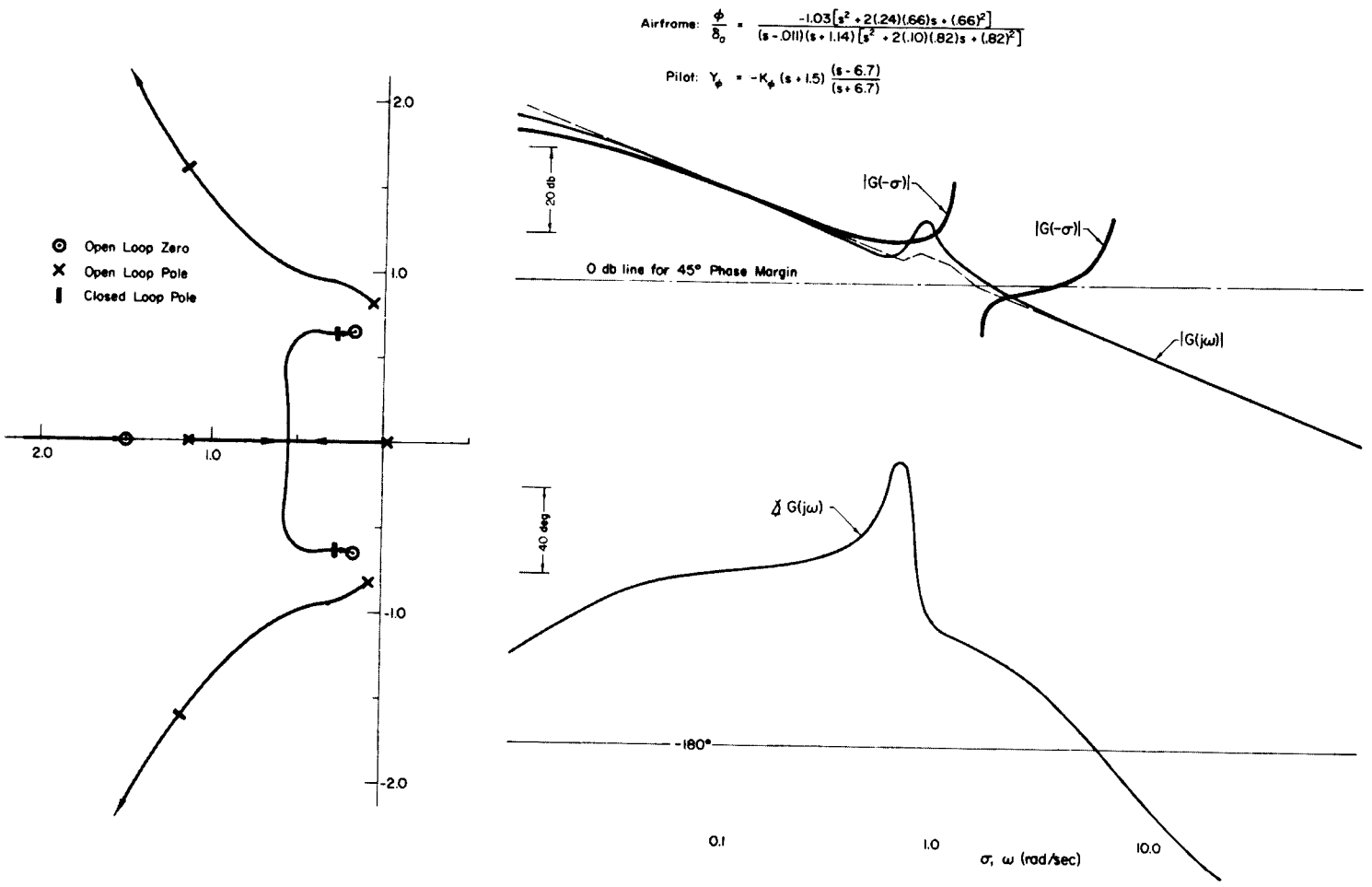

Figure 5. Subsonic Jet, Bank-Angle Closure

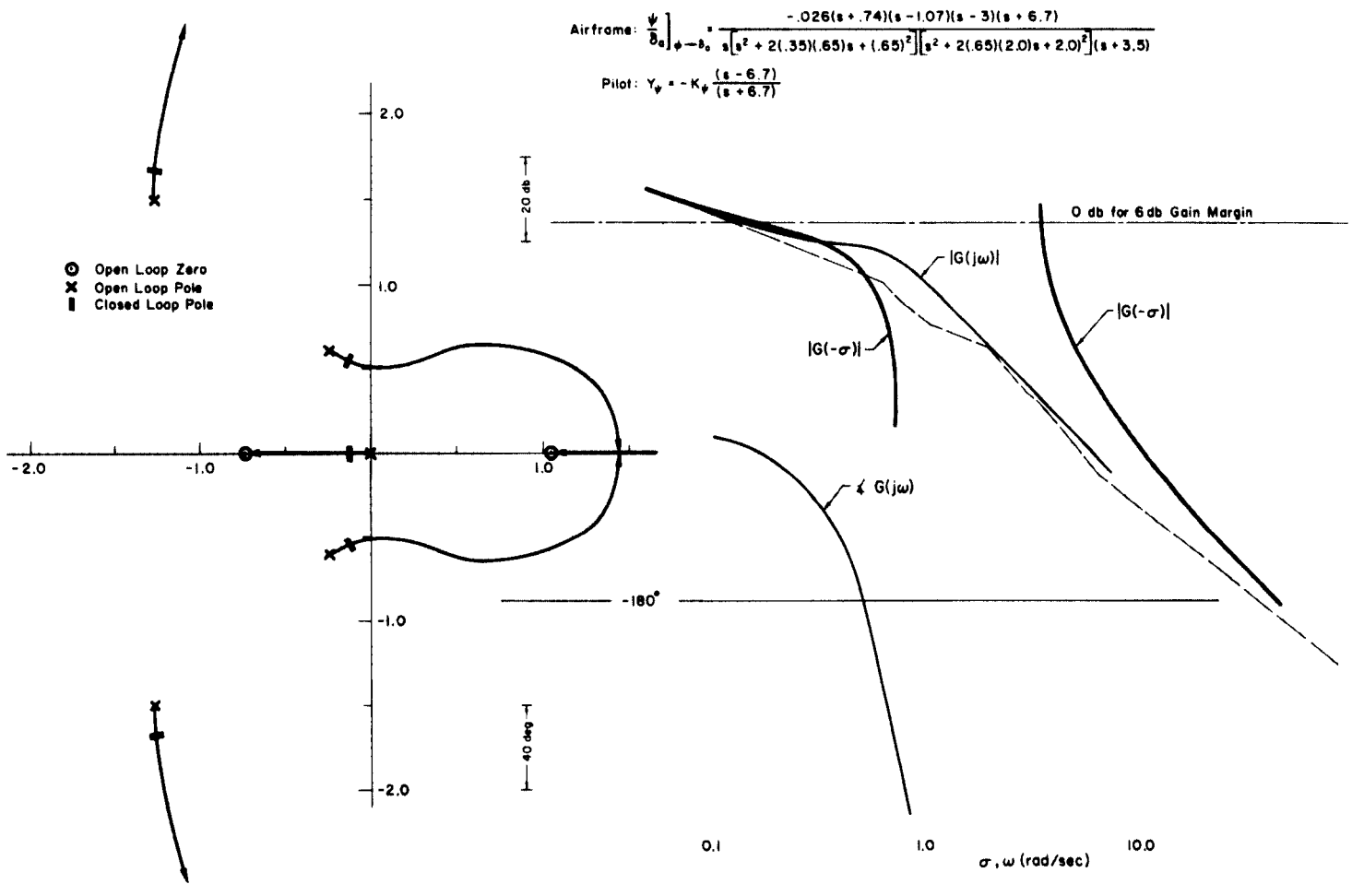

Figure 6. Subsonic Jet, Heading Closure

$$\text{Airframe: } \frac{r}{\delta_r} = \frac{-.38\,(s + 1.13)\left[s^2 + 2(-.0035)(.40)s + (.40)^2\right]}{(s - .011)(s + 1.14)\left[s^2 + 2(.10)(.82)s + (.82)^2\right]}$$

$$\text{Pilot: } Y_r = -K_r \frac{(s - 6.7)}{(s + 6.7)}$$

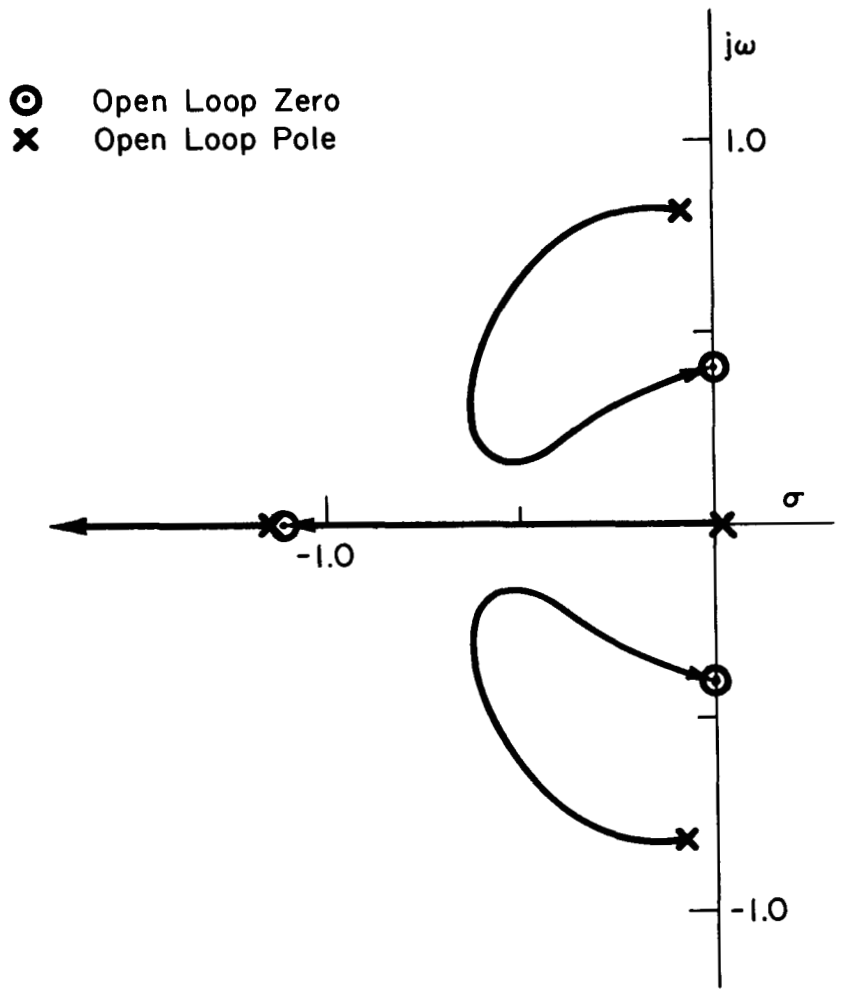

Figure 7. Subsonic Jet, Yaw-Rate Closure

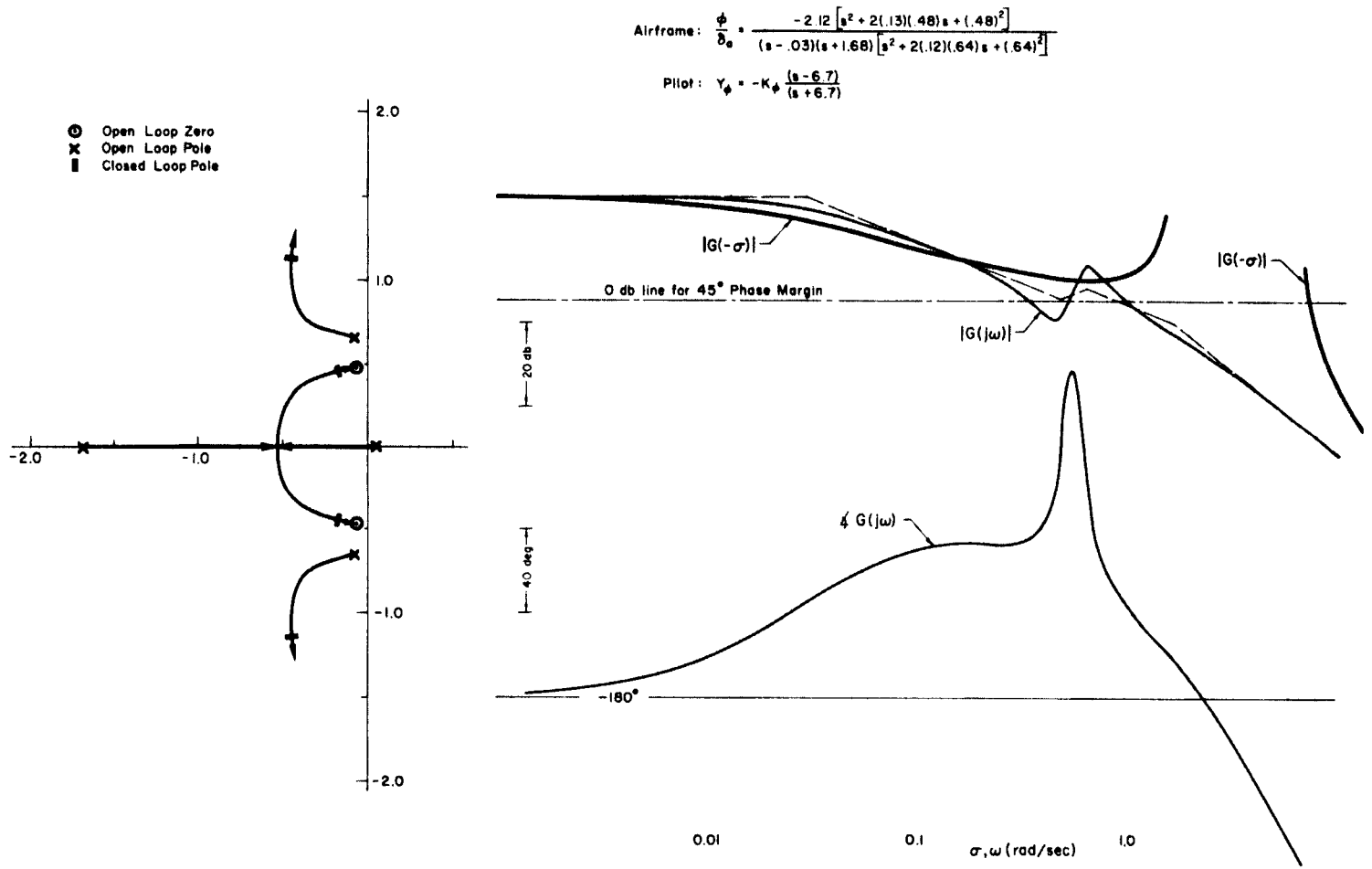

Figure 8. SCAT 16, Bare Airplane, Bank-Angle Closure

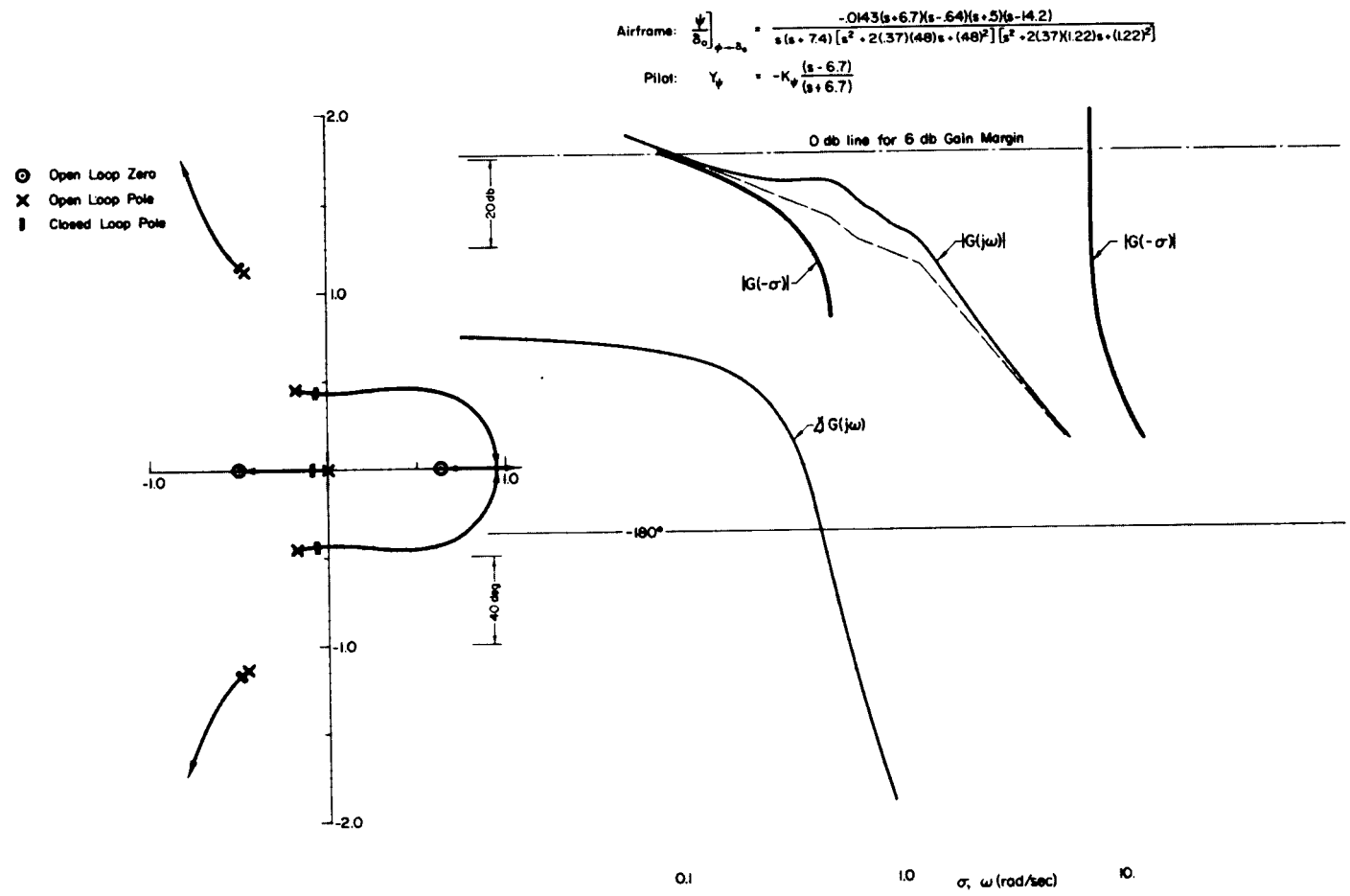

Figure 9. SCAT 16, Bare Airplane, Heading Closure

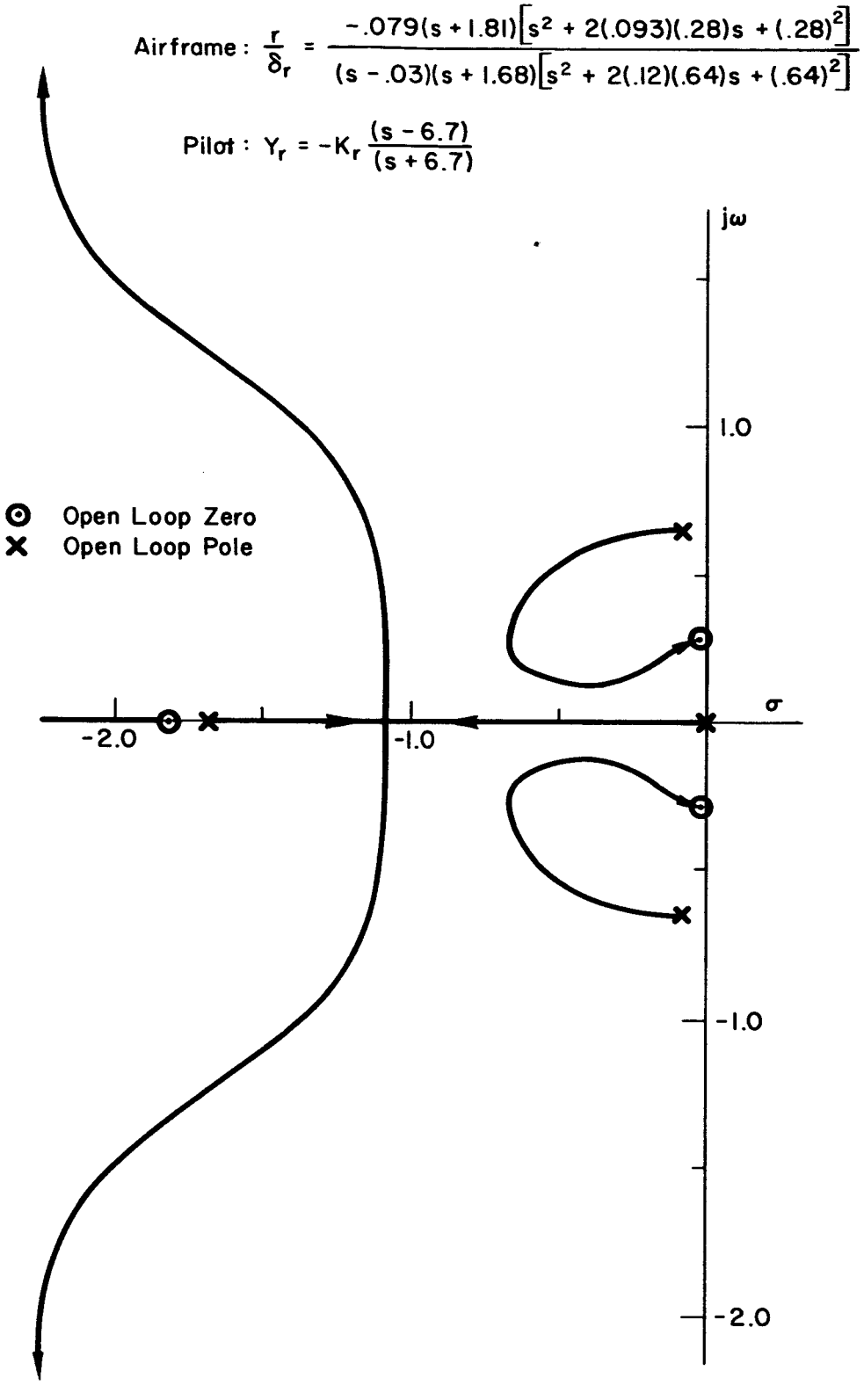

Figure 10. SCAT 16, Bare Airplane, Yaw-Rate Closure

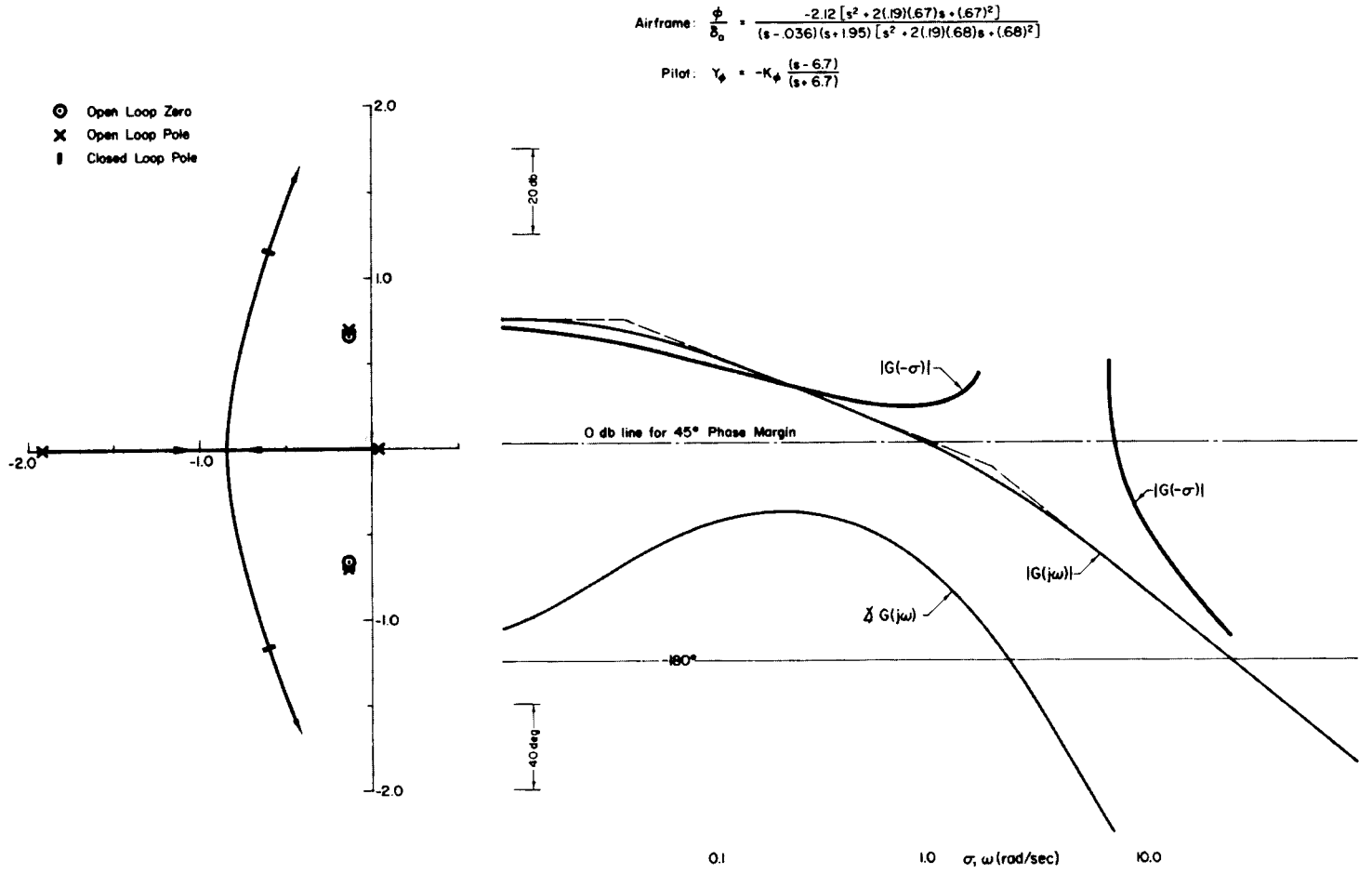

Figure 11. SCAT 16, Tested Augmentation, Bank-Angle Closure

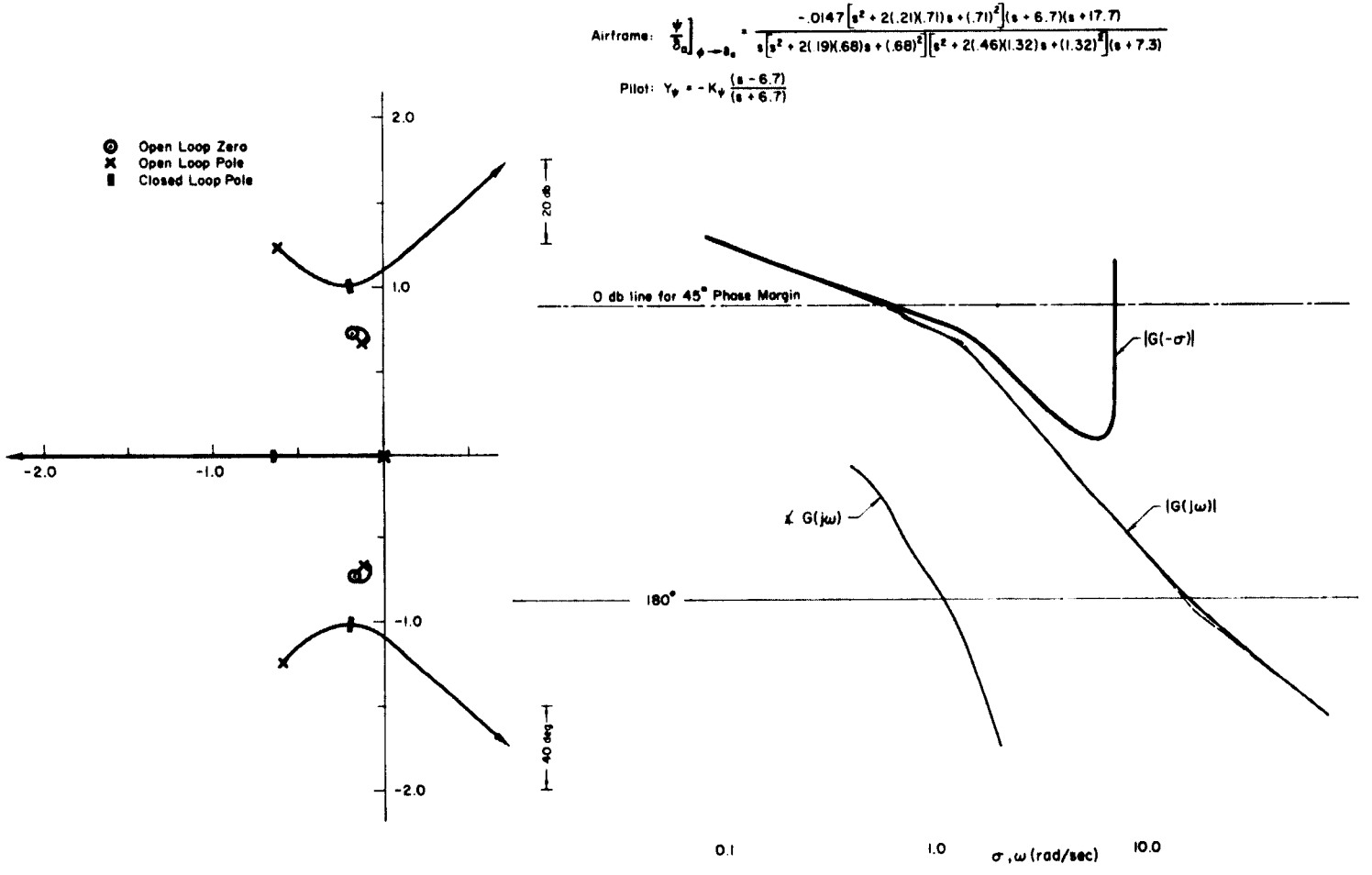

Figure 12. SCAT 16, Tested Augmentation, Heading Closure

$$\text{Airframe: } \frac{r}{\delta_r} = \frac{-.079(s+1.8)\left[s^2 + 2(.093)(.28)s + (.28)^2\right]}{(s-.036)(s+1.95)\left[s^2 + 2(.19)(.68)s + (.68)^2\right]}$$

$$\text{Pilot: } Y_r = -K_r \frac{(s-6.7)}{(s+6.7)}$$

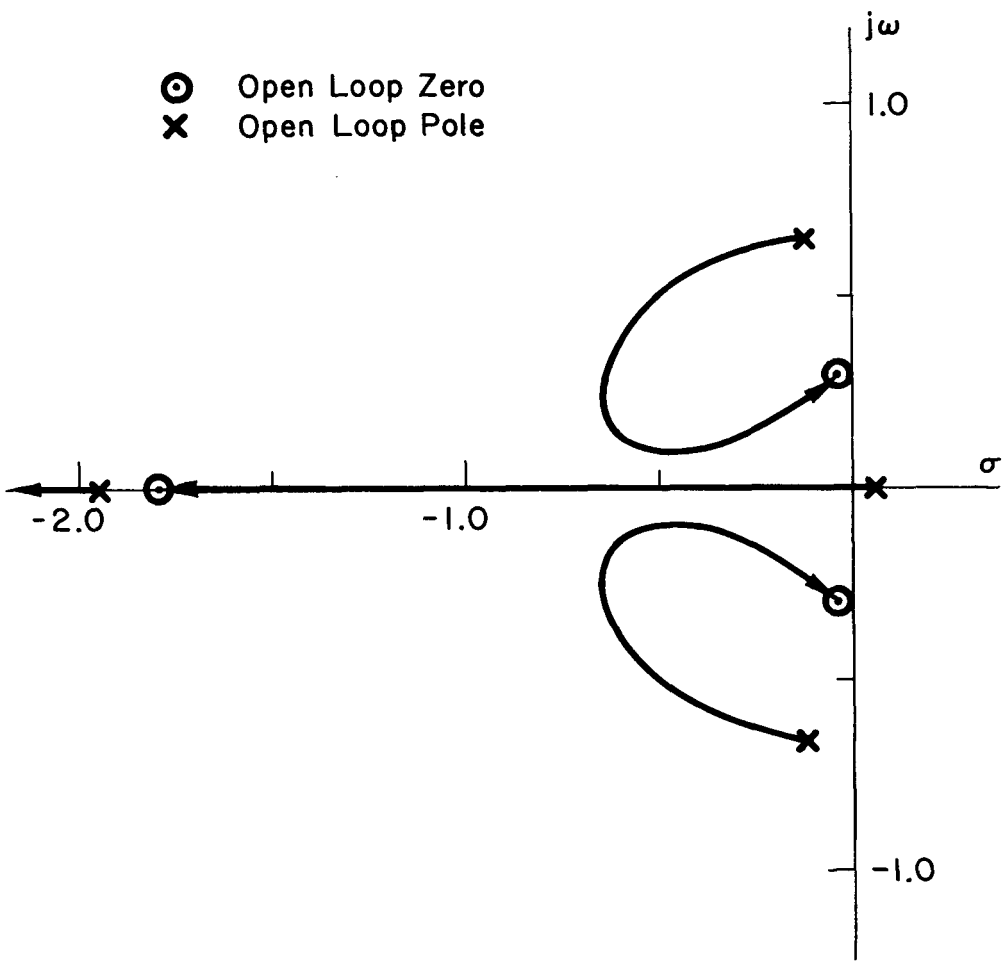

Figure 13. SCAT 16, Tested Augmentation, Yaw-Rate Closure

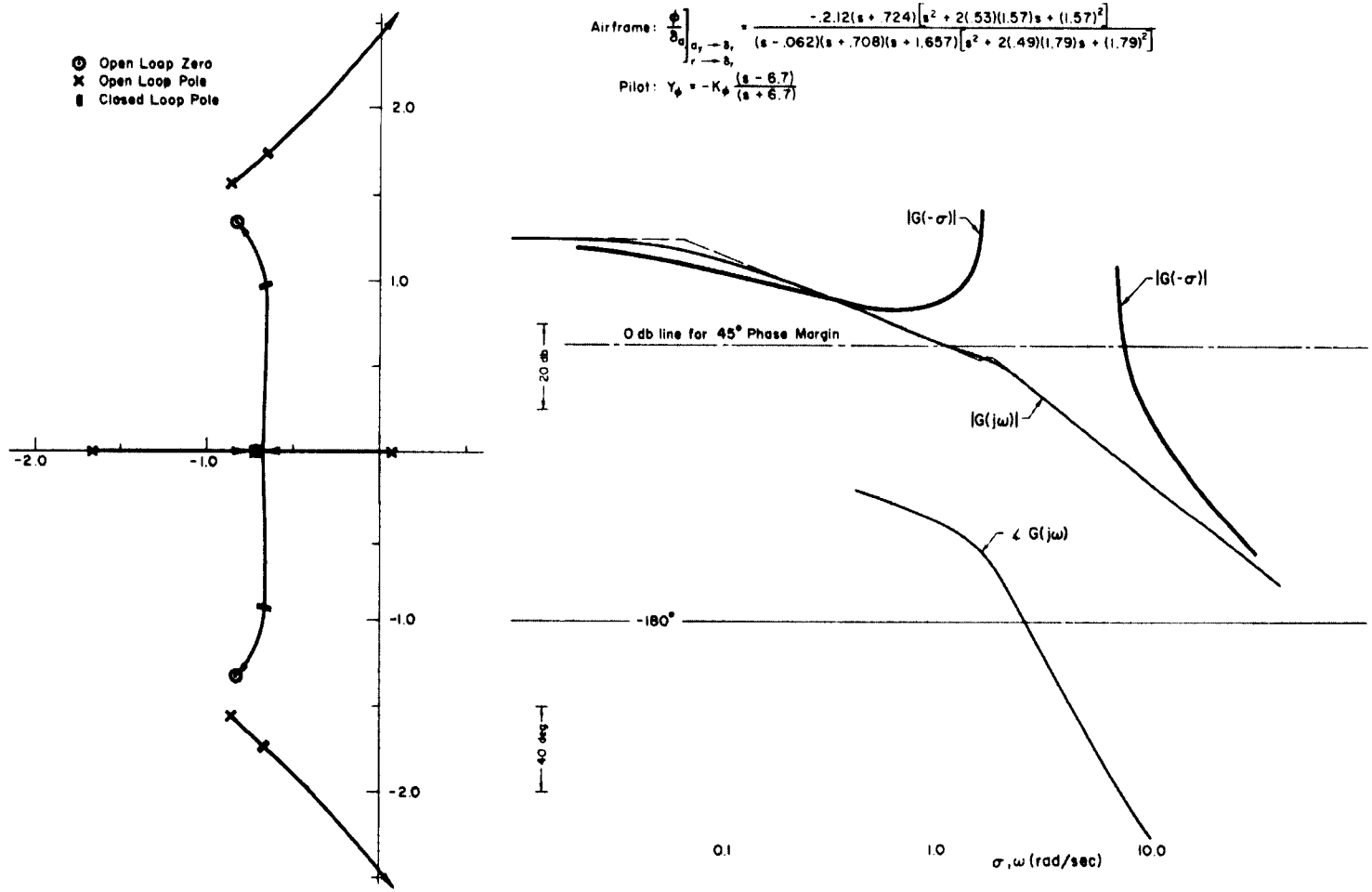

Figure 15. SCAT 16, Alternate Augmentation, Bank-Angle Closure

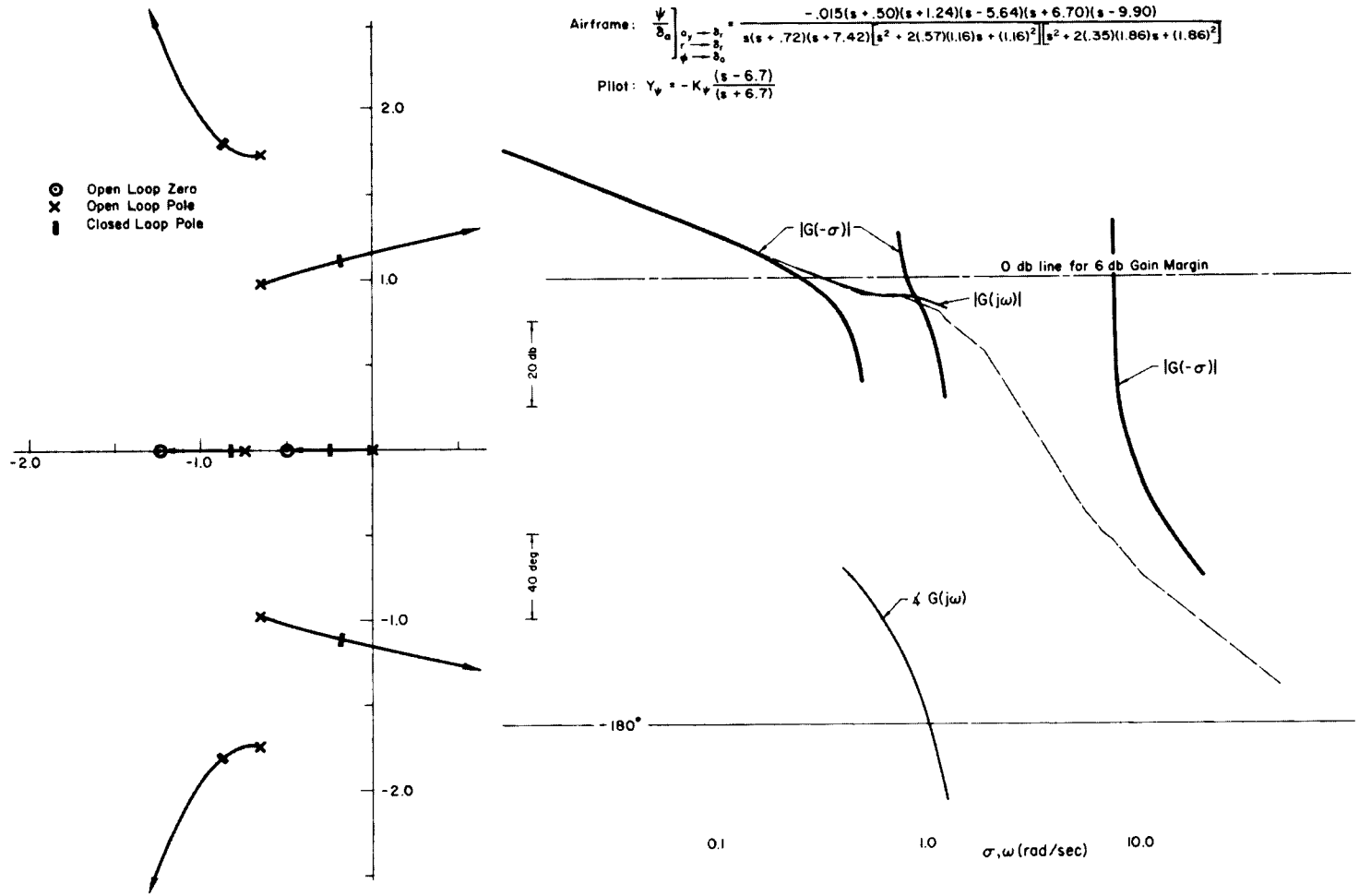

Figure 16. SCAT 16, Alternate Augmentation, Heading Closure

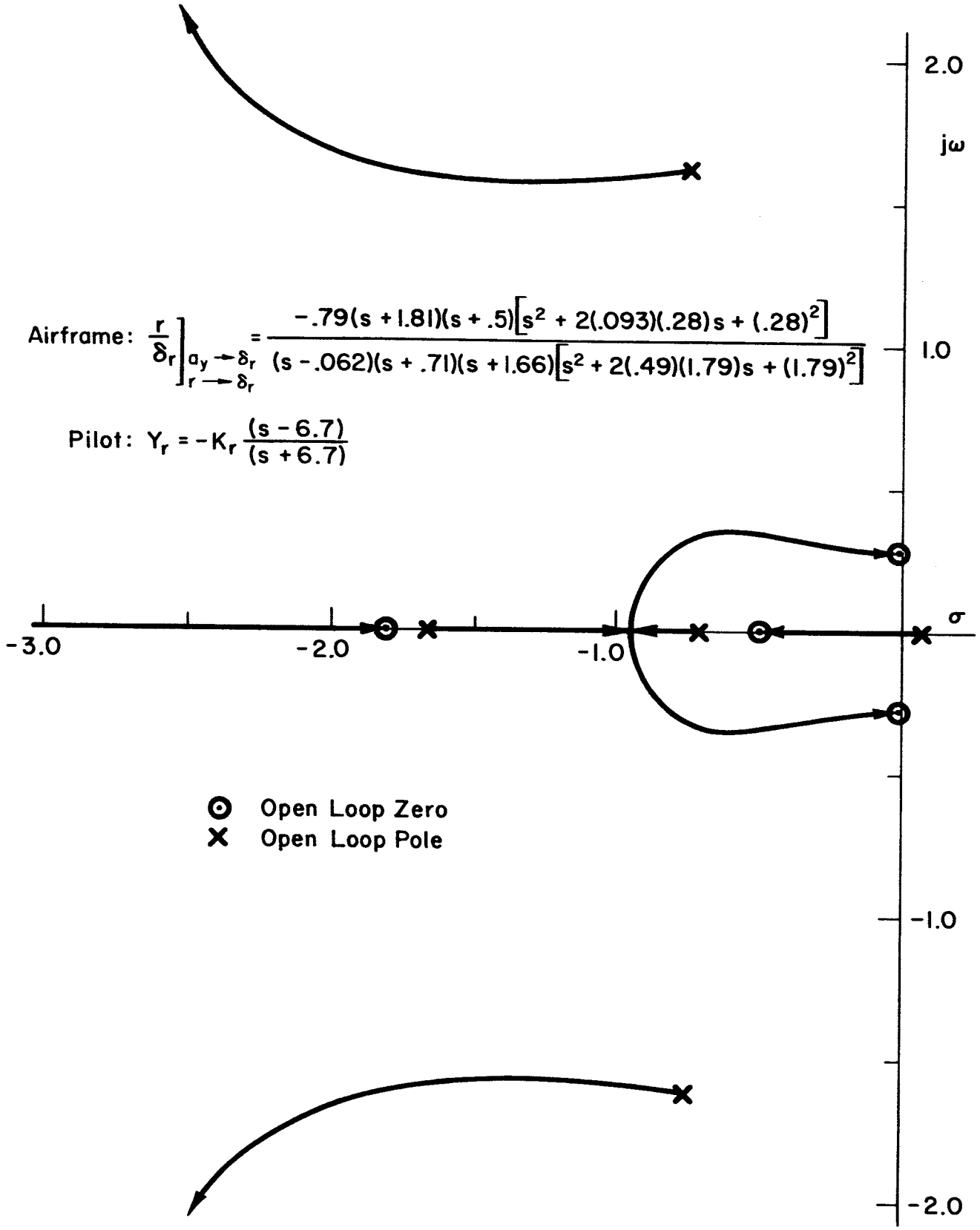

Figure 17. SCAT 16, Alternate Augmentation, Yaw-Rate Closure

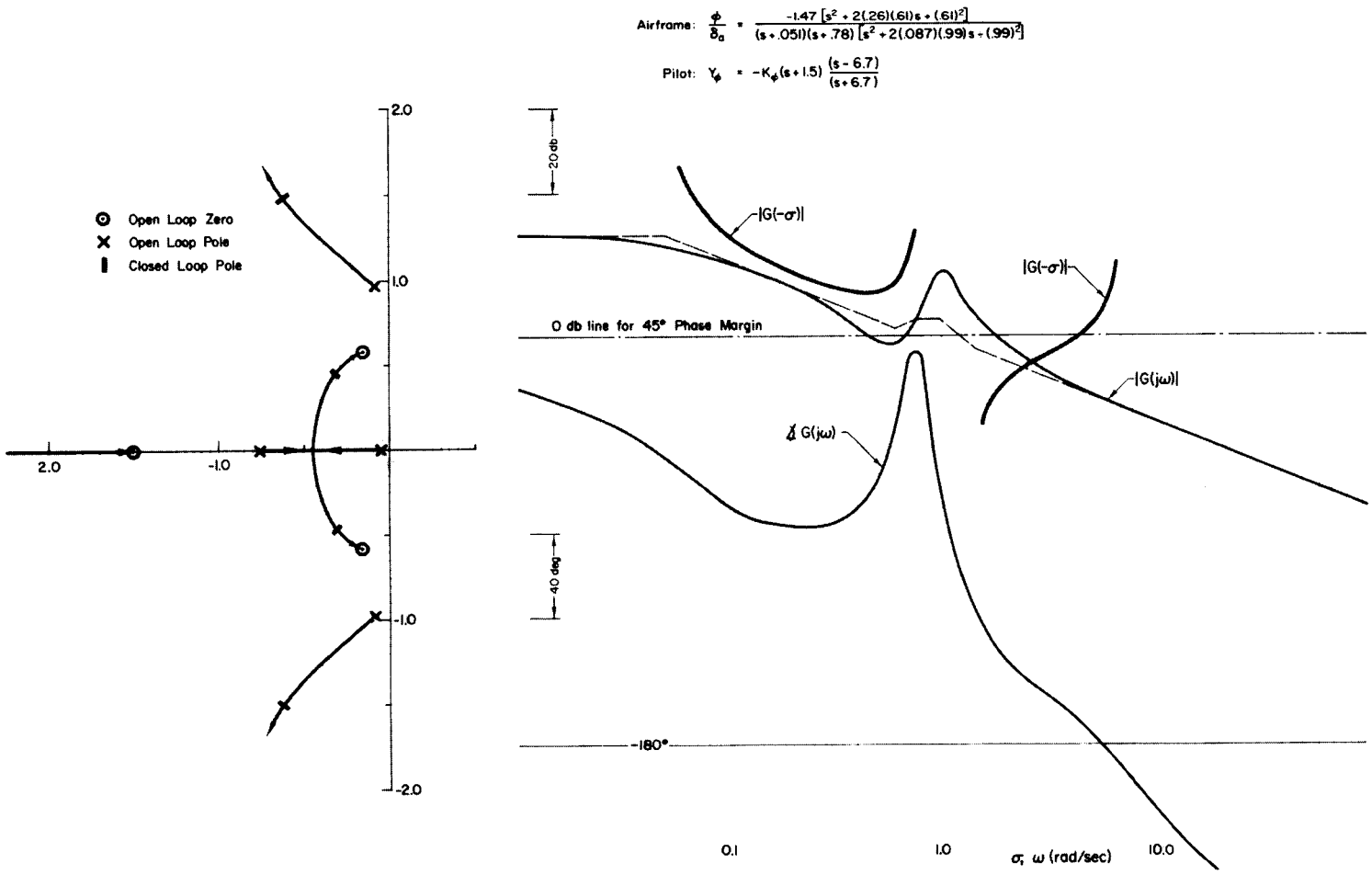

Figure 18. SCAT 17A, Bare Airplane, Bank-Angle Closure

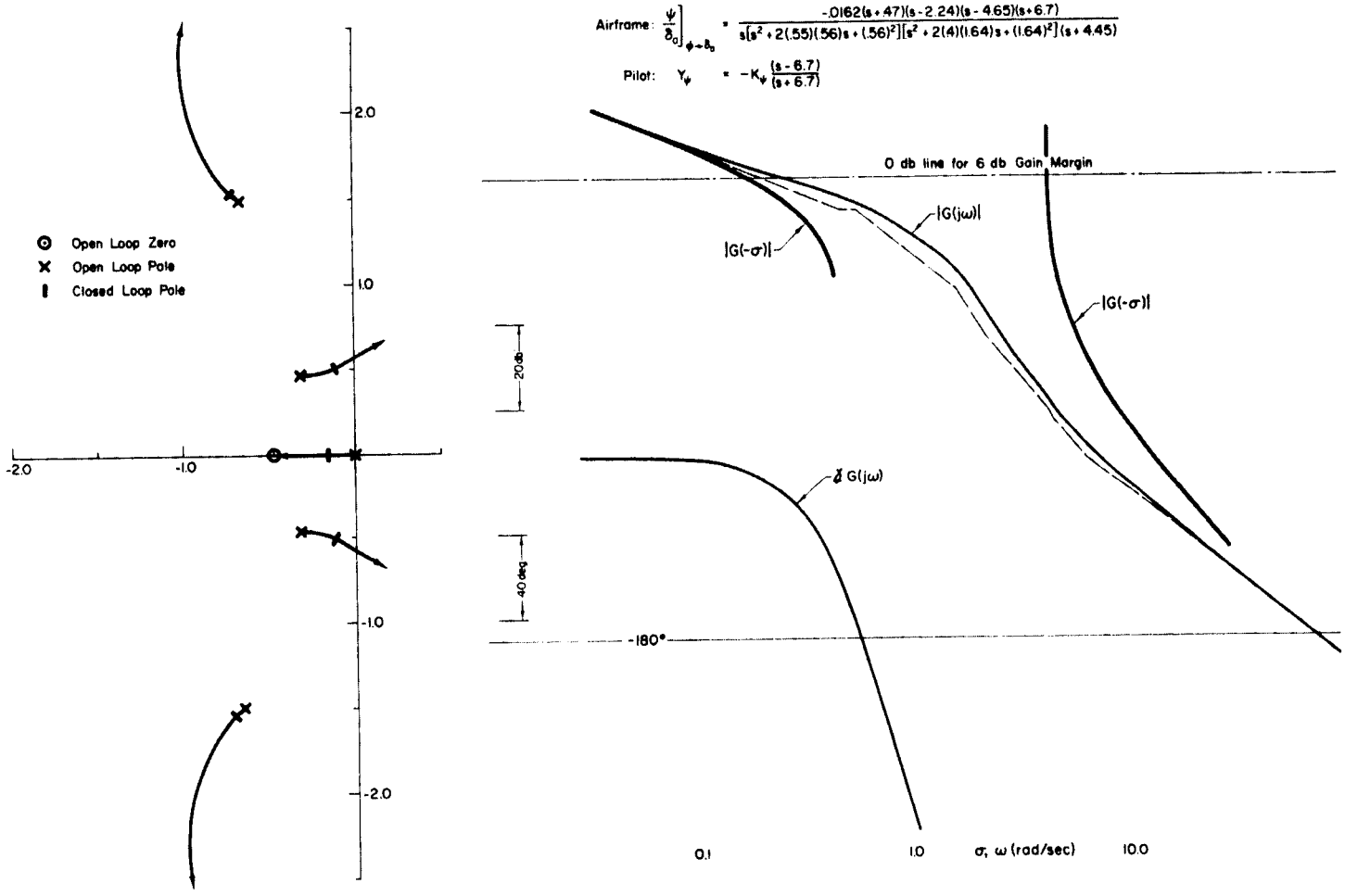

Figure 19. SCAT 17A, Bare Airplane, Heading Closure

$$\text{Airframe: } \frac{r}{\delta_r} = \frac{-.23(s + .76)\left[s^2 + 2(.025)(.60)s + (.60)^2\right]}{(s + .051)(s + .78)\left[s^2 + 2(.087)(.99)s + (.99)^2\right]}$$

$$\text{Pilot: } Y_r = -K_r \frac{(s - 6.7)}{(s + 6.7)}$$

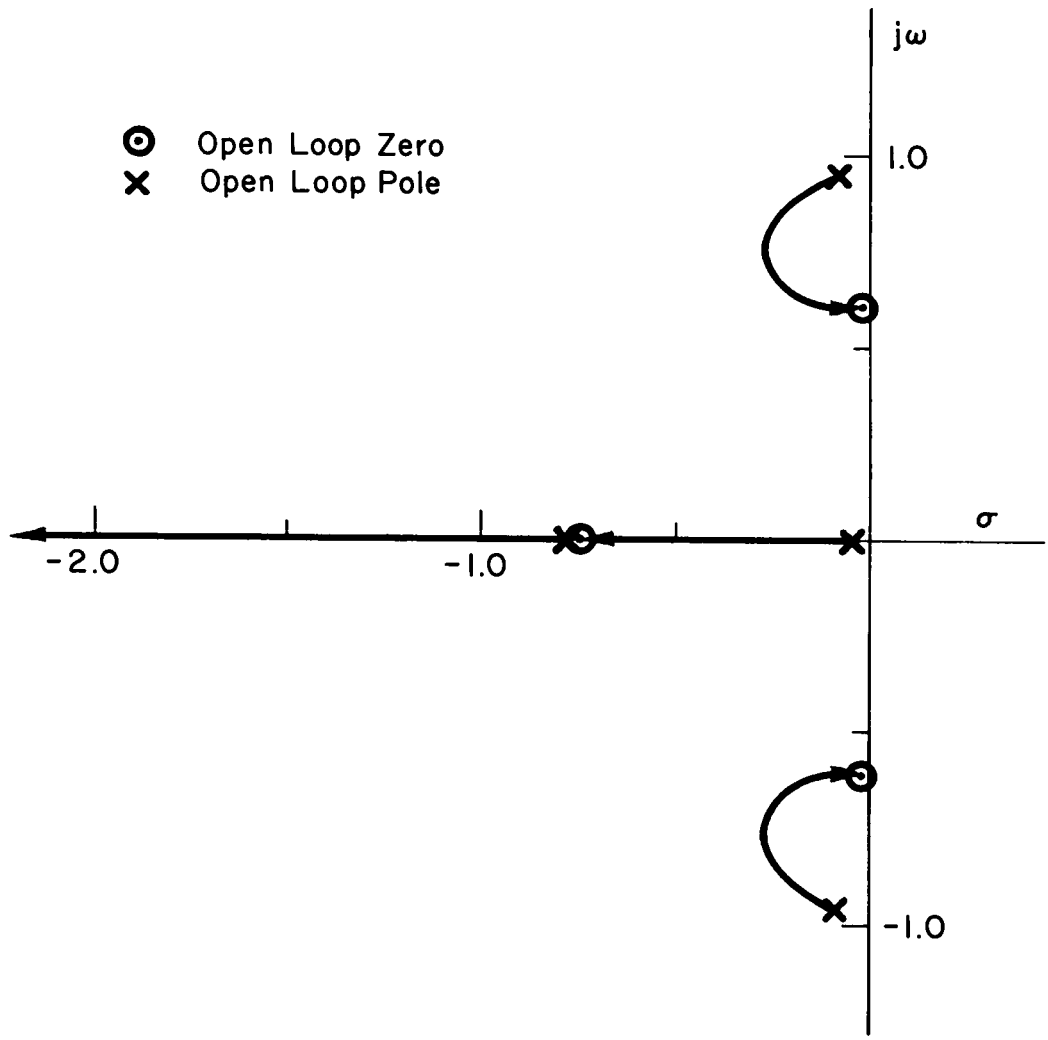

Figure 20. SCAT 17A, Bare Airplane, Yaw-Rate Closure

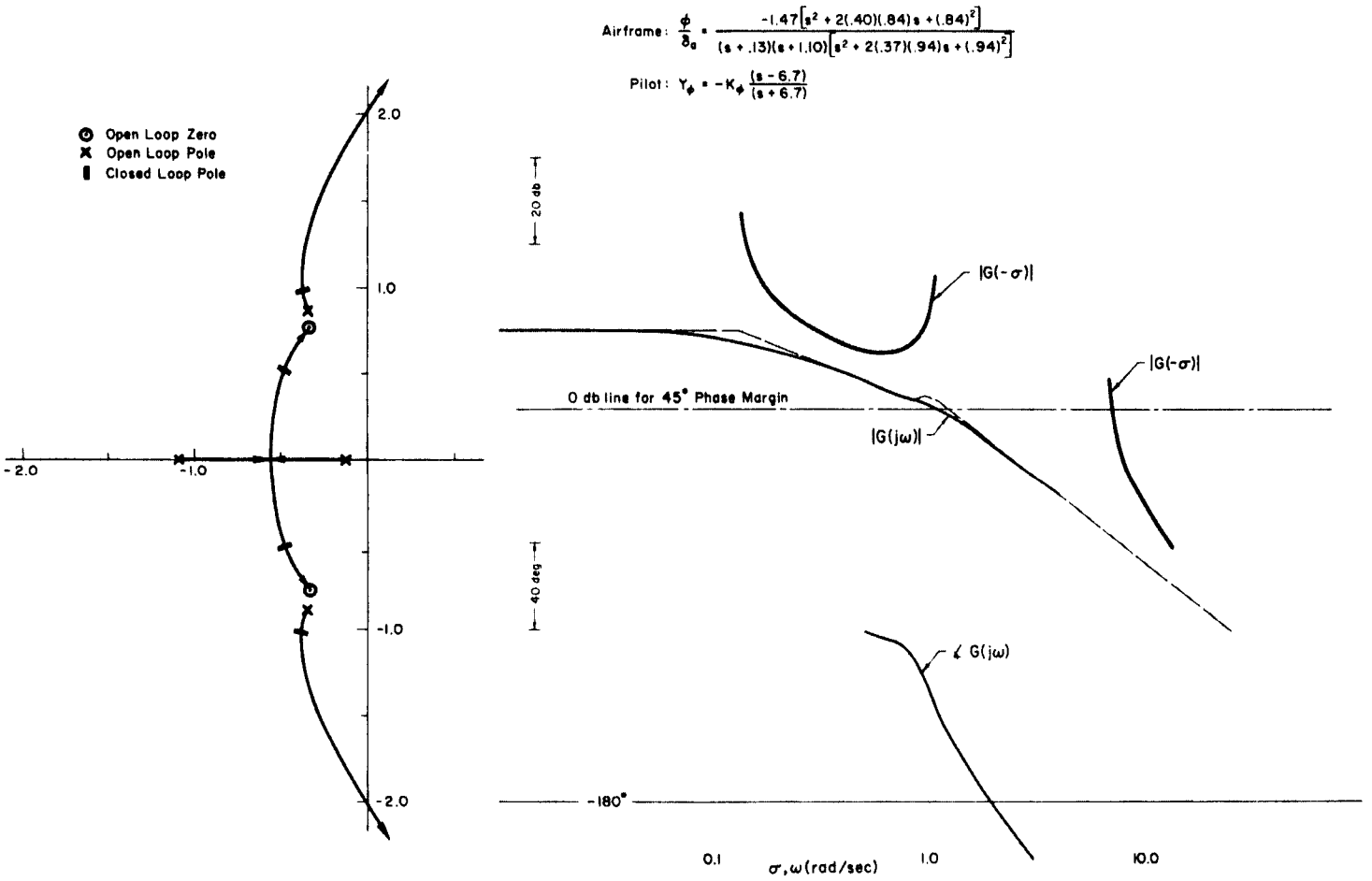

Figure 21. SCAT 17A, Tested Augmentation, Bank-Angle Closure

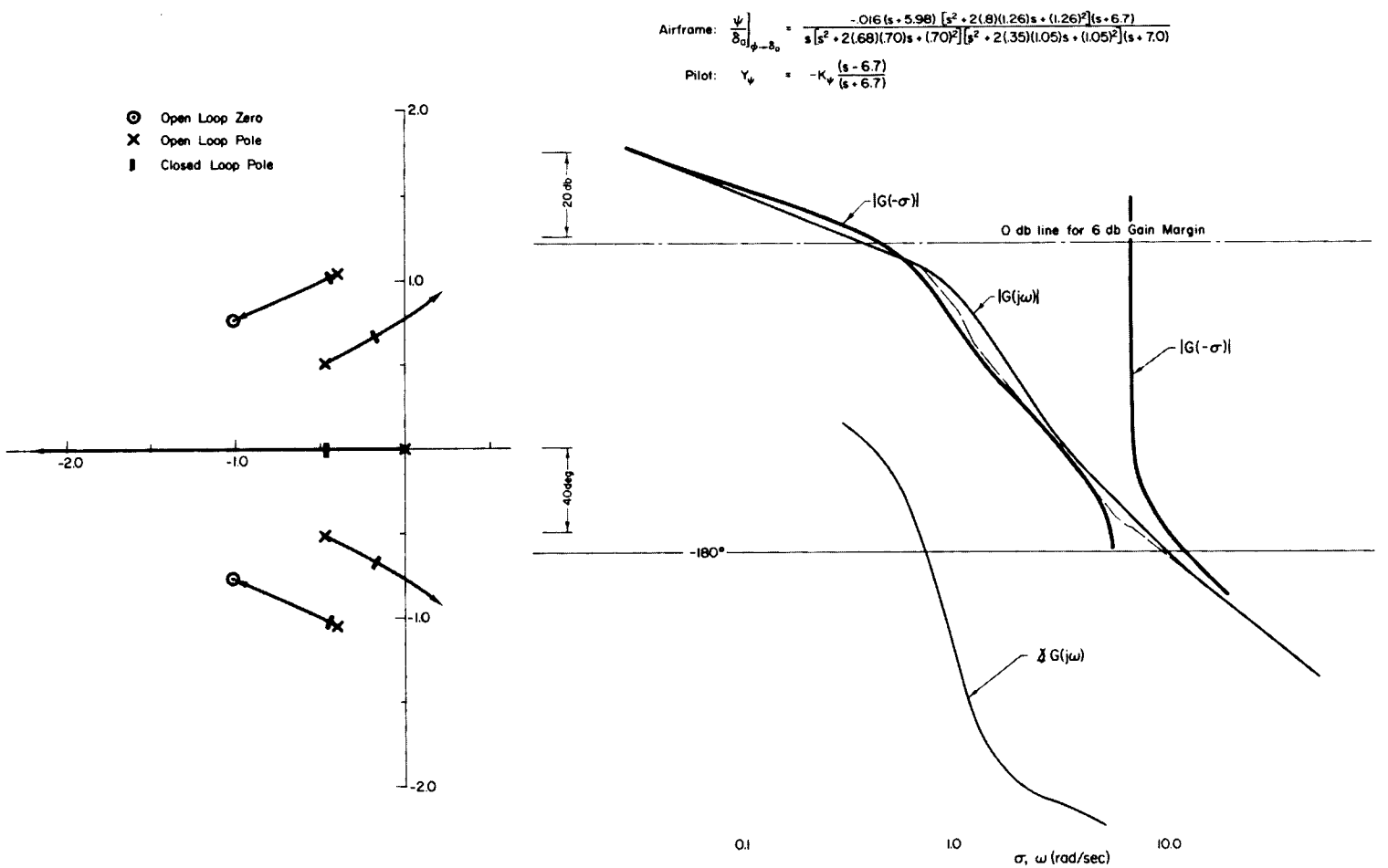

Figure 22. SCAT 17A, Tested Augmentation, Heading Closure

$$\text{Airframe: } \frac{r}{\delta_r} = \frac{-.23(s + 1.1)\left[s^2 + 2(.065)(.34)s + (.34)^2\right]}{(s + .13)(s + 1.1)\left[s^2 + 2(.37)(.94)s + (.94)^2\right]}$$

$$\text{Pilot: } Y_r = -K_r \frac{(s - 6.7)}{(s + 6.7)}$$

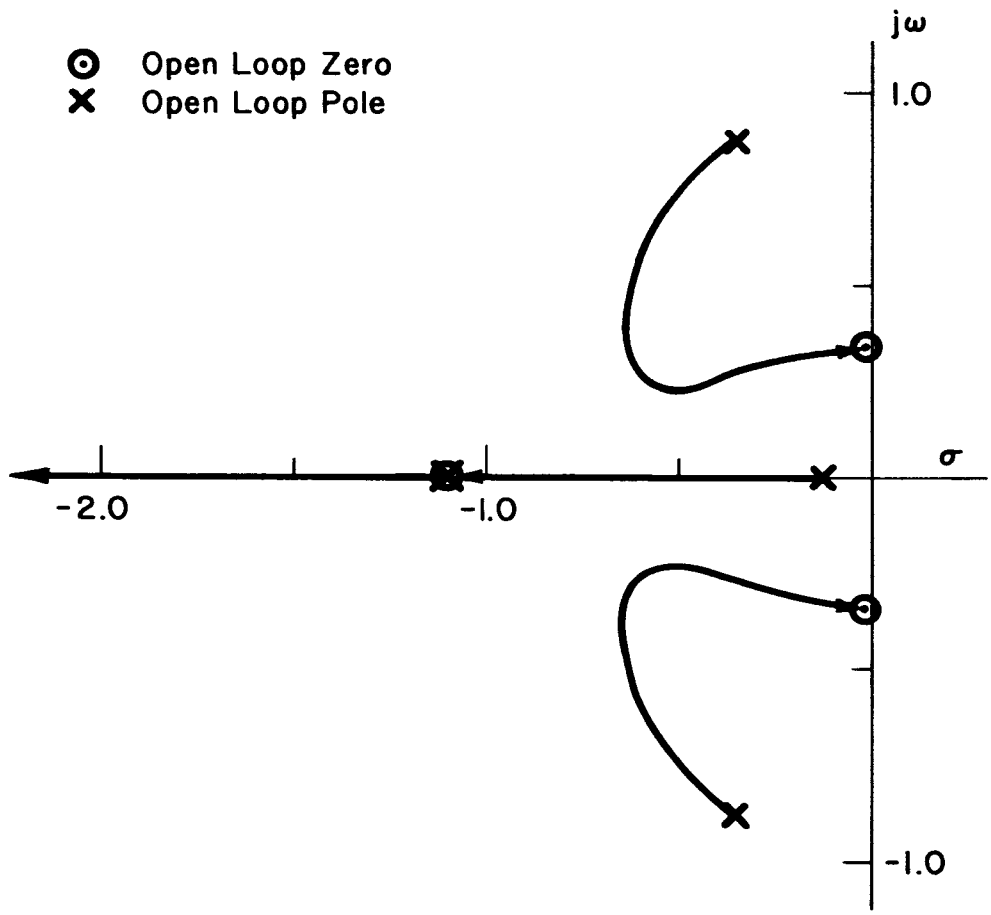

Figure 23. SCAT 17A, Tested Augmentation, Yaw-Rate Closure

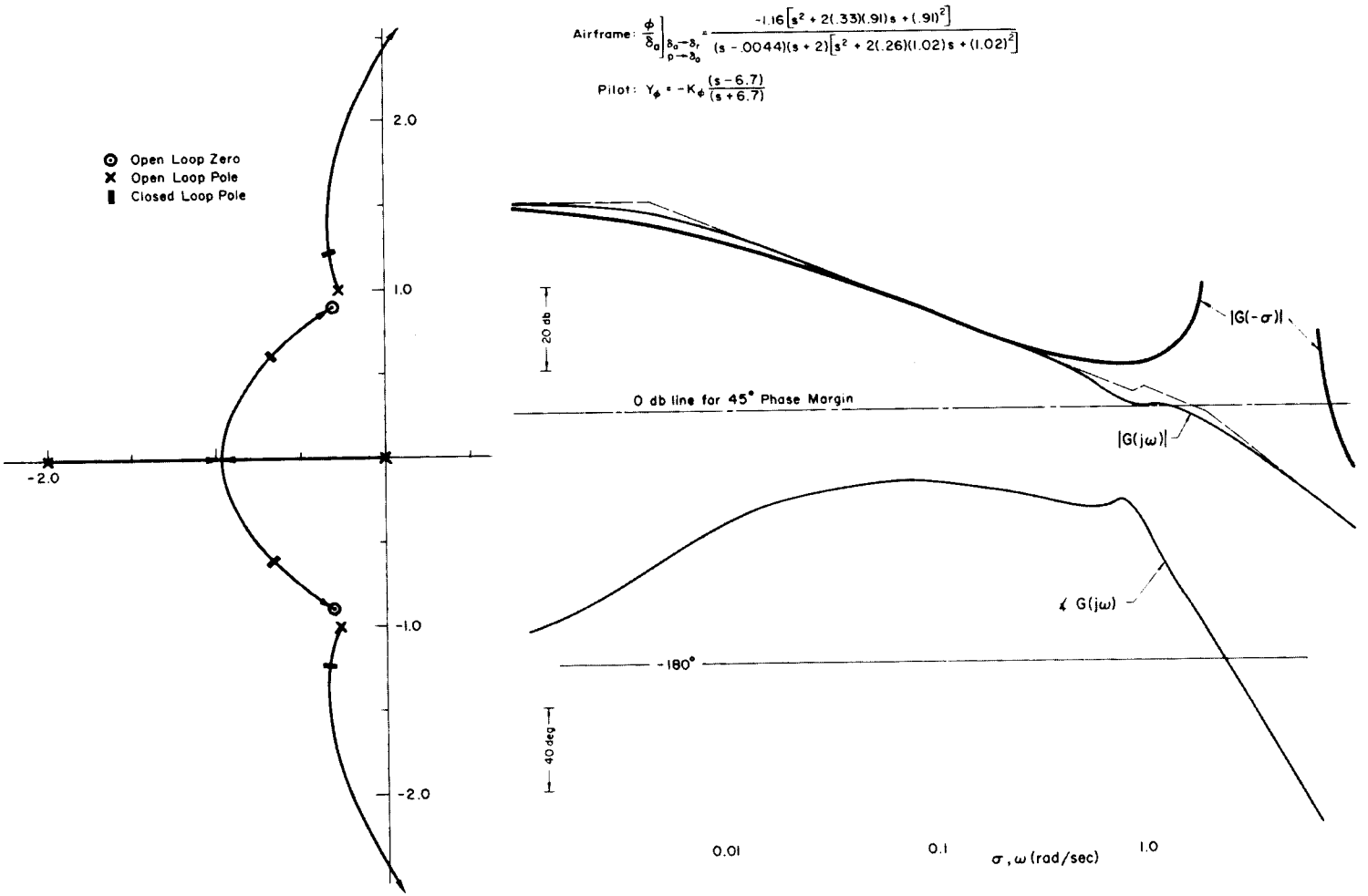

Figure 24. SCAT 17A, Alternate Augmentation, Bank-Angle Closure

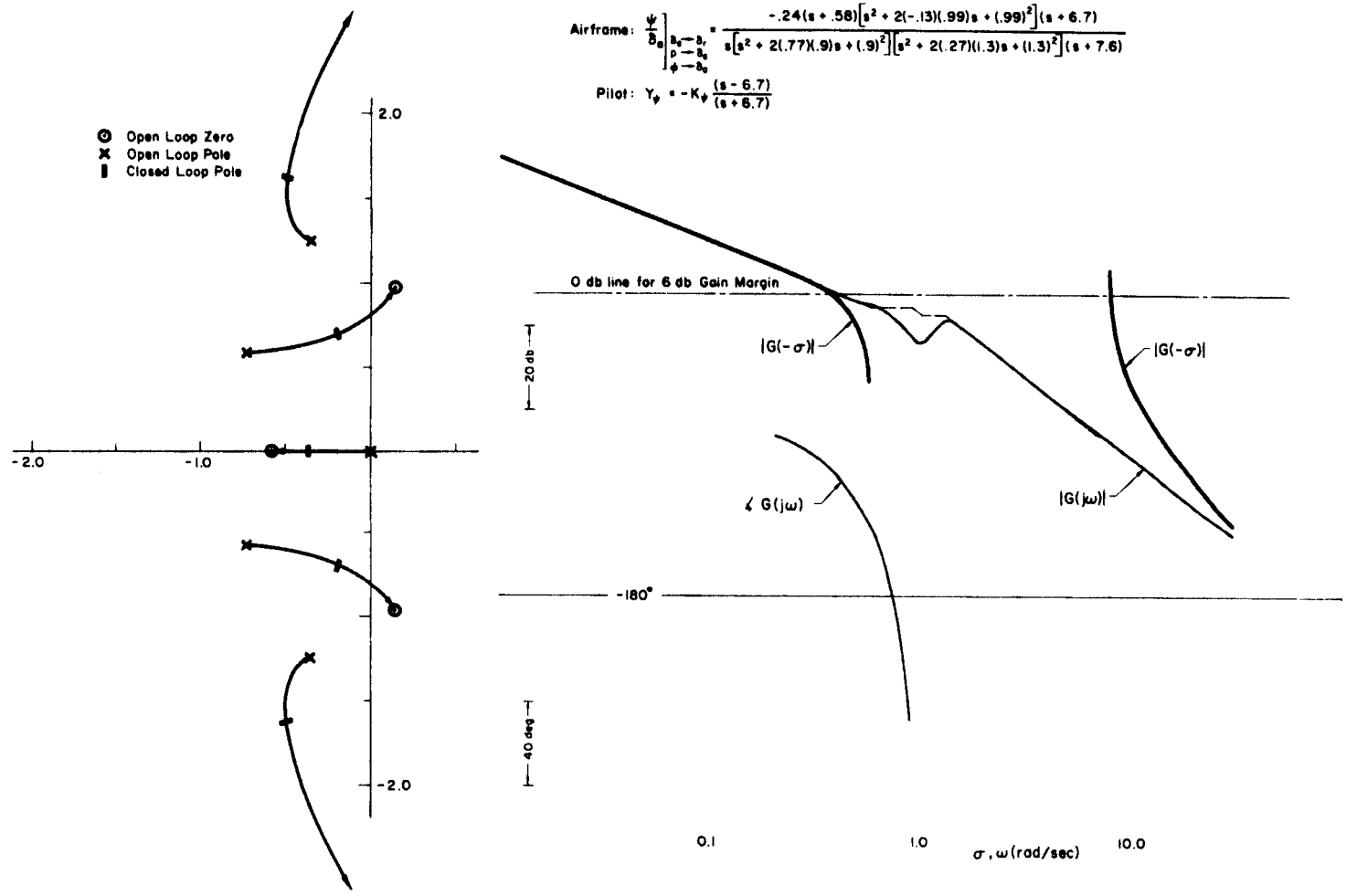

Figure 25. SCAT 17A, Alternate Augmentation, Heading Closure

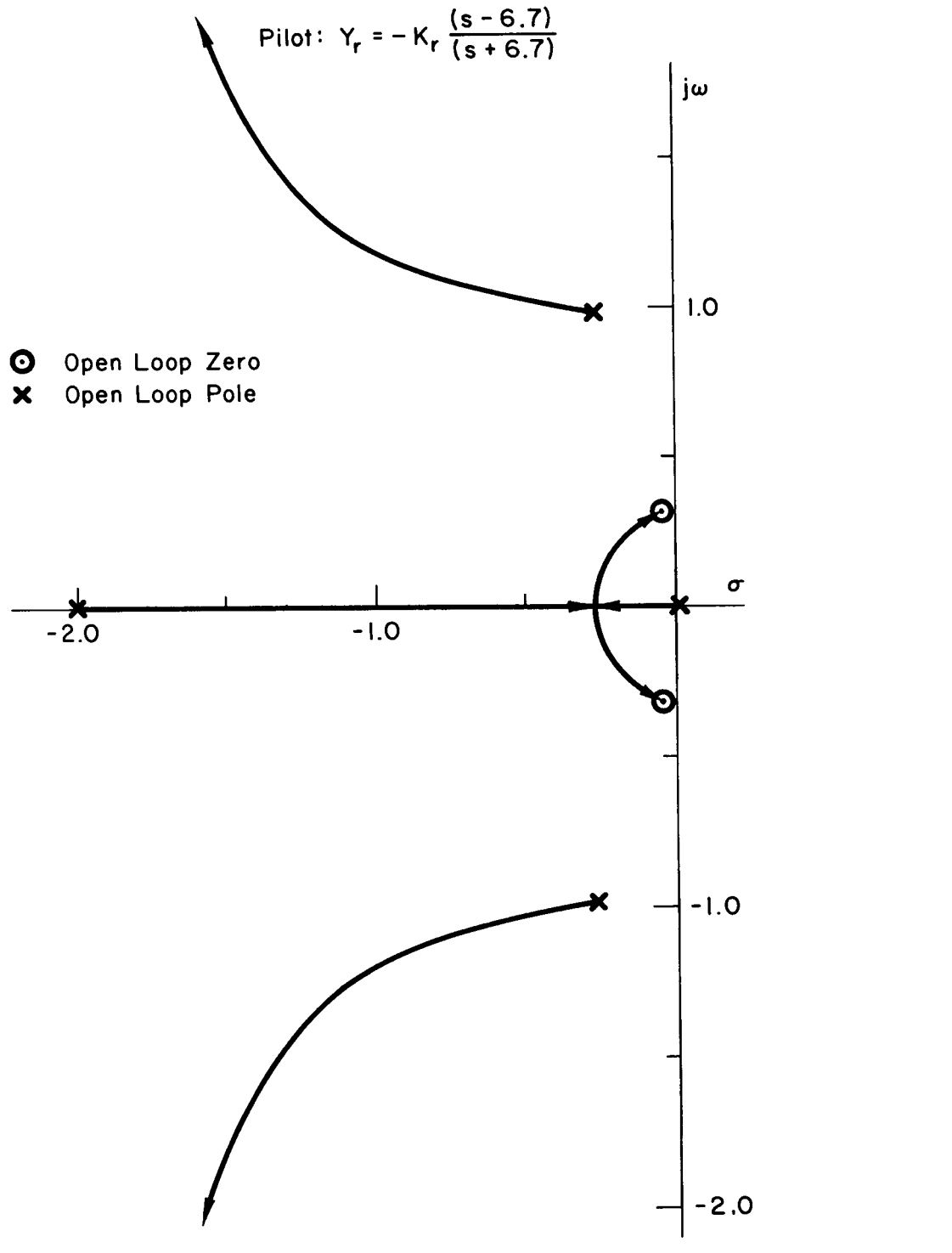

Figure 26. SCAT 17A, Alternate Augmentation, Yaw-Rate Closure

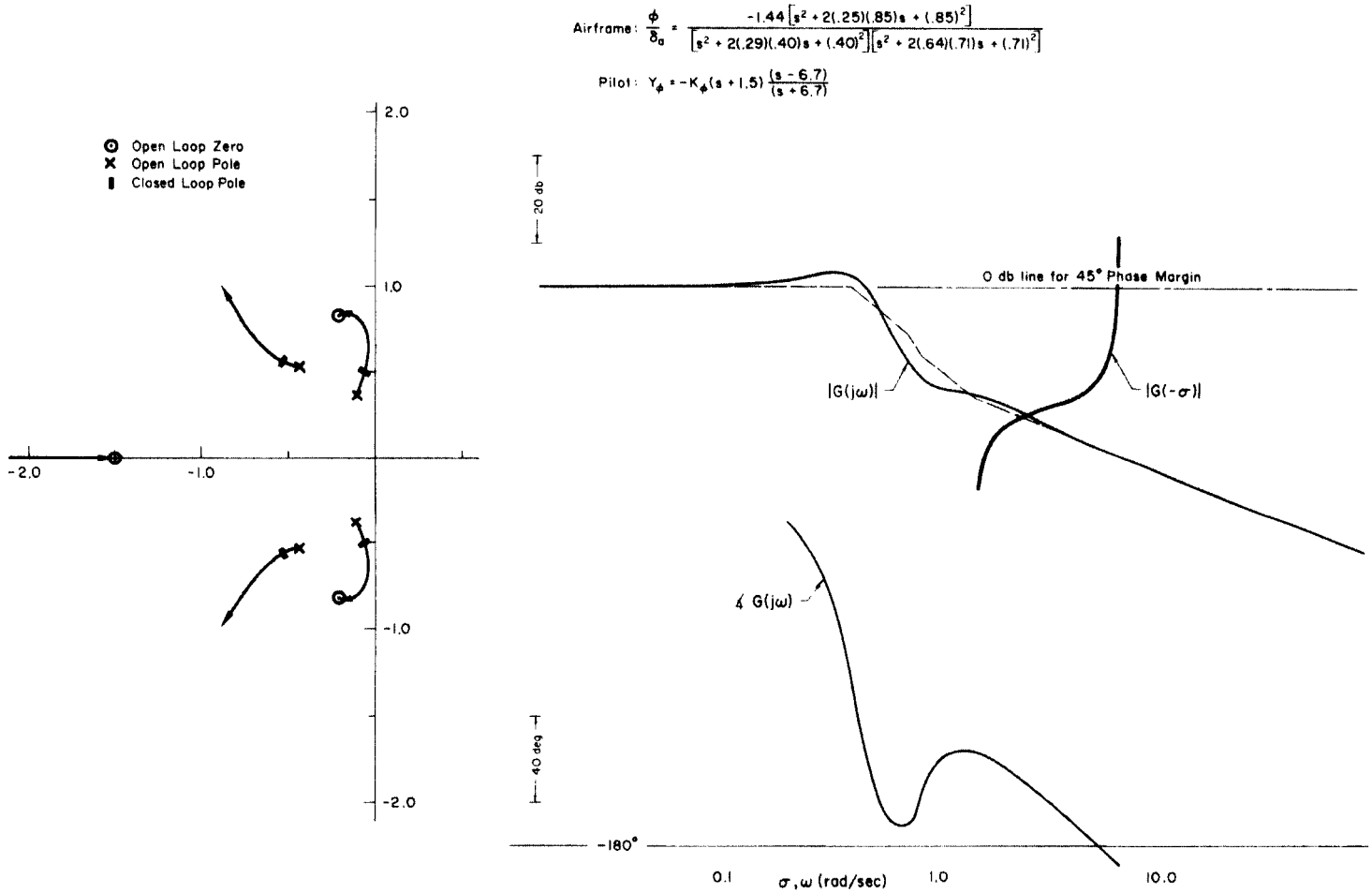

Figure 27. SCAT 17B, Bare Airplane, Bank-Angle Closure

$$\text{Airframe: } \frac{r}{\delta_r} = \frac{-.2\left[(s + .73)\left|s^2 + 2(-.11)(.60)s + (.60)^2\right.\right]}{\left[s^2 + 2(.29)(.4)s + (.4)^2\right]\left[s^2 + 2(.64)(.71)s + (.71)^2\right]}$$

$$\text{Pilot: } Y_r = -K_r \frac{(s - 6.7)}{(s + 6.7)}$$

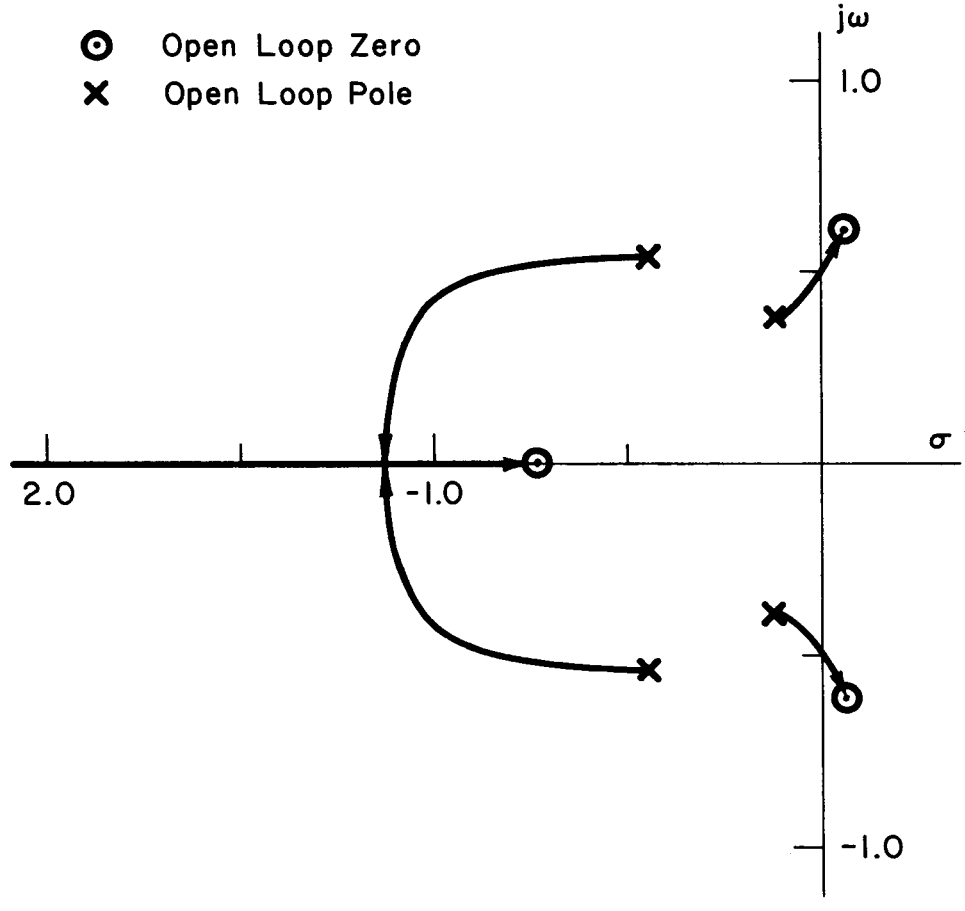

Figure 28. SCAT 17B, Bare Airplane, Yaw-Rate Closure

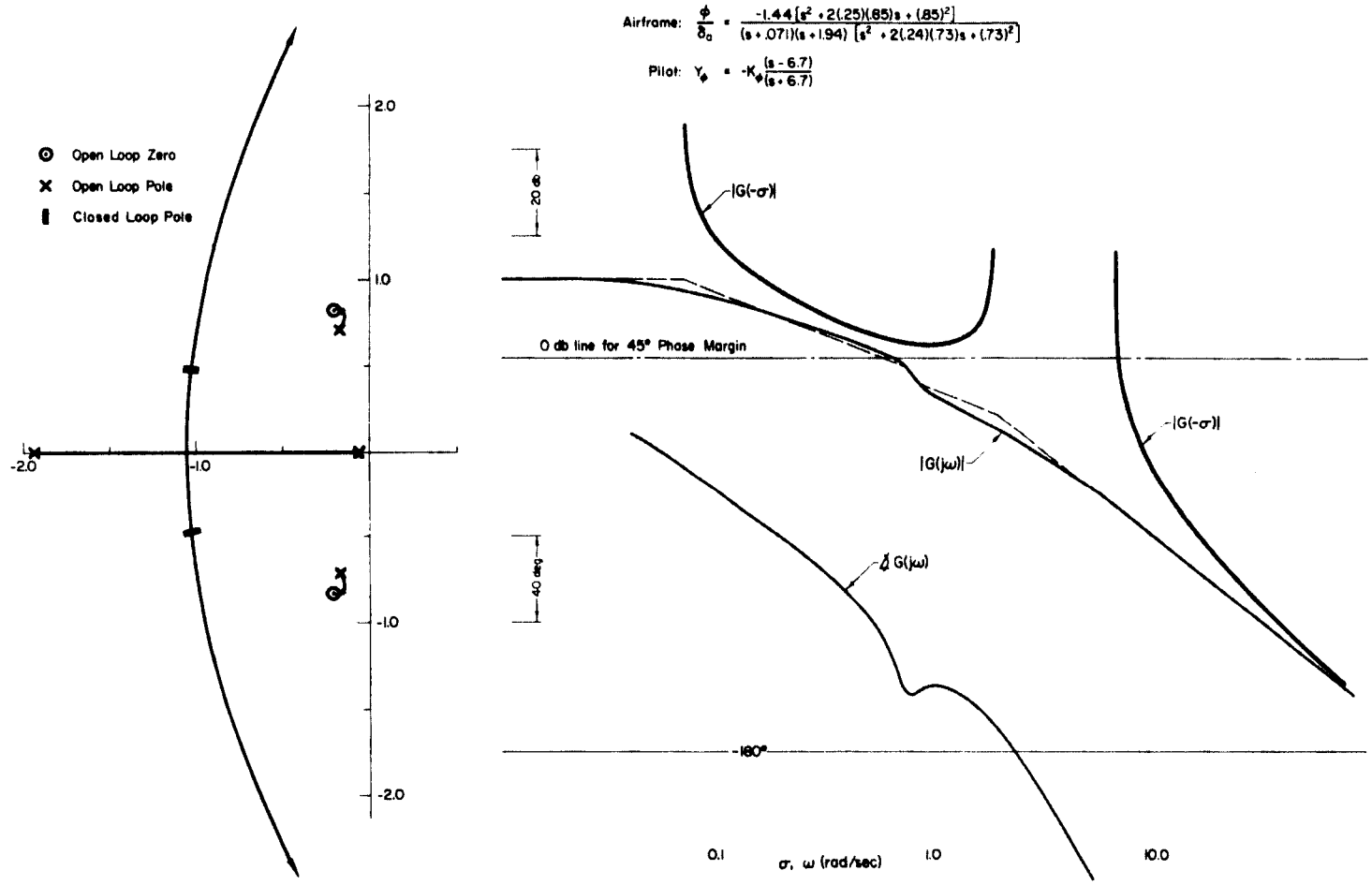

Figure 29. SCAT 17B, Tested Augmentation, Bank-Angle Closure

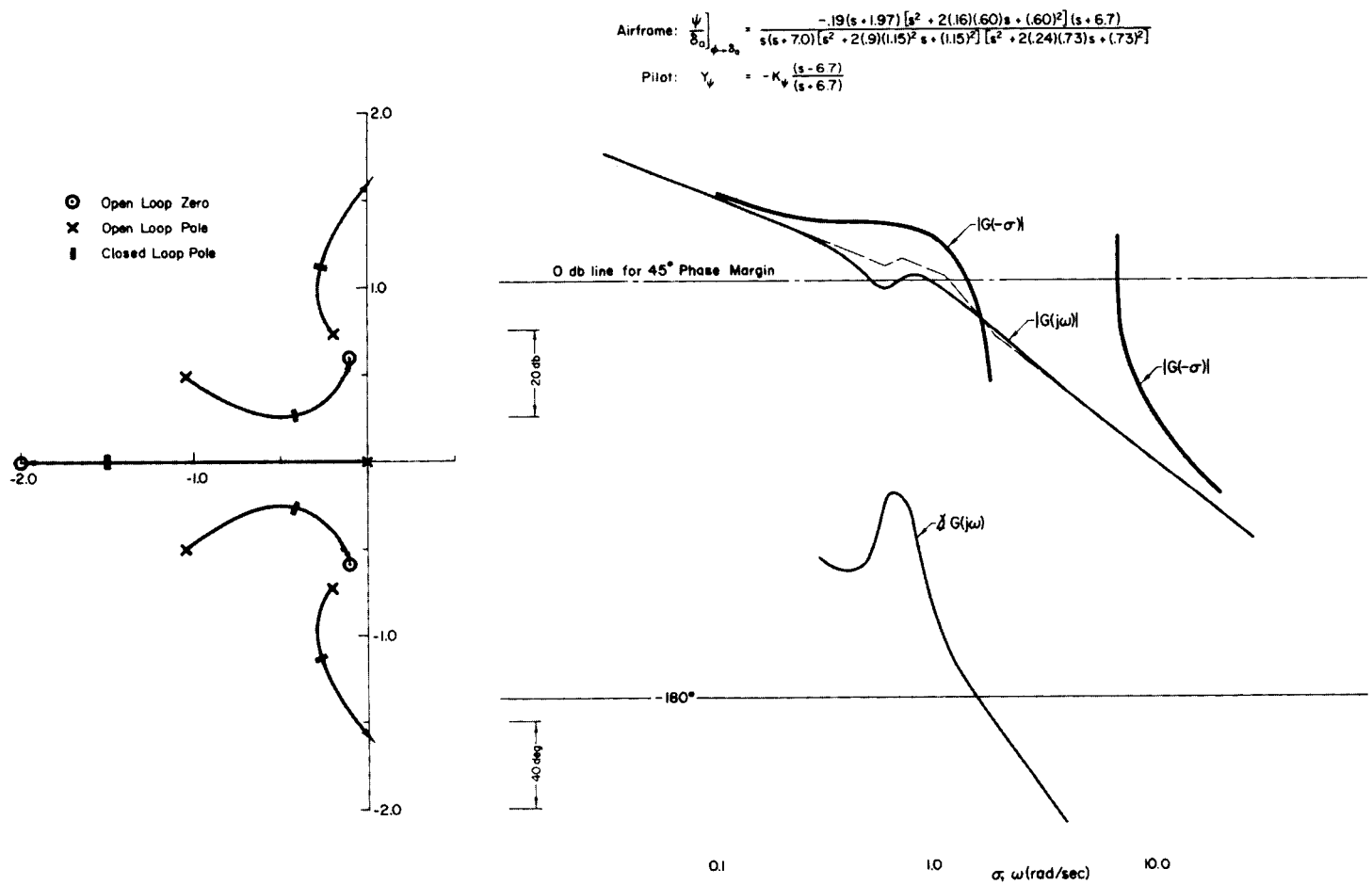

Figure 30. SCAT 17B, Tested Augmentation, Heading Closure

$$\text{Airframe: } \frac{r}{\delta_r} = \frac{-.215(s+1.94)\left[s^2 + 2(.122)(.37)s + (.37)^2\right]}{(s+.071)(s+1.94)\left[s^2 + 2(.24)(.73)s + (.73)^2\right]}$$

$$\text{Pilot: } Y_r = -K_r \frac{(s-6.7)}{(s+6.7)}$$

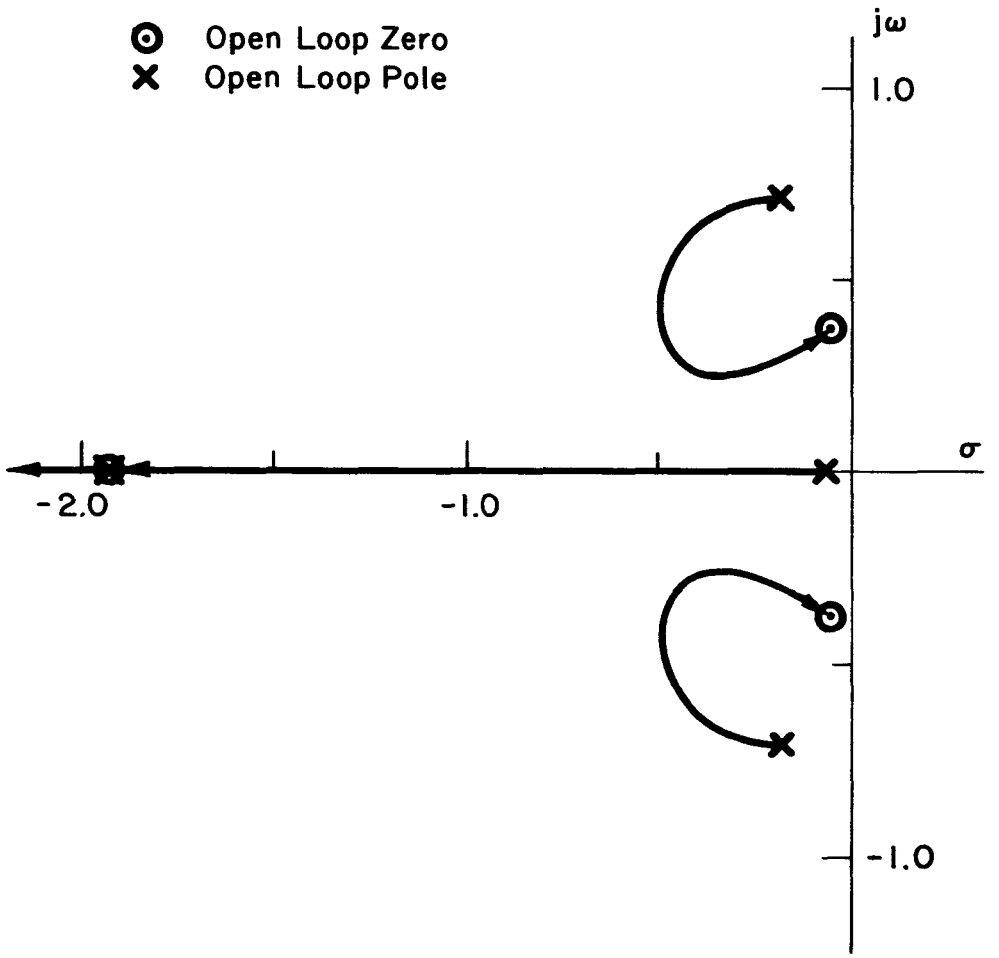

Figure 31. SCAT 17B, Tested Augmentation, Yaw-Rate Closure

J. DESIRABLE VALUES

From the comparison of the handling-quality factors for the several configurations tested and the correlations with pilot comments, preliminary estimates have been made of the desirable values for the various factors. This analysis indicates that the values necessary for a good pilot rating are:

1. $\varphi \rightarrow \delta_a$ closure: "Good" closure with pilot lead < 0.7 sec
2. $\psi \rightarrow \delta_a$ closure with $\varphi \rightarrow \delta_a$ inner loop: $\omega_{co} > 0.3$ rad/sec
3. $r \rightarrow \delta_r$ closure: $\zeta_{max} > 0.5$
4. $|\varphi/\beta|_{DR} < 1.5$
5. $(\delta_r/\delta_a)_0$
6. $(\dot{\delta}_r/\delta_a)_0$

   The magnitude of the sum of these two parameters should be less than 1
7. $|\delta_r/\varphi|_{ss} < 0.3$
8. $T_R < 1$ sec
9. $p_{max} > 10$ deg/sec
10. $|N'_{\delta_r}| > 0.2$ sec^{-2}
11. $|L'_\beta/L'_{\delta_a}| < 1$
12. $(\Delta\psi_{max})_{t=2 \text{ sec}} > 5$ deg

TABLE I

SUMMARY OF HANDLING-QUALITY FACTORS

CONFIGURATION	CLOSED-LOOP CONTROL			$\lvert\varphi/\beta\rvert_{DR}$	TURN COORDINATION			ROLL RESPONSE		DECRAB		
	$\varphi \rightarrow \delta_a$	ω_{to} (rad/sec)	$r \rightarrow \delta_r$		$(\delta_r/\delta_a)_0$ (2)	$(\dot{\delta}_r/\delta_a)_0$ (2) (sec^{-1})	$(\delta_r/\varphi)_{ss}$ (2)	T_R (sec)	p_{max} (1) (deg/sec)	N'_{δ_r} (sec^{-2})	L'_β/L'_{δ_a}	$(\Delta\psi_{max})_{t=2\ sec}$ (deg)
Subsonic jet	Good — Moderate pilot lead	0.12	Very good — $\zeta_{max} > 0.9$	1.4	0	0.6	-0.08	0.9	9	-0.38	1.3	9.8
SCAT 16 Bare airplane	Very good — No pilot lead	0.10	Very good — $\zeta_{max} > 0.9$	1.2	1.6	3.1	-0.10	0.6	10	-0.08	0.6	3.5
SCAT 16 Tested augmentation	Very good — No pilot lead	0.59	Very good — $\zeta_{max} > 0.9$	1.2	1.6	-2.1	-0.36	0.5	16	-0.08	0.7	3.0 (4)
SCAT 16 Alternate augmentation	Very good — No pilot lead	0.31	Very good — $\zeta_{max} > 0.7$	1.4	1.6	3.1	-0.10	0.6	15	-0.08	2.3 (5)	2.0 (4)
SCAT 17A Bare airplane	Good — Moderate pilot lead	0.20	Good — $\zeta_{max} = 0.35$	2.2	1.0	0.8	-0.18	1.2	11	-0.23	1.6	8.3
SCAT 17A Tested augmentation	Very good — No pilot lead	0.38	Very good — $\zeta_{max} = 0.9$	1.5	1.0	-0.1	-0.38	0.9	16 (3)	-0.23	1.3	5.5 (4)
SCAT 17A Alternate augmentation	Very good — No pilot lead	0.42	Very good — $\zeta_{max} > 0.6$	1.2	0 (2)	0.8	-0.31	0.5	7 (3)	-0.23	2.2	7.7
SCAT 17B Bare airplane	Very bad — Destabilizes lateral phugoid	——	Very bad — Destabilizes lateral phugoid	4.8	0	-0.6	-0.21	Lateral phugoid		-0.21	1.8	7.9
SCAT 17B Tested augmentation	Very good — No pilot lead	0.90	Very good — $\zeta_{max} = 0.9$	1.7	0	-0.4	-0.21	0.5	14 (3)	-0.21	1.8	7.9

Notes: (1) Maximum pilot aileron equals 15 deg — Assumes no limits on augmenter authority

(2) δ's are pilot inputs, not actual surface positions — Assumes no limits on augmenter authority

(3) These values could be increased by using pilot's aileron input as p command

(4) These values could be increased by using pilot's rudder input as β or a_y command

(5) 1.7 of this value is due to the lateral acceleration feedback

(6) Shading indicates factors which are deficient

SECTION V

STABILITY AUGMENTER MECHANIZATION

The previous section considered the handling qualities of three SST design with and without various types of augmentation. This section illustrates the assessment of competing mechanizations for a given type of augmentation and compares the operational penalties imposed upon each design by the required augmentation. Only the simpler type of augmentation (the alternate augmentation for SCAT 16 and 17A, and the tested augmentation for SCAT 17B) is considered for each design.

The mechanization of possible competing augmentation systems at this time poses several problems. Although the general airframe configurations for the three vehicles have been established, there is little information regarding the structural characteristics of the vehicles. It is impossible to establish the effects or manifestations of fuselage bending modes and, hence, the resulting number or location of sensors. It is also impossible to define the details of control surfaces and actuation means. As an example of the latter, Ostgaard (Ref. 12) predicts as many as twenty surface actuators may be required for the SST. Thus it may be impractical to employ the conventional series augmenter servo as a separate component in the control system. Multi-input (e.g., manual, augmenter, and/or autopilot) surface actuators may have to be employed. On the other hand, existing electrohydraulic valves are not yet proven capable of surviving (without cooling), for extended periods, the high temperature environment which will be encountered in the SST. Electromechanical servos could be designed to survive this high temperature environment, but the problem of achieving fail-soft or fail-operational capabilities (equivalent to those of the electrohydraulic servos) arises.

These problems cannot be resolved here and actually need not be. The intent of this section is to illustrate a <u>first cut</u> at determining

the relative reliability, maintenance, cost, etc., contributions of the competing systems. The resulting relative qualities can be scaled up or down at some later date to achieve a measure of the absolute values when such details as the number of servos and/or actuators can be established. In the light of past commercial airline requirements, it can be assumed that unproven, highly advanced equipments or techniques will be avoided to the greatest extent possible—at least in control applications. We can therefore assume that the present state-of-art components and mechanizational techniques will be employed and, to simplify the analysis, assume that sufficient cooling will be provided to allow usage of electrohydraulic servos.

The following subsection will present a summary of mechanizational considerations and ground rules. In subsection B a selection will be made of the most promising mechanizational scheme for each vehicle. Final assessments and tradeoffs between the three vehicles will be made in subsection C.

A. GROUND RULES

Before attempting to define mechanizational schemes, it is pertinent to summarize the ground rules and/or considerations which have a bearing on the mechanization. These ground rules are as follows:

1. Three airframe configurations are to be considered:

    a. SCAT 16
    b. SCAT 17A
    c. SCAT 17B

2. Each airframe has been evaluated at a single flight condition, the landing approach. The minimum lateral augmentation requirements, based on handling-quality considerations only, for the competing airframe configurations are:

VEHICLE	AUGMENTATION FEEDBACKS	COMMENTS
SCAT 16	a_y, $r \rightarrow \delta_r$	May be a_y command for final decrab maneuver
SCAT 17A	$p \rightarrow \delta_a$; $\delta_a \rightarrow \delta_r$	Stick position may be p command
SCAT 17B	$p \rightarrow \delta_a$	

3. Only the landing approach has been analyzed; however it is assumed that an equivalent situation exists during takeoff. Augmentation and gain compensation requirements have not been established for other mission phases or flight conditions.

4. No consideration is given to the automatic flight control system, AFCS, modes of operation or the requirement for augmentation as an inner loop of the AFCS.

5. For the SCAT 17B, the augmentation system reliability must equal or exceed the reliability requirement for a complete AFCS, namely, no more than one fatal accident in 10^7 landing attempts (flights).

6. From the standpoint of the FAA and the airlines, the relative ranking of design qualities will be:

    a. Fail safety
    b. Reliability
    c. Maintainability
    d. Bulk (weight and volume)
    e. Cost

7. Nuisance failures and false alarms must be held to a minimum in order to minimize turn-around time and maintenance actions.

B. SELECTION OF MECHANIZATIONS

Actual field experience with augmenters in military aircraft indicates system mean-time-between-failures, MTBF, for a single-axis augmenter, can be expected to fall in the range $140 < \text{MTBF} < 1000$ hr, depending on the complexity of the system mechanization. Assuming a flight time of 3 hr and an MTBF of 600 hr, the probability of failure of a nonredundant system operating from takeoff through landing is

$$P_F \doteq \frac{t}{\text{MTBF}} = \frac{3}{600} = \frac{1}{200}$$

Thus it could be expected that one landing in every 200 would be made without the aid of augmentation. To reduce the failure probability requires some form of redundancy.

Table F-I of Appendix F presents a hierarchy of feasible multiplicity schemes versus major operational, maintenance, and hardware design qualities. With few exceptions, as the level of multiplicity increases, these design qualities demonstrate an orderly progression of

Increasing failure protection

Increasing allowable augmenter authority

Increasing mean time to total system failure

Increasing dollar costs, weight, power requirements, etc.

Decreasing mean time between maintenance action

Increasing false alarm rate

It has been established in the previous section that, for the SCAT 16 and 17A, augmentation is desirable but not mandatory. Augmentation is mandatory, however, for the SCAT 17B. Based on the design quality considerations of Table F-I, tradeoff and selection of the mechanization category for each augmentation configuration can be made as follows:

1. SCAT 16 and 17A

A hard-over failure during the approach and landing (or takeoff) could result in the aircraft achieving a dangerous attitude before the pilot could determine the cause of aircraft motion and apply the necessary correction. The system must be sufficiently reliable to build pilot confidence in its availability and usefulness. False alarms must be eliminated if possible. The system must require a minimum of maintenance and allow the fastest possible turn-around. Bulk and cost are to be minimized.

The minimum system meeting the fail-pulse requirement is Category IIA (Table F-I); however, Category IIIb offers considerably increased reliability at the expense of bulk and cost. Both configurations reflect the minimum maintenance requirement in that neither is susceptible to false alarms and yet both allow direct isolation of a failure to a specific channel. Both Categories IIa and IIIb will therefore be investigated further.

2. SCAT 17B

The requirement for fail-operational automatically sets the augmentation configuration at Category VI or higher. Of these, Category VIII, although slightly more complicated due to the additional voters, inherently offers higher reliability and lower mean time between maintenance action. Category VIII is therefore the obvious choice.

Possible mechanizational schemes and the resulting MTBF calculations for a single channel are presented in Tables II, III, and IV for SCAT 16, 17A, and 17B, respectively. In view of the low resulting MTBFs it is obvious that reliability per flight must be drastically increased over single-channel reliability. Furthermore, fail-safety considerations

TABLE II

SCAT 16 MECHANIZATION (PER CHANNEL)

$a_y, r \rightarrow \delta_r$

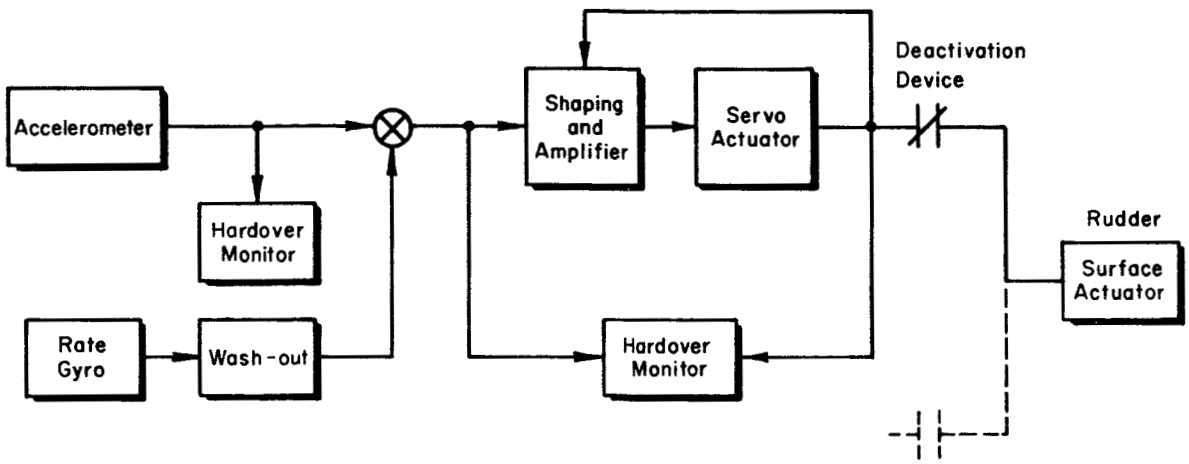

COMPONENT	FAILURE RATE (PER 10^6 HR)	DATA SOURCE (REFERENCE)
Rate gyro	150	13, 14
Accelerometer	50	13, 14
Accelerometer hard-over monitor	6	15
Washout and miscellaneous	20	14, 15
Amplifier (3 stages)	150	14
Servo valve	500	14
Actuator hard-over monitor	20	15
Cylinder	30	13
Feedback pot	100	14
Hydraulic solenoid	60	13
Power supply	50	14
Integrated test circuitry	60	15
Engage switch	60	14
	1256	

$$MTBF = \frac{1}{1256 \times 10^{-6}} \doteq 800 \text{ hr}$$

TABLE III

SCAT 17A MECHANIZATION (PER CHANNEL)

$p \rightarrow \delta_a$; $\delta_a \rightarrow \delta_r$

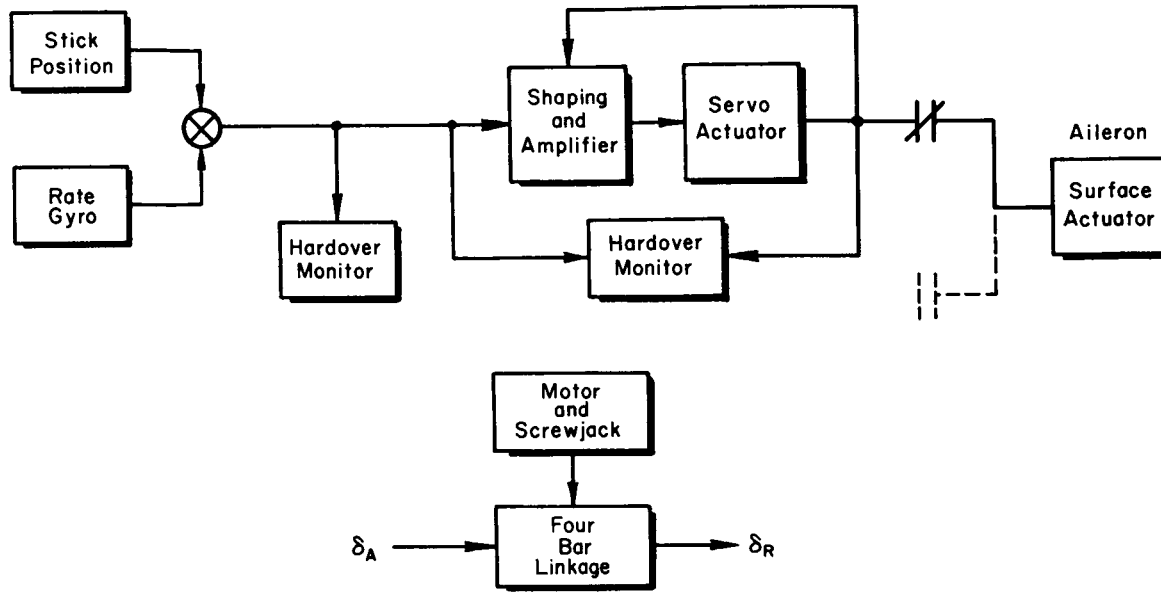

COMPONENT	FAILURE RATE (PER 10^6 HR)	DATA SOURCE (REFERENCE)
Stick position sensor	80	14
Rate gyro	150	13, 14
Sensor hard-over monitor	6	15
Amplifier (2 stages)	100	14
Miscellaneous circuitry	20	14
Servo valve	500	14
Actuator hard-over monitor	20	15
Cylinder	60	13
Feedback pot	100	14
Hydraulic solenoid	60	13
Power supply	50	14
Integrated test circuitry	60	15
Engage switch	60	14
Motor and screw jack	100	14
	1366	

$$MTBF = \frac{1}{1366 \times 10^{-6}} \doteq 730 \text{ hr}$$

TABLE IV

SCAT 17B MECHANIZATION (PER CHANNEL)

$p \rightarrow \delta_a$

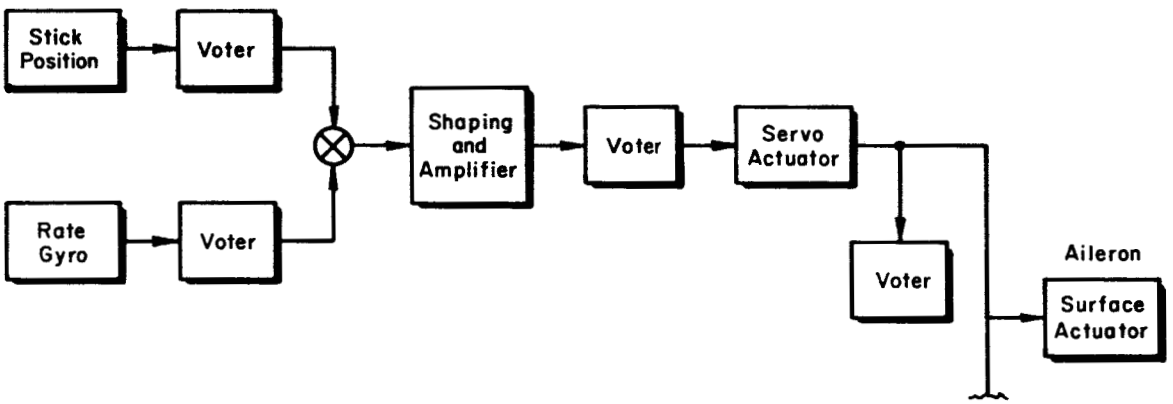

COMPONENT	FAILURE RATE (PER 10^6 HR)	DATA SOURCE (REFERENCE)
Stick position sensor	80	14
Rate gyro	150	13, 14
Amplifier (2 stages)	100	14
Miscellaneous shaping circuitry	20	14
On-line voters (3)	120	14
Off-line voters (4/3)	80	14
Servo valve (2/3)	333	14
Cylinder (2/3)	40	13
Feedback pot (2/3)	67	14
Hydraulic solenoid (2/3)	40	13
Power supply	50	14
Engage switch (1/3)	20	14
Model (1/3)	20	14
	1120	

$$\text{MTBF} = \frac{1}{1120 \times 10^{-6}} \doteq 890 \text{ hr}$$

dictate the minimum levels of redundancy noted above. Additional redundancies and/or operational usage leads to three possible situations:

> **Situation I.** Minimum, fixed-gain, fail-safe augmenter operated during takeoff and landing only. The augmenter is turned off during climb-out and is not re-engaged until a few minutes prior to landing.
>
> **Situation II.** Augmenter operated during the entire flight. Stand-by redundant system employed in SCAT 16 and 17A. The augmentation is assumed to be gain-compensated at an additional failure rate contribution of 250×10^{-6} per hour per channel.
>
> **Situation III.** Dual-redundant system for SCAT 16 and 17A and triple-redundant system for SCAT 17B, each operated throughout the flight with a stand-by, fixed-gain Category IIa augmenter available for emergency back-up for landing. If the cruise augmenter fails during flight, the landing augmenter is not turned on until the landing is to be undertaken. If the cruise augmenter is still operable during approach, the special landing and takeoff augmenter remains in stand-by. The cruise augmenter is assumed to be gain-compensated at an additional failure rate contribution of 250×10^{-6} per hour per channel. This mechanization requires a minimum of three independent hydraulic power sources.

The flight (mission) profile will be assumed to be divisible into three phases:

1. Warmup and takeoff, 10 min.
2. Climb, cruise, and letdown, 160 min.
3. Approach and landing, 10 min.

Thus, the total flight time is 3 hr and systems which are turned on only for takeoffs and landings will be operated for 20 min. per flight.

The probability of system failure per flight, P_F, probability of maintenance required per flight, P_M, probable maintenance hours per flight, M, and total system hardware "cost" (using the formulas in Appendix F), C, are presented in Table V for the three aircraft configurations and three usage situations. Note in Table V that the difference in hardware "cost" between a fixed-gain and a variable-gain

system is considered negligible. These values are also plotted in Fig. 32 and 33.

TABLE V

AUGMENTER COMPARISON SUMMARY

	CATEGORY	P_F ($\times 10^6$)	P_M ($\times 10^3$)	M ($\times 10^3$)	C
SITUATION I					
SCAT 16.....	IIa	420	0.42	0.35	1
SCAT 17A.....	IIa	460	0.46	0.38	1
SCAT 17B.....	VIII	0.155	2.4	2.0	3
SITUATION II					
SCAT 16.....	IIIb	10.2	4.5	3.7	2
SCAT 17A.....	IIIb	11.8	4.8	4.0	2
SCAT 17B.....	VIII	18.4	26	22	3
SITUATION III					
SCAT 16.....	IIIb + IIa	0.0021	4.5	3.7	3
SCAT 17A.....	IIIb + IIa	0.0027	4.8	4.0	3
SCAT 17B.....	VIII + IIa	0.0036	26	22	4

Recalling that the SCAT 16 and 17A vehicle configurations are capable of being landed without augmenters in an emergency situation, it would appear that the Situation II case would suffice for these vehicles from a handling-quality standpoint. That is, employing the Category IIIb mechanization throughout the normal mission wherein one system is active and a second is available on stand-by, roughly one landing in one hundred thousand would be made without augmentation. This would be accomplished at a reasonable maintenance expenditure (approximately 4.5 maintenance actions per thousand flights) and hardware cost (dollar and bulk).

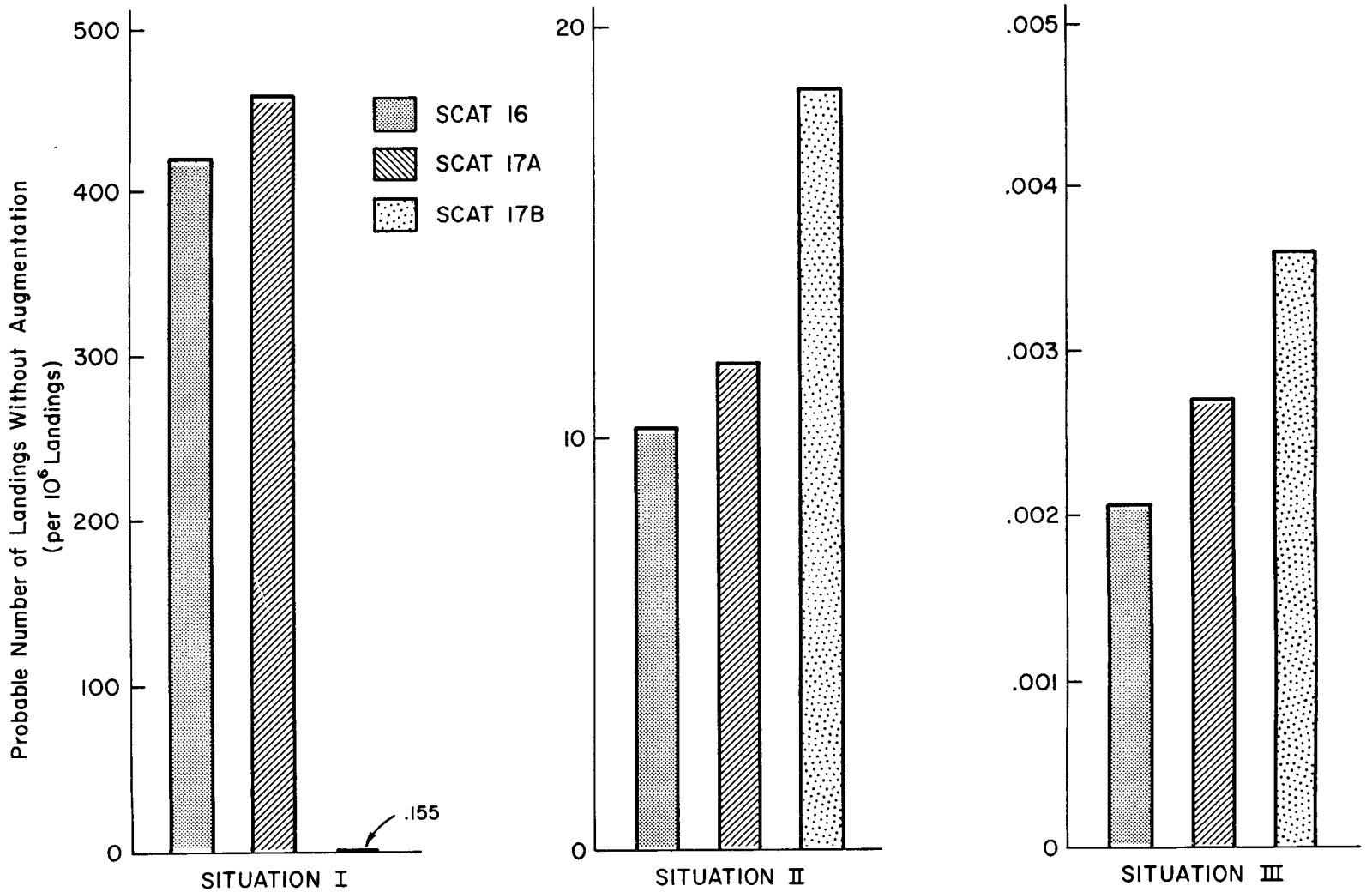

Figure 32. Probable Number of Landings Without Augmentation

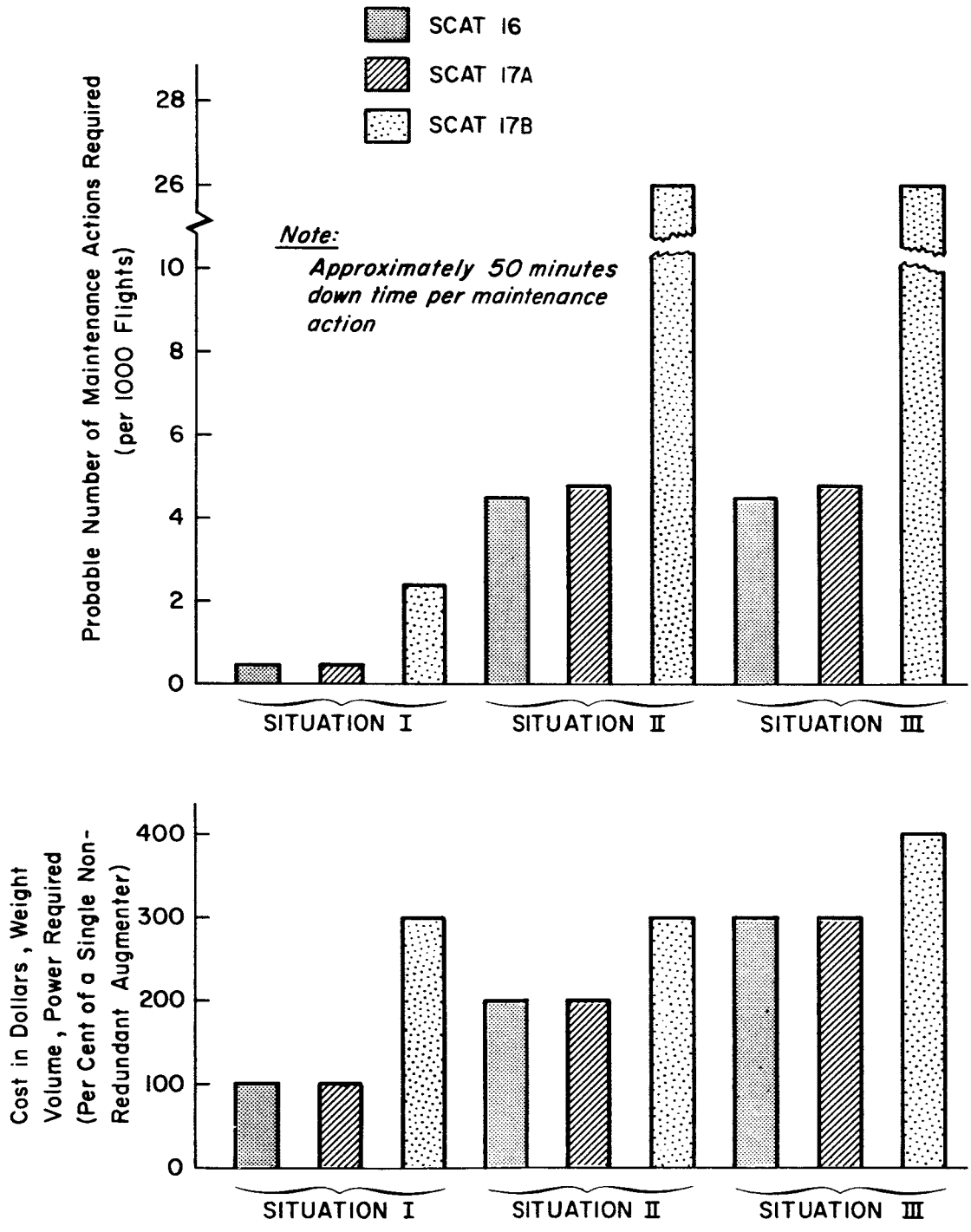

Figure 33. Probable Number of Maintenance Actions and Augmenter "Cost"

For the SCAT 17B vehicle, which is considered unflyable without augmentation, one is forced to select the Situation III case wherein a triple-redundant augmenter is employed as the nominally active system and a separate landing augmenter (fixed-gain) is available as an emergency device. This mechanization would probably require the further complexity of automatically switching to the emergency stand-by system in event of complete failure of the triple-redundant system during the actual approach and landing. This is necessary to eliminate the pilot's time lag in determining that total failure of the triple system has occurred and in then activating the stand-by system. It is also desirable to eliminate the extra burden on the flight crew during a most critical time period. If the triple-redundant system were to fail prior to the approach phase, suitable means would have to be provided to avoid its automatically turning on the landing augmenter. With this combination, the reliability requirement of one failure in 10^7 landings is actually exceeded by a factor of 30. The system cost in terms of maintenance actions (26/1000 flights) and hardware is extremely high, however, and obviously is due to the characteristics of the SCAT 17B which make a fail-operational system mandatory.

For fully automated landings in which the augmenter is an inner loop to the path control modes and the same 10^{-7} probability of failure is imposed on the complete AFCS, it is likely that the Situation III case would become a requirement for all three vehicle augmenters. That is, with the added complexity involved, the reliability apportionment for the inner loops would be much more stringent than it is for the present manual control situation.

As a final comment, it is to be recalled that these calculations are rough estimates based on current aircraft-type components. It might be expected that components will be improved during the time span between now and the date of actual design of the SST and hence the reliability of components will improve. This has not necessarily

proven to be the case in the past. For example, vendors have steadily improved upon the design and manufacture of flight control system components over the past ten years. Yet, actual field data indicate that the over-all system failure rate has been increasing for augmentation systems during this same time span. It is concluded that the system performance requirements, complexity, and environmental severity are outdistancing the component improvements. There is no reason to believe this same situation will not also be true for the SST.

SECTION VI

SUMMARY

The design of a stability augmentation system must include the three essential steps:

1. Analysis of the handling qualities of the basic airframe to determine what deficiencies, if any exist.
2. Determination of stability augmentation requirements for satisfactory handling qualities.
3. Assessment of the operational tradeoffs among the various mechanizational possibilities.

A simple analytical method for performing these steps has been presented. The method was developed for the lateral-directional augmentation of large transport-type aircraft in landing approach, but portions can be applied to other situations.

Factors for the handling-quality evaluations of steps 1 and 2 have been developed. Preliminary estimates of the values of these factors necessary for a good pilot rating have been developed from previous studies and from tests of several supersonic transport configurations evaluated on the Transport Landing Simulator of the Ames Research Center of the NASA, as follows:

1. $\varphi \rightarrow \delta_a$ closure: "Good" closure with pilot lead < 0.7 sec
2. $\psi \rightarrow \delta_a$ closure with $\varphi \rightarrow \delta_a$ inner loop: $\omega_{co} > 0.3$ rad/sec
3. $r \rightarrow \delta_r$ closure: $\zeta_{max} > 0.5$
4. $|\varphi/\beta|_{DR} < 1.5$
5. $(\delta_r/\delta_a)_0$
6. $(\dot{\delta}_r/\delta_a)_0$

   The magnitude of the sum of these two parameters should be less than 1
7. $|\delta_r/\varphi|_{ss} < 0.3$
8. $T_R < 1$ sec

9. $p_{max} > 10$ deg/sec

10. $|N'_{\delta_r}| > 0.2$ sec^{-2}

11. $|L'_{\beta}/L'_{\delta_a}| < 1$

12. $(\Delta\psi_{max})_{t=2\text{ sec}} > 5$ deg

It is recommended that a combined analytical–simulator study be undertaken to better define the parameter values necessary for a good rating and to refine the definitions of handling-quality factors.

The results of one of the example augmentation system assessments are of special interest. The handling qualities of configuration SCAT 17B were considered unacceptable even for emergency operation and pilot opinion was that the airplane could not be landed. With a simple roll damper the handling qualities were considered acceptable for normal operation; however, with current state-of-the-art components the reliability requirement of one failure, or less, in 10^7 flights is not quite met by a triple-redundant augmenter used only during takeoffs and landings. The requirement could be met by a triple-redundant augmenter used throughout the flight plus a single-channel back-up system to be used only during landings (this system requires three independent hydraulic supplies). The operational penalties (in terms of maintenance, weight, bulk, and cost) for such a system are obviously severe.

REFERENCES

1. Ashkenas, I. L., and Duane T. McRuer, The Determination of Lateral Handling Quality Requirements from Airframe–Human Pilot System Studies, WADD TR 59-135, June 1959.

2. Durand, T. S., and H. R. Jex, Handling Qualities in Single-Loop Roll Tracking Tasks: Theory and Simulator Experiments, ASD-TDR-62-507, November 1962.

3. Ashkenas, I. L., and D. T. McRuer, A Theory of Handling Qualities Derived from Pilot–Vehicle System Considerations, IAS Paper 62-39, January 1962. (Also published in Aerospace Engineering, Vol. 21, No. 2, February 1962.)

4. Creer, Brent Y., John D. Stewart, Robert B. Merrick, and Fred J. Drinkwater III, A Pilot Opinion Study of Lateral Control Requirements for Fighter-Type Aircraft, NASA Memo 1-29-59A, March 1959.

5. McNeill, Walter,E., and Robert C. Innis, "A Simulator Study of the Lateral–Directional Handling Qualities of Two SCAT Configurations in the Landing Approach," Proceedings of NASA Conference on Supersonic-Transport Feasibility Studies and Supporting Research, September 17–19, 1963, NASA TM X-905, December 1963. (Report CONFIDENTIAL, title UNCLASSIFIED)

6. Etkin, B., An Analytical Study of the Ability of a Slender Delta-Wing Aeroplane to Perform a Sidestep Manoeuvre at Low Speed, Royal Aircraft Estab. Tech. Note Aero 2623, May 1959.

7. Pinsker, W. J. G., Further Consideration of the Control Requirements for a Slender Delta Aircraft to Perform Sidestep Manoeuvres at Approach Speeds, Royal Aircraft Estab. Tech. Note Aero 2735, January 1961.

8. Perry, D. H., W. G. A. Port, and J. C. Morrall, A Flight Study of the Sidestep Manoeuvre During Landing, Aeronautical Research Council R and M 3347, July 1961.

9. Tomlinson, B. N., An Extensive Theoretical Study of the Ability of Slender Wing Aircraft to Perform Sidestep Manoeuvres at Approach Speeds, Royal Aircraft Estab. Tech. Note Aero 2837, August 1962. (Report CONFIDENTIAL, title UNCLASSIFIED)

10. Ashkenas, I. L., and D. T. McRuer, Approximate Airframe Transfer Functions and Application to Single Sensor Control Systems, WADD TR 58-82, June 1958.

11. McRuer, D. T., I. L. Ashkenas, and C. L. Guerre, A Systems Analysis View of Longitudinal Flying Qualities, WADD TR 60-63, January 1960.

12. Ostgaard, M. A., Flight Control System Design for Supersonic Transport, ASD, Flight Control Laboratory, unpublished paper.

13. Johnston, Donald E., and Tulvio S. Durand, A Compilation of Component Field Reliability Data Useful in Systems Preliminary Design, WADD TR 60-330, March 1961. (Report SECRET, title UNCLASSIFIED)

14. Johnston, D. E., and D. H. Weir, An Assessment of Operational and Cost Tradeoff Factors for a Typical High Performance AFCS, Systems Technology, Inc., TR-119-1, June 1962.

15. Boskovich, B., G. H. Cole, et al, YG910A Triple-Redundant Self-Adaptive Yaw Axis Stability Augmentation System for the B-58 Aircraft, Minneapolis-Honeywell Regulator Co. Tech. Proposal 3E-S-1, 4 February 1963.

16. Krendel, Ezra S., and Duane T. McRuer, "A Servomechanisms Approach to Skill Development," J. Franklin Inst., Vol. 269, No. 1, January 1960.

17. McRuer, Duane T., and Ezra S. Krendel, "The Man-Machine System Concept," Proc. IRE, Vol. 50, No. 5, May 1962.

18. McRuer, Duane T., Unified Analysis of Linear Feedback Systems, ASD TR 61-118, July 1961.

19. McRuer, D. T., I. L. Ashkenas, and H. R. Pass, Analysis of Multi-loop Vehicular Control Systems, ASD-TDR-62-1014, March 1964.

APPENDIX A

TRANSFER FUNCTIONS

The lateral transfer functions used herein are based on the following form of the equations of motion (body-fixed axes*):

$$\begin{bmatrix} s - Y_v & -\dfrac{sW_o + g\cos\theta_o}{V_{T_o}} & \dfrac{sU_o - g\sin\theta_o}{sV_{T_o}} \\ -L'_\beta & s(s - L'_p) & -L'_r \\ -N'_\beta & -sN'_p & (s - N'_r) \end{bmatrix} \begin{Bmatrix} \beta \\ \dfrac{p}{s} \\ r \end{Bmatrix} = \begin{Bmatrix} Y^*_\delta \\ L'_\delta \\ N'_\delta \end{Bmatrix} \delta \quad \text{(A-1)}$$

where δ can be either δ_a or δ_r

Additional variables are given by

$$\dot{\varphi} = p + r\tan\theta_o \quad \text{(A-2)}$$

$$\dot{\psi} = \frac{r}{\cos\theta_o} \quad \text{(A-3)}$$

$$a_y = V_{T_o}(Y_v\beta + Y^*_\delta\delta) = V_{T_o}\dot{\beta} - W_o p + U_o r - g\cos\theta_o\varphi \quad \text{(A-4)}$$

$$a'_y = a_y + l_x\dot{r} - l_z\dot{p} \quad \text{(A-5)}$$

The transfer function of a dependent variable is written in the form

$$\frac{\lambda(s)}{\delta(s)} = \frac{N_{\lambda\delta}(s)}{\Delta(s)} \quad \text{(A-6)}$$

where $\lambda = \beta$, p, r, φ, etc.

---

*For stability axes $W_o = 0$, $U_o = V_{T_o}$, and θ_o is the flight path angle.

The denominator, $\Delta(s)$, is given by

$$\begin{aligned}\Delta(s) = {} & s^4 + s^3(-Y_v - L_p' - N_r') \\ & + s^2\left[\frac{1}{VT_o}(U_o N_\beta' - W_o L_\beta') + L_p' N_r' - L_r' N_p' + Y_v(L_p' + N_r')\right] \\ & + s\left[\frac{U_o}{VT_o}(L_\beta' N_p' - L_p' N_\beta') + \frac{W_o}{VT_o}(L_\beta' N_r' - L_r' N_\beta') \right. \\ & \qquad \left. - Y_v(L_p' N_r' - L_r' N_p') - \frac{g}{VT_o}(L_\beta' \cos\theta_o + N_\beta' \sin\theta_o)\right] \\ & + \frac{g}{VT_o}\left[(L_\beta' N_r' - L_r' N_\beta') \cos\theta_o + (L_p' N_\beta' - L_\beta' N_p') \sin\theta_o\right] \qquad \text{(A-7)}\end{aligned}$$

The numerators are given by

$$\begin{aligned}N_{\beta_\delta} = {} & s^3 Y_\delta^* + s^2\left[-Y_\delta^*(L_p' + N_r') + \frac{1}{VT_o}(W_o L_\delta' - U_o N_\delta')\right] \\ & + s\left[Y_\delta^*(L_p' N_r' - L_r' N_p') + \frac{U_o}{VT_o}(L_p' N_\delta' - L_\delta' N_p') \right. \\ & \qquad \left. + \frac{W_o}{VT_o}(L_r' N_\delta' - L_\delta' N_r') + \frac{g}{VT_o}(L_\delta' \cos\theta_o + N_\delta' \sin\theta_o)\right] \\ & + \frac{g}{VT_o}\left[(L_r' N_\delta' - L_\delta' N_r') \cos\theta_o + (L_\delta' N_p' - L_p' N_\delta') \sin\theta_o\right] \qquad \text{(A-8)}\end{aligned}$$

$$\begin{aligned}N_{p_\delta} = {} & s^3 L_\delta' + s^2\left[Y_\delta^* L_\beta' - L_\delta' Y_v + L_r' N_\delta' - L_\delta' N_r'\right] \\ & + s\left[Y_\delta^*(L_r' N_\beta' - L_\beta' N_r') + Y_v(L_\delta' N_r' - L_r' N_\delta') + \frac{U_o}{VT_o}(L_\delta' N_\beta' - L_\beta' N_\delta')\right] \\ & + \frac{g}{VT_o}(L_\beta' N_\delta' - L_\delta' N_\beta') \sin\theta_o \qquad \text{(A-9)}\end{aligned}$$

$$N_{r_\delta} = s^3 N'_\delta + s^2\left[Y^*_\delta N'_\beta - Y_v N'_\delta + L'_\delta N'_p - L'_p N'_\delta\right]$$
$$+ s\left[Y^*_\delta (L'_\beta N'_p - L'_p N'_\beta) + Y_v (L'_p N'_\delta - L'_\delta N'_p) + \frac{W_o}{V_{T_o}}(L'_\delta N'_\beta - L'_\beta N'_\delta)\right]$$
$$+ \frac{g}{V_{T_o}}(L'_\delta N'_\beta - L'_\beta N'_\delta) \cos \theta_o \qquad \text{(A-10)}$$

$$N_{\varphi_\delta} = \frac{N_{p_\delta} + \tan \theta_o N_{r_\delta}}{s} \qquad \text{(A-11)}$$

$$N_{\psi_\delta} = \frac{N_{r_\delta}}{s \cos \theta_o} \qquad \text{(A-12)}$$

$$N_{a_y} = V_{T_o} s N_{\beta_\delta} - W_o N_{p_\delta} + U_o N_{r_\delta} - g \cos \theta_o N_{\varphi_\delta}$$
$$= V_{T_o}(Y_v N_{\beta_\delta} + Y^*_\delta \Delta) \qquad \text{(A-13)}$$

$$N_{a'_y} = N_{a_y} + l_x s N_{r_\delta} - l_z s N_{p_\delta} \qquad \text{(A-14)}$$

APPENDIX B

NUMERICAL DATA

Numerical values of reference dimensions, inertias, dimensionless stability derivatives, dimensional derivatives, and transfer function factors for the various configurations are summarized in the following series of tables.

TABLE B-I

REFERENCE DIMENSIONS

PARAMETER	UNITS	SUBSONIC JET	SCAT 16	SCAT 17A	SCAT 17B
S	ft^2	2,892	3,000	5,100	5,200
b	ft	142.4	69.7	105	106.3
U_o	ft/sec	223	231.4	218.1	243.2
W_o	ft/sec	7.79	17	46.4	29.9
m	slugs	5,590	7,540	7,860	6,520
I_x	10^6 slug-ft^2	3.3	2.63	1.86	2.8
I_z	10^6 slug-ft^2	8.3	13.1	13.35	16
I_{xz}	10^6 slug-ft^2	0	0	0	0
θ_o	deg	-0.86	1.2	9	4
α_o	deg	2	4.2	12	7

TABLE B-II

DIMENSIONLESS STABILITY DERIVATIVES

PARAM.	SUBSONIC JET	SCAT 16		SCAT 17A		SCAT 17B	
		Bare	Tested Aug.	Bare	Tested Aug.	Bare	Tested Aug.
C_{y_β}	-0.82	-0.492	-0.492	0.109	0.109	-0.143	-0.143
$C_{y_{\delta_a}}$	0	0	0	0	0	0	0
$C_{y_{\delta_r}}$	0	0	0	0	0	0	0
C_{l_β}	-0.18	-0.249	-0.297	-0.142	-0.116	-0.180	-0.180
C_{l_p}	-0.42	-2.20	-2.52	-0.172	-0.317	-0.264	-0.660
C_{l_r}	0.35	1.33	1.52	0.338	0.127	0.156	0.156
$C_{l_{\delta_a}}$	-0.14	-0.417	-0.417	-0.086	-0.086	-0.1014	-0.1014
$C_{l_{\delta_r}}$	0.010	0.0177	0.0177	0.0203	0.0203	0.0211	0.0211
C_{n_β}	0.13	0.211	0.422	0.145	0.294	0.151	0.151
C_{n_p}	-0.12	-0.709	0.709	-0.138	0.131	0.327	0.026
C_{n_r}	-0.20	-0.406	-1.22	-0.597	-1.22	-0.586	-0.586
$C_{n_{\delta_a}}$	-0.009	-0.0141	-0.0141	-0.0067	-0.0067	-0.077	-0.077
$C_{n_{\delta_r}}$	-0.13	-0.0773	-0.0773	-0.0952	-0.0952	-0.0871	-0.0871

TABLE B-III

DIMENSIONAL STABILITY DERIVATIVES

PARAM.	UNITS	SUBSONIC JET	SCAT 16		SCAT 17A		SCAT 17B	
			Bare	Tested Aug.	Bare	Tested Aug.	Bare	Tested Aug.
Y_v	sec^{-1}	-0.112	-0.054	-0.054	0.019	0.019	-0.033	-0.033
$Y^*_{\delta_a}$	sec^{-1}	0	0	0	0	0	0	0
$Y^*_{\delta_r}$	sec^{-1}	0	0	0	0	0	0	0
L'_β	sec^{-2}	-1.33	-1.27	-1.51	-2.42	-1.97	-2.54	-2.54
L'_p	sec^{-1}	-0.99	-1.68	-1.93	-0.69	-1.27	-0.81	-2.02
L'_r	sec^{-1}	0.82	1.02	1.16	1.35	0.51	0.48	0.48
L'_{δ_a}	sec^{-2}	-1.03	-2.12	-2.12	-1.46	-1.46	-1.43	-1.43
L'_{δ_r}	sec^{-2}	0.074	0.090	0.090	0.35	0.35	0.30	0.30
N'_β	sec^{-2}	0.38	0.22	0.43	0.34	0.70	0.37	0.37
N'_p	sec^{-1}	-0.11	-0.11	0.11	-0.077	0.073	0.17	0.014
N'_r	sec^{-1}	-0.19	-0.062	-0.19	-0.33	-0.68	-0.31	-0.31
N'_{δ_a}	sec^{-2}	-0.026	-0.014	-0.014	-0.016	-0.016	-0.19	-0.19
N'_{δ_r}	sec^{-2}	-0.38	-0.079	-0.079	-0.23	-0.23	-0.21	-0.21

TABLE B-IV

TRANSFER FUNCTION FACTORS

PARAMETER	SUBSONIC JET	SCAT 16		SCAT 17A		SCAT 17B	
		Bare	Tested Aug.	Bare	Tested Aug.	Bare	Tested Aug.
	$\Delta = \underbrace{\left(s + \frac{1}{T_s}\right)\left(s + \frac{1}{T_R}\right)}_{\text{or}} \left(s^2 + 2\zeta_d\omega_d s + \omega_d^2\right)$ or $\left(s^2 + 2\zeta_1\omega_1 s + \omega_1^2\right)$						
$1/T_s$ (ζ_1)	-0.011	-0.030	-0.036	0.051	0.130	(0.29)	0.071
$1/T_R$ (ω_1)	1.14	1.68	1.95	0.78	1.10	(0.40)	1.94
ζ_d	0.10	0.12	0.19	0.087	0.37	0.64	0.24
ω_d	0.82	0.64	0.68	0.99	0.94	0.71	0.73
	$N_{\varphi\delta_a} = A_\varphi\left(s^2 + 2\zeta_\varphi\omega_\varphi s + \omega_\varphi^2\right)$						
A_φ	-1.03	-2.12	-2.12	-1.47	-1.47	-1.44	-1.44
ζ_φ	0.24	0.13	0.19	0.26	0.40	0.25	0.25
ω_φ	0.66	0.48	0.67	0.61	0.84	0.85	0.85
	$N_{\psi\delta_a} = \frac{A_\psi}{s}\left(s + \frac{1}{T_{\psi_1}}\right)\underbrace{\left(s + \frac{1}{T_{\psi_2}}\right)\left(s + \frac{1}{T_{\psi_3}}\right)}_{\text{or}}$ or $\left(s^2 + 2\zeta_\psi\omega_\psi s + \omega_\psi^2\right)$						
A_ψ	-0.026	-0.014	-0.014	-0.016	-0.016	-0.19	-0.19
$1/T_{\psi_1}$	0.74	0.50	17.7	0.47	5.98	1.97	1.97
$1/T_{\psi_2}$ (ζ_ψ)	-1.07	-0.64	(0.21)	-2.24	(0.80)	(0.16)	(0.16)
$1/T_{\psi_3}$ (ω_ψ)	-2.97	-14.2	(0.71)	-4.65	(1.26)	(0.60)	(0.60)
	$N_{r\delta_r} = A_r\left(s + \frac{1}{T_r}\right)\left(s^2 + 2\zeta_r\omega_r s + \omega_r^2\right)$						
A_r	-0.38	-0.079	-0.079	-0.23	-0.23	-0.21	-0.21
$1/T_r$	1.13	1.81	1.80	0.76	1.10	0.73	1.94
ζ_r	-0.0035	0.093	0.093	0.025	0.065	-0.11	0.12
ω_r	0.40	0.28	0.28	0.60	0.34	0.60	0.37

APPENDIX C

PILOT MODEL

When flying an airplane the pilot can be considered to be operating in one of the following modes (Ref. 16 and 17):

1. Precognitive
2. Pursuit
3. Compensatory

When the pilot is operating in the precognitive mode, he is applying a learned set of control manipulations without any feedback of the actual airplane motion. For example, on a calm day a skilled pilot could execute a turn entry in a precognitive manner, i.e., his movements of the ailerons and rudder could be a completely predictable learned sequence which he could do with his eyes closed. Because precognitive behavior is essentially open-loop control, the pilot cannot operate in this mode unless all inputs, disturbances, and airplane responses to the controls are completely known. Predictability is a necessary but not sufficient condition for precognitive behavior.

When the situation is not predictable, the pilot will operate in either the pursuit or compensatory mode. In either of these two modes the pilot is operating closed-loop, i.e., he is using the sensed motion of the airplane to modify his control actions. In the pursuit mode the pilot is able, either mentally or through an appropriate display, to separate the airplane motions due to his control movements from those due to external disturbances (gusts). For example, in making a visual approach with a moderate amount of turbulence the pilot can distinguish between the motions due to his control inputs and gusts. When he cannot separate the motions he is in the compensatory mode; an instrument approach during severe turbulence is an example.

The above modes of pilot behavior have also been postulated as steps in human skill development (Ref. 16). When first confronted with

a control task, the behavior of a human operator is compensatory. As he becomes more familiar with the task, he may be able to separate his input effects from the disturbance effects and operate in the pursuit mode. Finally, if the disturbances are predictable, the control may become precognitive. The amount of training necessary to progress from one mode to the other depends on the size and predictability of the disturbances and the complexity of the controlled element.

An excellent example of this progression is given in Ref. 16:

> The foregoing hypothesized development can be given intuitive substance by considering, in an introspective manner, how certain common motor skills have developed. As an illustration, consider learning to steer an automobile. Many beginners start by relating a fixed object on the automobile to a guideline on the road. Thus a novice, concentrating on the many details of driving, steers the automobile so that a constant distance is maintained between the hood ornament and the curbing. This is an effective compensatory display since the operator is attending to the error only. As the driver in training acquires facility and confidence he is able to increase his perceptual capacity for external stimuli, so his effective field of view or perceptual aperture increases. In the course of this process he becomes aware of the separate characteristics of the hood ornament and the curbing. In other words, he can attend to input signal and control responses independently. He thus achieves a pursuit display type of organization of his visual field, and can make use of the regularities and predictable features of the road. Finally, on achieving complete familiarity with the controlled element, the driver can view the entire visible field, sampling it as necessary, and can steer the automobile as necessary with deft, discrete movements. The interval between these short duration open loop control responses is dependent on the degree to which the road winds, the speed of the car, and the amount of traffic. Other examples of driving in an open loop fashion for brief intervals of time occur during such emergency maneuvers as steering out of a skid.

After an operator has learned a particular control task his behavior may vary, depending on the disturbances. Thus, for a particular maneuver a pilot might operate in the pursuit mode on a calm

day and in the compensatory mode in the presence of severe turbulence. For this study the critical task is an instrument approach in the presence of beam noise and severe turbulence, and the pilot should be operating in the compensatory mode. It has been shown that even when the pilot is operating in the pursuit mode, a compensatory model of the pilot gives a good prediction of the closed-loop characteristic roots, albeit a conservative estimate of the closed-loop performance.

A highly successful analytical model of compensatory pilot behavior has been formed from numerous single-loop tracking experiments (Ref. 3). While the model does not give a point-by-point match of the operator's response, it does closely match his time-averaged response characteristics. In this model the pilot's transfer function is represented by

$$Y_p = \frac{K_p(T_L s + 1)e^{-\tau s}}{(T_I s + 1)(T_N s + 1)}$$

where τ is the reaction-time delay ($\tau \doteq 0.15$ sec), T_N is the neuromuscular lag ($T_N \doteq 0.1$ sec), and K_p, T_L, and T_I are adjustable by the pilot.

It has been shown that the pilot will generally adjust his gain, lead, and lag in much the same way a servo designer would do if presented with the same control task with the variable compensation

$$\frac{K_p(T_L s + 1)}{T_I s + 1}$$

There are, however, limits on these pilot parameters, the most restrictive limit being the amount of lead the pilot can generate. The maximum value of T_L is unknown, but if the pilot is required to generate much more of a lead than $T_L = 2$ sec, his behavior becomes quite nonlinear and his opinion of the system is very poor.

The pilot adjusts his characteristics to minimize the deviations of the airplane from the ILS beam. When interpreted in the language

of the servo analyst, this minimization becomes the adjustment rules:

1. The closed-loop system must be stable.
2. When the closed-loop system can be approximated by a third-order system, the damping ratio of the closed-loop oscillatory roots should be 0.35 or more.
3. For the landing approach situation, phase margins should be on the order of 40 to 60 deg.
4. The closed-loop system should have good low-frequency response, i.e., for frequencies less than the bandwidth of the equivalent input, the open-loop amplitude ratio should be much greater than 1. The equivalent input is the airplane-alone response to the turbulence.

Pilot opinion is a function of the pilot's success in suppressing the disturbances and of the characteristics he must adopt. Highest pilot ratings are for tasks where the pilot can act as a pure gain. His opinion will be degraded slightly if he is required to generate lags. Tasks which require pilot lags take longer to learn well and require more training. The most severe degradations in pilot rating are due to requirements for pilot lead. If the pilot is required to generate a 1-sec lead his opinion will not be greatly degraded, but with a 2-sec lead his rating of the system will be poor.

Pilot opinion will also be very poor if the control sensitivity or gain is much too high or low. Unfortunately it is not possible at this time to analytically predict the optimum control gain as this depends on the task and type of control device; however, it is a simple task to determine the optimum gain from simulator studies. Because of this gain effect, the predictions of pilot opinion and rankings of various characteristics should be based on the use of the optimum gain for each set of characteristics.

The above discussion has only considered the pilot in single-loop tasks. The extension to multiloop situations appears straightforward if two additional factors are considered. The first factor is the

loop-closure adaptability of the pilot. In flying an airplane the pilot has several parameters available to him for control, and he may select any one of a number of combinations of loop closures or pilot techniques. For example, he will normally control pitch attitude with elevator, but he can control altitude with either elevator or throttle. By trial and error the pilot will ultimately select the set of loop closures which makes it easiest for him to control the airplane. In the analysis of the multiloop pilot–airplane situation, it is therefore necessary to consider many different pilot techniques to establish the most likely one.

The second multiloop factor is a possible increase in the pilot's transport lag (time delay) because he may have to scan several instruments to get the data for closing the loops. For multiloop tasks in which the pilot must sample several instruments, his transport lag will be increased above the value measured in single-loop tasks. For the analyses described in this report an effective reaction-time delay, which combines the neuromuscular and reaction-time lags, of 0.3 sec was used. This in turn was approximated by a first-order Padé form so that the pilot model actually used was

$$Y_p = \frac{K_p(T_L s + 1)}{(T_I s + 1)} \frac{(-0.15s + 1)}{(0.15s + 1)}$$

$$= \frac{-K_p(T_L s + 1)(s - 6.7)}{(T_I s + 1)(s + 6.7)}$$

APPENDIX D

UNIFIED SERVO ANALYSIS METHOD

The basic problem in servo analysis is: Given the open-loop transfer function, $G(s)$, what are the closed-loop characteristics of the system? The heart of the servo analysis problem is then to find the zeros of $1 + G(s)$, i.e., those values of s for which $G(s) = -1$. These values of s are the closed-loop poles of the system. For very simple systems the roots can be found directly by factoring the characteristic equation, $1 + G(s) = 0$. For most systems factoring is impractical and provides the designer with no appreciation for the effects of the various open-loop parameters. Consequently, a number of graphic tools have been developed to provide information about the closed-loop system.

The most significant feature of the Unified Servo Analysis Method (Ref. 18) is the combined use of the root locus diagram and the generalized Bode diagram. The conventional Bode diagram is a graph of the amplitude and phase of the open-loop transfer function, $G(s)$, versus frequency, ω, where $s = j\omega$. In the generalized Bode the amplitude and phase of $G(s)$ are plotted for variations in s other than just along the imaginary axis. The most useful of these plots is the "Siggy," which is the graph of the amplitude and phase of $G(s)$ for $s = \pm\sigma$, where σ is a real number, i.e., for s varying along the real axis. Note that the phase of a Siggy plot is either 0 or 180 deg since $G(\pm\sigma)$ must be a real number, either positive or negative. The portions of the Siggy for which the phase is 180 deg, $G(\pm\sigma)$ negative, are the more significant, as they graphically illustrate the variations of the real closed-loop roots with gain. When the phase is 180 deg, the intersections of the Siggy and the zero-db line (amplitude equals unity) define all real closed-loop poles because, by definition, the closed-loop roots are those values of s for which $G(s) = -1$.

A simple example of the combined use of root locus and Bode diagrams is given in Fig. D-1. The Bode diagram has the conventional

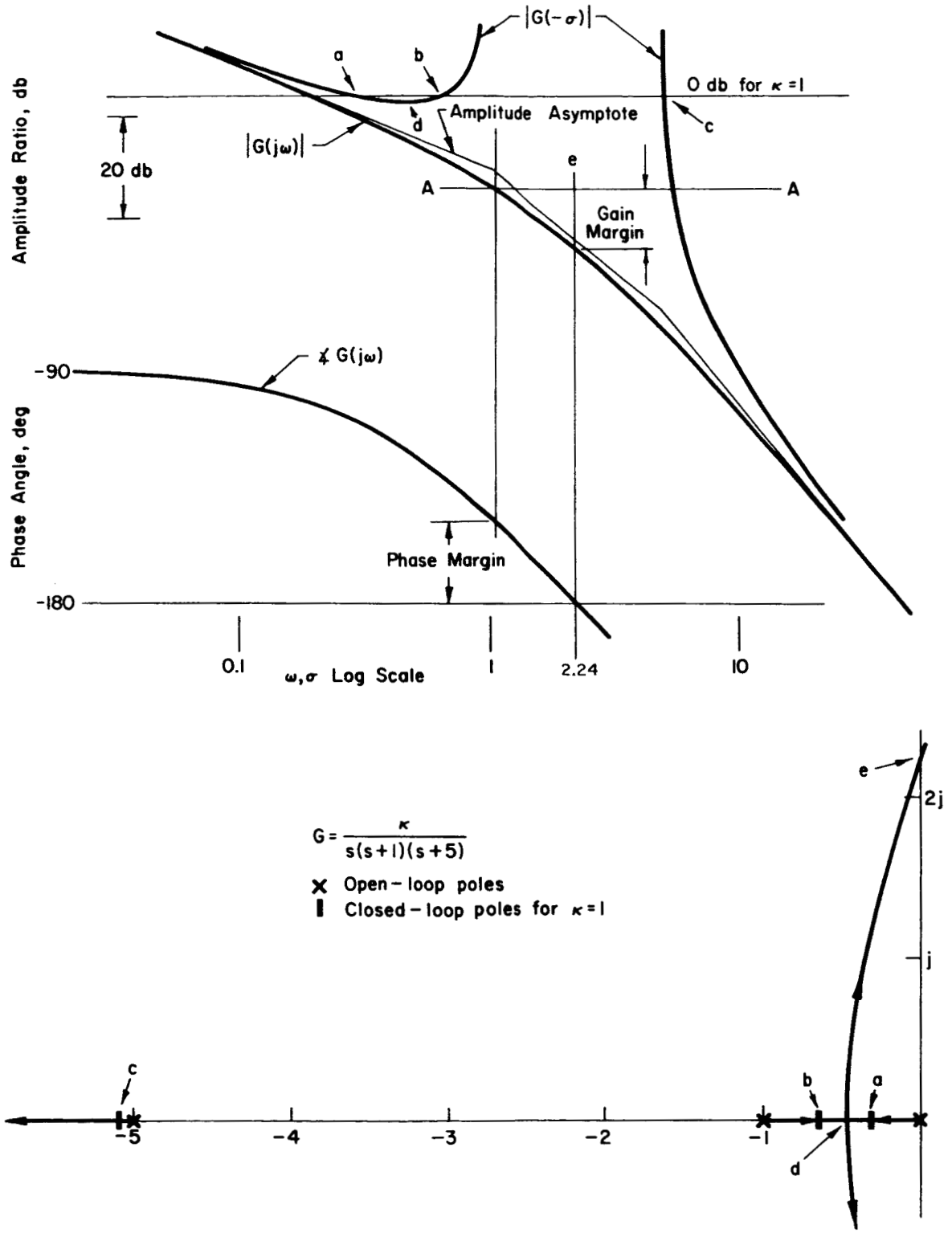

Figure D-1. Example of the Combined Use of Root-Locus and Bode Diagrams

Bode plots as well as those portions of the Siggy for which the phase is 180 deg. To illustrate the use of the Siggy in locating real roots, consider the case of $\kappa = 1$. From the intersection of the Siggy and the zero-db line, it can be seen that the real roots are at $s = -0.31$, -0.64, and -5.05, points a, b, and c, also shown on the root locus. The Siggy also shows the frequency, 0.45 (point d of both plots), and the gain, $\kappa = 1$ db $= 1.12$, at which two of the real roots are identical.

As illustrated in Fig. D-1 for the zero-db line along A-A, the conventional Bode indicates the phase margin, 32 deg, and the gain margin, 11.5 db, directly. It also shows the gain, $\kappa = 29.5$ db $= 30$ in linear units, and the frequency, 2.24, at which the system becomes neutrally stable (point e of both plots).

The principal advantage of the root locus is that it graphically illustrates the movement of the closed-loop roots in the s plane as the gain is varied. Unless various gain values are indicated on each branch of the locus, the locations of all the closed-loop roots for a specified gain are not obvious. The generalized Bode, on the other hand, shows all the real roots directly as a function of gain. Because of the logarithmic scales, it is also simple to include roots which are different by several orders of magnitude.

Perhaps the most useful property of the Bode is the ability to indicate which open-loop poles and zeros have the most influence on the closed-loop characteristics. On the Bode it is simple to see in what frequency regions $|G(j\omega)| \gg 1$ or $|G(j\omega)| \ll 1$. In those regions for which $|G(j\omega)| \gg 1$, $G/(1+G) \doteq 1$ and the closed-loop poles are nearly equal to open-loop zeros. Consequently, variations in the open-loop poles and zeros in these frequency regions have little effect on the closed-loop characteristics. Similarly, in regions for which $|G(j\omega)| \ll 1$, $G/(1+G) \doteq G$ and the closed-loop poles are nearly equal to the open-loop poles. Consequently, variations in the open-loop zeros in these regions have little effect on the closed-loop poles.

The combined use of root locus and generalized Bode plots results in a powerful analysis technique. The advantages of the individual plots are complementary and tend to offset the shortcomings of one another.

APPENDIX E

MULTILOOP ANALYSIS TECHNIQUE

The multiloop analysis technique developed by STI provides a valuable tool for analyzing or synthesizing a control system for a vehicle with two or more independent controls. This technique is very useful for analyzing the lateral dynamics of an airplane when there are a number of aileron and rudder feedbacks. A detailed development of the method is given in Ref. 19; however, the basic principles can be illustrated by the following simple example.

Consider a three-degree of freedom system with two separate controls. The equations of motion can be written as

$$\begin{bmatrix} a_{11}(s) & a_{12}(s) & a_{13}(s) \\ a_{21}(s) & a_{22}(s) & a_{23}(s) \\ a_{31}(s) & a_{32}(s) & a_{33}(s) \end{bmatrix} \begin{Bmatrix} X_1(s) \\ X_2(s) \\ X_3(s) \end{Bmatrix} = \begin{bmatrix} b_{11}(s) & b_{12}(s) \\ b_{21}(s) & b_{22}(s) \\ b_{31}(s) & b_{32}(s) \end{bmatrix} \begin{Bmatrix} \delta_1(s) \\ \delta_2(s) \end{Bmatrix} \quad \text{(E-1)}$$

or, more compactly, $$[A(s)][X(s)] = [B(s)][\delta(s)] \quad \text{(E-2)}$$

Examples of the resultant conventional transfer functions are given in Eq. E-3 and E-4.

$$\frac{X_1}{\delta_1} = \frac{N_{X_1\delta_1}}{\Delta} = \frac{\begin{vmatrix} b_{11} & a_{12} & a_{13} \\ b_{21} & a_{22} & a_{23} \\ b_{31} & a_{32} & a_{33} \end{vmatrix}}{\begin{vmatrix} a_{11} & a_{12} & a_{13} \\ a_{21} & a_{22} & a_{23} \\ a_{31} & a_{32} & a_{33} \end{vmatrix}} \quad \text{(E-3)}$$

$$\frac{X_3}{\delta_2} = \frac{N_{X_3\delta_2}}{\Delta} = \frac{1}{\Delta}\begin{vmatrix} a_{11} & a_{12} & b_{12} \\ a_{21} & a_{22} & b_{22} \\ a_{31} & a_{32} & b_{32} \end{vmatrix} \quad \text{(E-4)}$$

A central question in an analysis of this system is: If X_1 is fed back to δ_1 through equalization Y_1 [i.e., $\delta_1(s) = -Y_1(s)X_1(s)$], what is the response of X_2 to δ_2? Using conventional block-diagram algebra and transfer functions like Eq. E-3 and E-4, one would obtain the expression:

$$\left(\frac{X_2}{\delta_2}\right)_{X_1 \rightarrow \delta_1} = \frac{\Delta N_{X_2\delta_2} + Y_1\left(N_{X_1\delta_1} N_{X_2\delta_2} - N_{X_2\delta_1} N_{X_1\delta_2}\right)}{\Delta\left(\Delta + Y_1 N_{X_1\delta_1}\right)} \qquad \text{(E-5)}$$

By working with the matrix equations, E-1 and E-2, directly, one obtains the equivalent but simpler-looking result given in E-6.

$$\left(\frac{X_2}{\delta_2}\right)_{X_1 \rightarrow \delta_1} = \frac{N_{X_2\delta_2} + Y_1 N_{\delta_1\delta_2}^{X_1X_2}}{\Delta + Y_1 N_{X_1\delta_1}} \qquad \text{(E-6)}$$

The coupling numerator $N_{\delta_1\delta_2}^{X_1X_2}$ in E-6 is defined by

$$N_{\delta_1\delta_2}^{X_1X_2} = \begin{vmatrix} b_{11} & b_{12} & a_{13} \\ b_{21} & b_{22} & a_{23} \\ b_{31} & b_{32} & a_{33} \end{vmatrix}$$

The primary advantage of using coupling numerators and the multi-loop technique is a greatly increased physical understanding of the effects of feedbacks (a secondary benefit is a significant computational reduction). It becomes a far easier task to keep track of all the effects of each feedback as evidenced from a comparison of E-6 with E-5. In some cases it has been found that the most beneficial feature of one feedback is that it modifies a particular numerator (for example, $N_{X_2\delta_2}$ in E-6) so that a second feedback can produce the desired changes in the system. This was not evident at all when the more conventional methods were employed.

APPENDIX F

REDUNDANCY IN STABILITY AUGMENTERS

To place the major consequences of multiplicity or redundancy in automatic flight control systems in a perspective which facilitates tradeoffs between potential competing mechanizations, it is convenient to form a matrix of practical redundant mechanizations versus major operational, maintenance, and hardware design qualities. Such a matrix can serve a second purpose by focusing attention on areas requiring special consideration in achieving a successful design for any given mechanization.

One form of such a matrix is presented in Table F-I. In this table the system configuration hierarchy progresses from a conventional single active channel to a triple-redundant configuration with both on-line and off-line monitor-voters. The design quality assessments are expressed in general terms; however the quantitative values indicated therein are based on detailed investigations of military squadron-level operations (conducted as a part of previous STI studies) backed up by a comprehensive library of aircraft operational reliability, maintainability, and cost data which have been gathered by STI over a period of nearly ten years. This material reflects actual field experience with the A3J, A4D, B-52, B-58, F8U, F9F, F-100, F-102, S2F, X-15, 707, and numerous other aircraft.

Definitions and assumptions necessary to develop the table are presented below.

1. System Configuration

a. A single active channel consists of sensing (S), actuation (A), and the necessary interconnecting and shaping electronics (E).

b. A hard-over monitor (H) consists of a simple logic circuit triggered either by signal amplitude or by a specific

combination of sensor output sign and amplitude and actuator output sign and amplitude.

c. A model channel consists of sensor and electronic units, identical to that of an active channel, plus an electronic model of the actuator dynamics (M).

d. A decision element (D) consists of a single threshold device which will disengage its associated active channel whenever the difference between the outputs of the actuator and its model exceeds some predetermined error (threshold).

e. A voter (V) consists of solid-state circuitry and-or gates operating as

(1) Majority rule for off-line voting,
(2) Mid-value select for on-line voting.

f. Actuators connected by unbroken lines are assumed to be dual tandem.

2. Failure Protection

a. Fail-hard. System can fail such that the surface will deflect to the limit of augmenter authority. A failed augmenter must be detected and turned off by the pilot.

b. Fail-pulse. System can fail such that the suface will momentarily deflect to the limit of augmenter authority. The system is then automatically turned off by its monitor.

c. Fail-soft. System is capable of automatic disconnection in the presence of any single failure without substantial disturbance to the aircraft.

d. Fail-operational. System is capable of withstanding any single failure without substantial alteration of system performance.

Note from the matrix that the following groupings can be made:

Failure Protection	Configuration	
	First Failure	Second Failure
Fail-hard	I, IIIa	IIIa, IVb-2, V
Fail-pulse	II, IIIb, IVa, V	IIIb, IVa, VI, VIII*
Fail-soft	IVb-1, IVb-2	VII, VIII*
Fail-operational	VI, VII, VIII	VIII*

3. Mean Time Between Failure

a. All systems are in the constant hazard or constant failure rate portion of their useful lives and failures are random with an exponential distribution. Hence the system mean time between failure is a measure of the system reliability.

b. Mean time between failure is the reciprocal of the summation of the failure rate contributions of all components comprising the system configuration.

c. Mean time between failure of a model channel is twice that of a complete channel.

d. The failure contribution of a stand-by system is negligible when not energized. This is recognized to be optimistic; however, it is considered valid on the basis that components containing moving parts (e.g., sensors, actuators, relays, switches, etc.) are by far the greatest failure contributors.

---

*Configuration VIII can fail-pulse only if both failures are in the positional servo and if the second failure is a hard-over failure. It will fail-soft if the first and second failures occur in two of any other three parallel units. For any other combination of first, second, or third failures it is fail-operational.

e. On-line or off-line majority voters are solid-state circuits resulting in negligible contribution to the total system failure rate (in the quantities indicated herein).

f. The mean time to second failure assumes that the first and second failures are completely independent, that the equipment associated with the first failure is effectively isolated from the unfailed equipment upon occurrance of the first failure, and thus the remaining equipment enters a new period having the MTBF indicated.

4. Probability of Complete Systems Failure

a. The basic expression for probability of failure for Configuration I is

$$P_F = 1 - P_S = 1 - e^{-t/T} \doteq \frac{t}{T} \quad \text{where} \quad \frac{t}{T} \ll 1$$

t = the mission time

T = the system MTBF

b. Approximate expressions are employed in many instances to avoid lengthy entries in the table.

c. The entry for Configuration VIII is valid only for the case of three voters per channel. The general expression is

$$P_F = 1 - \left[1 - \sum_{k=r_1}^{n} \binom{n}{k} (p)^k (1-p)^{n-k}\right]^j$$

where n = redundancy level

r_1 = number of failures to cause shutdown

p = probability of failure of each element

5. Mean Time Between False Alarms

a. There are many potential (and actual) causes of false alarms. Fundamentally the problem is that signals in parallel paths differ, for one reason or another, by an amount sufficient to cause the decision device or voter to take action even though a time failure has not occurred. Potential causes include:

(1) Difference in channel or component nulls, drift, or wear-out.

(2) Differences in integration rates. Leads to squeeze modes.

(3) Differences in component or channel nonlinearities.

(4) Differences in component tolerance build-ups.

(5) Crosstalk in between wires in cable bundles.

(6) Power supply variations (where each channel has a different supply).

(7) Requirement for relatively low disconnect thresholds.

(8) A single outer loop operating on one phase of electrical power while one or more of the redundant augmenters are operating on other phases.

b. The mean times to false alarm presented here are based on current experience with two dual-redundant systems which have been flying for some time, the X-15 and the A3J-1. For both aircraft the false alarm rate appears to be approximately eight times the actual augmenter failure rate. False alarms tend to occur at low q flight conditions where gains are highest in variable-gain systems, i.e., landing, takeoff, and high altitude.

c. The mean times to false alarm for Configurations VI, VII, and VIII are extrapolations of the dual-redundant case

since there is no flight experience with triple redundancy. For Configurations VI and VII it is assumed the voter contains three differencing devices, hence the false alarm rate is increased by a factor of three. The purpose of the on-line voters in Configuration VIII is to reduce the possibility of false alarms by avoiding error build-up through the separate channels. This is accomplished by a mid-signal selection process in each on-line voter. A common signal is then fed to the succeeding blocks. For the three stages of voting indicated, it would be expected that the error build-up, hence false alarms, would be approximately one-third that of a dual system.

6. Authority Limitation

Whether authority limitation is, or is not, of consequence depends on

a. Fail-safety requirements (structural, controllability, etc.).

b. Required authority for augmentation purposes.

c. Use of the augmentation system as the inner loop of the AFCS.

d. Specific actuator design and installation.

7. Mean Time Between Maintenance Actions

a. Assuming the maximum failure protection capability of the system must be available prior to aircraft takeoff, maintenance action will be required following every flight on which a channel trip-out is obtained (false alarm or actual failure).

b. The rate of required maintenance is the sum of the false alarm rate and the failure rate.

8. Mean Time to Accomplish Repair

a. From visits to military squadrons, maintenance records, etc., it has been determined that the average time to work off a squawk at the flight line level is approximately 2-1/2 hr. Of this time approximately 1-1/2 to 1-3/4 hr is fixed, i.e., apply power, open up equipment bay, obtain part from stock, button up aircraft.

b. Assuming each augmenter channel to contain built-in self-test features, it is estimated that the time to trouble-shoot the system, remove and reinstall the proper component, and to verify proper channel operation will vary from 1/4 to 3/4 hr, depending on the specific redundant configuration. Thus the estimated mean time to accomplish repair is $\tau = 2$ hr for military operations.

c. It is assumed that since electrical and hydraulic power are readily available to commercial aircraft during ground operation and parts supply can be located essentially adjacent to the aircraft, the fixed maintenance time can be reduced to approximately 1/2 hr. Assuming a further increase in skill level (and incentive) for the commercial mechanic in accomplishing trouble-shooting, it is estimated that the mean time to accomplish repair will reflect a base of $\tau \doteq 50$ min. for commercial airline operations.

d. Assuming that the probability of successful repair has an exponential distribution with time, the availability of a down aircraft can be expressed as

$$A = 1 - e^{-t/\tau}$$

where t is the maintenance time interval allowable.

TABLE F-I

MULTIPLICITY MATRIX

CATEGORY	SYSTEM CONFIGURATION	OPERATIONAL ASPECTS: 1st FAILURE	2nd FAILURE	FAILURE PROTECTION: 1st FAILURE	2nd FAILURE	PROBABILITY OF COMPLETE FAILURE (FIRST APPROXIMATION)	MEAN TIME TO FALSE ALARM	AUTHORITY LIMITATION: FAILURE 1st	FAILURE 2nd	MAINTENANCE ASPECTS: SYSTEM COMPLEXITY: SENSORS	EQUIVALENT ELECT BOXES	ACTUATORS	MEAN TIME BETWEEN MAINT. TECHNICAL ACTION (MTBMA)	MEAN TIME TO ACCOMP. REPAIR (MTTAR)	HARDWARE ASPECTS: COST (1 UNIT ≈ $7000)	WEIGHT (1 UNIT ≈ 18 lb)	VOLUME (1 UNIT ≈ 500 in³)	POWER REQUIRED	WIRES IN AIRCRAFT BUNDLES	REMARKS
I	SINGLE ACTIVE CHANNEL	FAIL HARD	N.A.	T	N.A.	$P_A = \frac{1}{T}$	N.A.	REQ'D	N.A.	1	1	1	T	T	1	1	1	1	1	
II a	SINGLE ACTIVE CHANNEL (HARD.) + MONITOR	FAIL PULSE	N.A.	~T	N.A.	$\sim P_{F_A}$	N.A.	REQ'D	N.A.	1	1	1	~T	T	1	1	1	1	1	1. MONITOR CAN ONLY IDENTIFY HARDOVER FAILURE. 2. COMPLEXITY INCREASE, OVER CATAGORY I, IS NEGLIGIBLE.
II b	SINGLE ACTIVE CHANNEL (MODEL CHANNEL)	FAIL PULSE	N.A.	$\frac{T}{1.5}$	N.A.	$\frac{3}{2}P_A$	$\frac{T}{8}$	REQ'D	N.A.	2	2*	1	$\frac{T}{9.5}$	1.1T	1.5	1.3	1.3	1.3	2	1. MONITOR CAN DETECT ANY DISCREPANCIES BETWEEN CHANNEL PERFORMANCES. 2. MONITOR THUS AFFORDS PILOT AN INDICATION OF FAILURE IN REGIONS WHERE CORRECT OPERATION OF THE AUGMENTOR IS NOT READILY APPARENT.
III a	SINGLE ACTIVE CHANNEL & PARALLEL STANDBY CHANNEL (CAN BE REDUCED PERFORMANCE)	FAIL HARD	FAIL HARD	T	T	$\frac{P_A^2}{2}$	N.A.	REQ'D	REQ'D	2	2	2	T	T	2	2	2	1	2	1. CHANGEOVER FROM A FAILED ACTIVE CHANNEL TO A STANDBY CHANNEL MUST BE ACCOMPLISHED MANUALLY.
III b	SAME + HARDOVER MONITOR	FAIL PULSE	FAIL PULSE	T	T	$\frac{P_A^2}{2}$	N.A.	REQ'D	REQ'D	2	2	2	T	T	2	2	2	1	2	1. CHANGEOVER FROM A FAILED ACTIVE CHANNEL TO A STANDBY CHANNEL CAN BE EITHER MANUAL OR AUTOMATIC. IN EITHER CASE A TIME DELAY IS INVOLVED TO ALLOW FAILED CHANNEL SERVO TO REACH NEUTRAL.
IV a	TWO ACTIVE CHANNELS WITH HARDOVER MONITORS SPLIT SURFACE	FAIL PULSE	FAIL PULSE	$\frac{T}{2}$	T	P_A^2	N.A.	REQ'D	REQ'D	2	2	2	$\frac{T}{2}$	T	2	2	2	2	2	1. CONFIGURATION ALLOWS UNINTERRUPTED (BUT REDUCED PERFORMANCE) OPERATION REGARDLESS OF TYPE OF FIRST FAILURE. 2. ALLOWS TRADEOFF BETWEEN MAGNITUDE OF PULSE AT FAILURE AND AUTHORITY LIMITATIONS.
IV b	TWO ACTIVE CHANNELS WITH DUAL TANDEM ACTUATOR 1. NO INTERROGATION PROVISION 2. INTERROGATION PROVISION	FAIL SOFT	N.A.	$\frac{T}{2}$	N.A.	$2P_A$	$\frac{T}{8}$	NOT REQ'D	N.A.	2	2	2	$\frac{T}{10}$	1.25T	2	2	2	2	2	
		FAIL SOFT	FAIL HARD	$\frac{T}{2}$	T	P_A^2		NOT REQ'D	REQ'D	2	2*	2		T					
V	SINGLE ACTIVE CHANNEL (MODEL PLUS STANDBY (CAN BE REDUCED PERFORMANCE CHANNEL)	FAIL PULSE	FAIL HARD	$\frac{T}{1.5}$	T	$\frac{5}{4}P_A^2$	$\frac{T}{8}$	REQ'D	REQ'D	3	3*	2	$\frac{T}{9.5}$	1.1T	2.5	3~	3~	1.3	3	1. ACTIVE CHANNEL MAY BE EITHER IIa OR IIb.
VI	TWO ACTIVE CHANNELS & PARALLEL MONITOR CHANNEL	FAIL OPERATIONAL	FAIL PULSE	$\frac{T}{2.5}$	$\frac{T}{1.5}$	$2P_A^2$	$\frac{T}{24}$	NOT REQ'D	NOT REQ'D	3	3*	2	$\frac{T}{26.5}$	1.35T	2.5*	3~	3~	3~	3	
VII	THREE ACTIVE CHANNELS	FAIL OPERATIONAL	FAIL SOFT	$\frac{T}{3}$	$\frac{T}{2}$	$3P_A^2$	$\frac{T}{24}$	NOT REQ'D	NOT REQ'D	3	3*	3	$\frac{T}{27}$	1.85T	3*	3*	3*	3*	3	1. REQUIRES THREE SEPARATE ACTUATOR POWER SOURCES.
VIII	TWO ACTIVE CHANNELS & PARALLEL MONITOR - MULTIPLE ON LINE VOTING	FAIL OPERATIONAL	FAIL@ OPERATIONAL	$\frac{T}{3}$	$\sim\frac{2T}{5}$	P_A^2	$\frac{T}{3}$	NOT REQ'D	NOT REQ'D	3	3**	2	$\frac{T}{6}$	T	3*	3~	3~	3~	3	1. P_A EXPRESSION HERE IS BASED ON THE SIMPLIFYING ASSUMPTION THAT EACH ELEMENT HAS A FAILURE PROBABILITY OF $P_A/3$.

*ASSUMES DISSIMILAR 1st AND 2nd FAILURES